



Activity Report
2016

1	Introduction.....	4
2	ITER Project.....	6
2.1	Activity for the development of Neutral Beam Injectors for ITER	6
2.1.1	SPIDER	8
2.1.2	MITICA.....	28
2.1.3	PRIMA buildings and plants	40
2.1.4	Host Supporting Activities	45
2.1.5	RF R&D	47
2.1.6	Development of flux-gate magnetic sensor	48
2.2	ITER NBI Physics activities.....	50
2.3	ITER Core Thomson Scattering	51
3	EUROfusion Programme	53
3.1	RFX-mod: experimental, modeling activities and upgrades.....	53
3.1.1	Analysis of experiments in RFP configuration	53
3.1.2	Analysis of experiments in Tokamak configuration.....	61
3.1.3	Analysis of experiments in ultra-low-q configuration.....	65
3.1.4	3-D modelling of RFP helical states	66
3.1.5	Transport studies	67
3.1.6	RFX-mod upgrade.....	69
3.2	Medium Size Tokamaks and JET	72
3.2.1	Activities on JET	73
3.2.2	European Medium Size Tokamak studies	74
3.3	Contribution to the ITER Physics.....	78
3.3.1	Preparation of Exploitation of JT-60SA.....	78
3.3.2	Exploitation of W7-X and Stellarator optimization.....	81
3.3.3	WP ISA Infrastructure support activities	84
3.3.4	ITER Modelling and some related support activities.....	85
3.3.5	Divertor Test Tokamak studies (DTT).....	88

3.4	NBI Accompanying program	88
3.4.1	NIO1 operation.....	88
3.4.2	Breakdown Modelling for HV Holding.....	93
3.4.3	Voltage Holding Prediction Model activities	95
3.4.4	Modelling of beam acceleration.....	96
3.4.5	Development of alternative concepts: the bent beam	103
3.4.6	Collaboration with other Laboratories and Institutions	103
3.5	Power Plant Physics & Technology Projects	108
3.5.1	Heating and Current Drive Systems for DEMO	108
3.5.2	Plant Level System Engineering, Design Integration and Physics Integration	112
3.5.3	Magnet System Protection	113
3.5.4	Diagnostic and Control.....	115
4	Broader Approach.....	117
4.1	Contribution to the JT-60SA project	117
4.2	Remote Participation.....	119
5	Socio economic studies	119
5.1	Fusion Energy as base-load electricity source	119
5.2	Long term scenarios for power generation and the role of Fusion	119
6	Industrial Collaborations	120
6.1	Model for the electrostatic design a new VCB prototype.....	120
6.2	Biomedical plasma applications	123
7	Education, Training and Information to the public	124
7.1	Education and Training	124
7.1.1	International Doctorate in Fusion Science and Engineering	124
7.1.2	Other education and training activities.....	124
7.2	Information to the public.....	125
8	PUBLICATIONS 2016	126

1 Introduction

The 2016 Activity Programme of Consorzio RFX was presented and evaluated at the 35th meeting of the Scientific-Technical Committee on 6 November 2015 and approved by the Consorzio RFX partners in the meeting on 22 February 2016. Despite the delay of the approval, the initial program was maintained and the main goals achieved.

The carried out research lines have been confirmed according to the initial prevision, being mainly addressed to the realization of the Neutral Beam Test Facility, the participation to the experimental and theoretical physics research in favor of ITER to which the exploitation of RFX-mod remains a pillar for a qualified contribution, the supply of the power converters to JT-60SA within the Broader Approach agreement and the contribution to the studies for DEMO.

The activity for the realization of the Neutral Beam Test Facility has produced, during the year 2016, a high and visible advancement in the installation and assembly of the 1 megavolt power supplies provided as contribution of Japan to the Facility: almost 80% of the components have been delivered to Padova and assembled.

Significant progress in the set-up of SPIDER, the test bed specifically devoted to the development of the beam source, has been obtained in the year with the installation completion of almost all the components and the start of the integration of the plants with the control system. Nevertheless the beam source delivery, which was planned in September 2016, has been further postponed to the middle of 2017 because of component quality problems.

In Sec. 2 the attained results on MITICA, the full size test bed of the ITER neutral beam, and SPIDER are reported together with the advancement in the host activities and the accompanying NBI physics studies.

The physics activity, related to the success of ITER, was based firstly on the analysis and elaboration of the experimental data obtained from RFX-mod, operated both in RFP and Tokamak configuration. New results and increased knowledge have been obtained in the fields of plasma-wall interaction, isotopic effect, impurity behavior, turbulence contribution to transport, fast particle dynamics and 3D physics for helical state studies. The RFX-mod proposed modifications in order to enhance its plasma performances have obtained the full endorsement from the evaluating international

panel and during the 2016 the different technical solutions have been analyzed and the modifications finalized.

In relation with the stop of the experimental activity at RFX-mod, it was increased the participation to JET and European Medium Size Tokamak experiments and to the preparation of the exploitation of the satellite Tokamak JT-60SA.

Increased effort was devoted to enhance the Consorzio competences in the neutral beam physics in view of the exploitation of SPIDER and MITICA. This was done through the experimental studies in NIO1, the small scale beam source operating at the Consorzio, and with strong cooperation with international laboratories. Significant results have been obtained in the optimization of the magnetic field configuration of the source which could improve, when adopted, the MITICA performances.

A supporting activity to the preliminary design of DEMO, in the framework of EUROfusion consortium, was maintained. It is based on the already available competences in Consorzio RFX and refers to the sectors of neutral beam plasma heating, power supplies, magnetic systems, diagnostics, vacuum and gas systems. Related to DEMO are the socio-economic studies to analyse the impact of fusion on the future energy scenarios.

The contribution to JT-60SA, through the supply of the power converters for the control of the Resistive Wall Modes, was progressed with the start of the procurement, the finalization of the design and the release of the next manufacturing phase.

In the year 2016, the results of the scientific and technological researches have been reported in 92 papers on national and international journals (74 in 2015), 62 publications in conference proceedings (92 in 2015), 25 communications and 65 participations in international and national conferences and workshops.

2 ITER Project

2.1 Activity for the development of Neutral Beam Injectors for ITER

The activities for the development of the Neutral Beam Test Facility (NBTF) Team, including those of the third parties, are foreseen by the existing agreements among ITER, Fusion for Energy and Consorzio RFX to realize the PRIMA Test facility at Padova¹.

The main areas of activity performed in 2016 by NBTF Team and third parties were:

- *Construction supervision* for the completion of PRIMA buildings and auxiliaries, including the plant commissioning, in order to be ready to host the experimental plants
- *Design* of components, diagnostics, protection and safety systems. The activity includes the preparation of the documentation for the call for tenders
- *R&D activities* for experimental qualification of critical items finalised to the confirmation of the design choices. The activities have been performed with the support of the HV Test Facility (HVPTF) and the RF laboratory
- *Technical follow up* of procurement contracts from the call for tender phase, issued by F4E, up to the installation, including factory and site acceptance tests of some plants
- *Interface management* among buildings/plants/components to guarantee the coherence of the overall design. To guarantee proper integration between experimental plants and PRIMA buildings, a full 3D integrated CAD model was developed
- *Management* of the contract for the installation of JADA components and of the overall installation activities on site
- *Procurement* by Consorzio RFX of plants or components for the Facility

During 2016 there was a considerable commitment of human resources to finalize the design of the Beam Line Components, to follow-up procurements, in particular SPIDER Beam Source and Cooling plant, to support JADA and INDA installations, and to perform to Host Site Activities and plant integrations.

Within the Framework Contract for the realization of the Control, Interlock and Safety systems by Consorzio RFX, signed in 2014 with Fusion for Energy, SPIDER CODAS

¹ V. Toigo, et al. "A substantial step forward in the realization of the ITER HNB system: The ITER NBI Test Facility" Fusion Eng. and Des., DOI: 10.1016/j.fusengdes.2016.11.007

and Interlock system was provided, installed and tested. In July 2016 both systems have been accepted.

Similarly, the procurement of the SPIDER diagnostics in charge to the Consorzio RFX, started in July 2015, has continued throughout 2016 with successful delivery of almost all the main diagnostic components. Together with the diagnostic delivery, the development of programs for data analysis was continued in order to be ready to interpret the results from the first plasma.

Finally, the last foreseen Framework Contract with Fusion for Energy, devoted to assign to Consorzio RFX the assembly and completion activities, has been signed in November allowing the start of the procurement of the HV Bushing Support Structure, a key component for the progress of the installation of components coming from Japan.

The SPIDER Beam Source procurement has continued to meet difficulties to progress in the construction – the delivery date to Padua was foreseen in September 2016 - so that the assembly activities, started in May 2016, have to be interrupted as a consequence of several ongoing issues on parts to be assembled. Recovery actions have been planned and the new delivery date has been postponed to June 2017.

Despite the beam source delay, significant progress in the procurement of all other SPIDER plants was achieved by the NBTF Team. In particular in 2016:

- the High Voltage Deck and Transmission Line have been definitively completed, installed, tested and, finally, accepted by Fusion for Energy.
- the Ion Source and Extraction Grid Power Supply has been installed and tested and is now ready to be integrated with the control (CODAS) and the interlock system;
- the vessel, including electric and hydraulic flanges, after delivered on Site was installed and accepted;
- the Beam Source Handling Tool has been delivered on Site and will be installed and tested by the beginning of 2017;
- the Vacuum and Gas Injection system was installed and the commissioning progressed during 2016; during the Site Acceptance Tests the cryopump capability to pump hydrogen was seen not satisfy the requirements. Actions are in progress in order to understand the cause and find a solution to this issue;
- the Cooling plant system, which installation started in November 2014 and

continued during 2015, has been concluded in November 2016. Soon after it started commissioning of the plant which will run until mid-2017;

- the Acceleration Grid Power Supply (AGPS), provided by INDA, was started the installation in July and prosecuted till the end of 2016. In January 2017 will start the commissioning and power tests on dummy load.

In conclusion, all SPIDER systems and components have been installed or are under installation completion except for the beams source; moreover, some systems have been tested and accepted. The start of SPIDER experiment remains related to the solution of the encountered issues and the delivery of the beam source.

The MITICA test bed realization was progressed with the completion of the design of the injector mechanical components and the procurement activities of almost all systems; only a couple of calls for tenders (Beam Line Components and cryo-pumps) remain to be launched and they are expected in the beginning of 2017. In particular, were signed by Fusion for Energy in 2016 the contracts for the procurement of the Beam Source, cryo-plant and SF₆ gas system.

The complexity of the installations into the on-site yard has required to set up an integrated organization able to manage, according to the Italian rules, the activities related to the Health and Safety, the Coordination of the Direction of the Works and the Plant integration. For all 2016, weekly meetings for the coordination of installations and integrations activities are held on a regular basis and the integrated plan for installations is regularly updated.

Finally, R&D activities were performed on High Voltage (HV) in vacuum using the High Voltage Padova Test Facility and on Radio Frequency (RF) with the aim of supporting the Beam Source realization and of training the NBTF staff.

The detailed status of the project and the main achievements in the year are described in the following sections.

2.1.1 *SPIDER*

2.1.1.1 SPIDER Vacuum Vessel

In the first quarter of 2016 the SPIDER Vacuum Vessel was made available for installation of GVS parts (pumps, pipes and cables) to be connected to the Vessel. The installation of two HV bushings (one electrical and one hydraulic) was completed in November 2015 and the foreseen HV electrical tests were positively completed on site in January 2016. During 2016 the NBTF Team has put a lot of effort of engineers and technicians to support and attend all the meetings and testing activities

performed on-site by the supplier, with particular care for electrical holding voltage and vacuum leak tests.

The installation was completed by the end of June (see Fig. 2.1.1) with the installation of the last hydraulic bushing; the electrical acceptance tests were successfully carried out achieving the target value of 130 kV for one hour with vacuum level of 3×10^{-7} mbar, after 4 hours of voltage conditioning (see Fig. 2.1.2).



Fig. 2.1.1 The finally assembled hydraulic bushings on the bottom side of SPIDER Vacuum Vessel

After successful completion of the acceptance tests the updated “as built” documentation was submitted by the supplier and the NBTF Team carried out the final checks, review and recommendation of technical documents, propaedeutic for the Vessel hand over.

2.1.1.2 SPIDER Beam Source

The contract for the supply of the SPIDER Beam Source (BS) was signed in 2012. In 2016 a high effort was required to the Team to perform the technical follow up of the contract due to the criticalities emerged in the procurement of some source components (cooling pipes and grids) resulting in further delivery date delay by the company.

The RFX personnel were strongly involved in meetings, inspections to the supplier site to verify the manufacturing progress and to witness intermediate tests according to the control plans.

At the beginning of 2016, the manufacturing of most critical parts was completed,

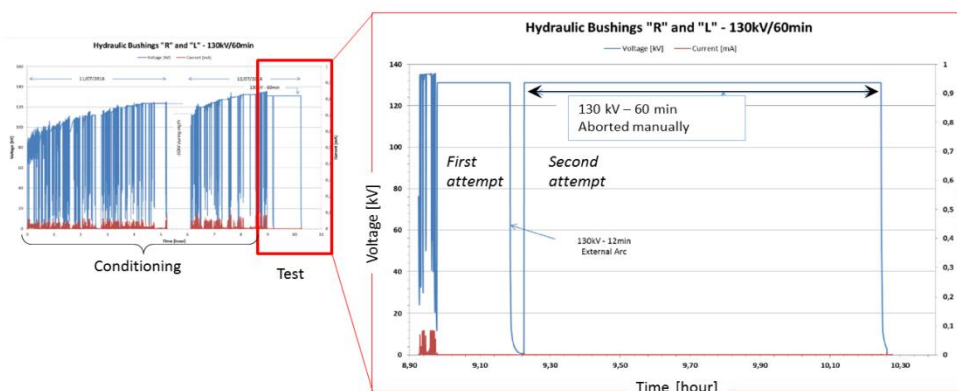


Fig. 2.1.2 Electrical tests results on SPIDER hydraulic bushings

including overall support structure and large plates for accelerator and ion source, which had required a change of sub-supplier in mid 2015. Then, constant and close follow-up of the initial phase of the assembly at the factory was ensured till May 2016, when issues were identified on hydraulic circuits and on Bias Plate and Plasma Grid, showing pollution and oxidation on the Molybdenum coated surfaces. Pictures of the SPIDER Beam Source as partially assembled inside the supplier's assembly room are shown in Fig. 2.1.3.

The large number of non-conformities on many parts to be assembled (pipes welded



(a)



(b)

Fig. 2.1.3 The SPIDER BS under assembly at the supplier's factory: view of the ion source plasma chamber (a) and of the Beam Source support structure (b)

joints, Mo coating of Plasma Grid and Bias Plate, absence of cleaning, oxidations inside the pipes and dimensional errors) paralyzed the assembly from June to October 2016.

In the second half of the year the progress of the source realization was very poor, notwithstanding the huge follow-up effort done by NBTF team. Several issues and non-conformities are still pending and need being discussed. Presently the procurement schedule shows end of June 2017 as final delivery date. The procurement of the Beam Source handling tool, whose manufacturing has proceeded substantially on schedule during 2016, will be completed with site acceptance tests at the beginning of 2017.

Furthermore the NBTF Team reviewed the documentation prepared by Iter Organization for the independent procurement of eight electromagnetic shields, to be installed on the source around each RF driver prior to the assembly into the vessel.

2.1.1.3 SPIDER Cs Ovens

The Cs ovens were foreseen to be supplied within SPIDER beam source contract, even if the detailed design was not included into the specification. As a consequence

of the excessive financial claim by the Beam Source supplier after Cs oven design finalization, this procurement had been delated from SPIDER contract and set under the direct responsibility of RFX. Final design was completed as foreseen, together with the preparation of the technical specification for the procurement, launched by RFX after the successful completion of an additional design review by Iter, Fusion for Energy and IPP. See a section view of the SPIDER Cs Oven in Fig. 2.1.4 Section

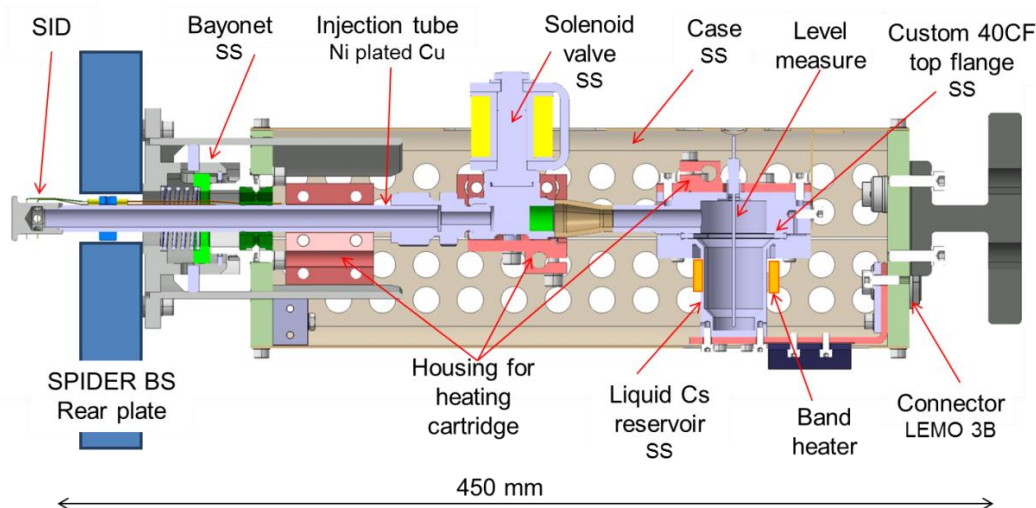


Fig. 2.1.4 Section view of a typical Cs Oven for SPIDER Beam Source

view of a typical Cs Oven for SPIDER Beam Source.

The realization started in September 2016, under full responsibility and with constant follow-up by RFX. The first oven prototype is expected to be delivered at the beginning of 2017 and the three ovens to be installed on the SPIDER beam source around mid 2017. In parallel, it was proposed and agreed to establish a Cs oven test facility at PRIMA site, in order to optimize the development and the exploitation of this crucial component for the source performances. The design of the Cs oven testing facility was completed (see Fig. 2.1.5 and Fig. 2.1.6 Plan view of the Cs Oven test bed room to be installed at PRIMA site inside Building 1.) and the specific design review by Iter, Fusion for Energy and IPP was held in December 2016.

At the beginning of 2017 the various procurements for the facility components and systems will be launched.

2.1.1.4 SPIDER Beam Dump

The SPIDER Beam Dump delivered at PRIMA site in 2015 required adjustments of the hypervapotron positions located on one of the two panels, in order to close some gaps that could cause beam shinethrough. In first quarter 2016 ITER Organization

identified a technical solution, also shared with NBTF Team, to adjust the positions and fix the hypervapotron with proper combs engaging the inlet/outlet cooling pipes. NBTF Team was then in charge for the design and procurement of a dedicated structure aiming to support the Beam Dump inside Building 1 to allow the works necessary for recovery of non-conformities and the installation of thermocouples and cables on the panels. This support structure was delivered and installed inside Building 1 by the NBTF Team in September 2016, allowing the activities for solving the shine through non-conformity in October. The installation of the Beam Dump inside Building 1 is shown in Fig. 2.1.7. Unfortunately the issue of beam shine through between adjacent hypervapotron elements was not solved during the recovery activity due to a lot of mismatches and problems on Beam Dump side. It was decided to stop the activity and to plan the restart in January 2017 after some modifications to the procured parts.

A fruitful collaboration was set up between ITER Organization and the NBTF Team to manage and solve the issue with procurements from local suppliers and efficient

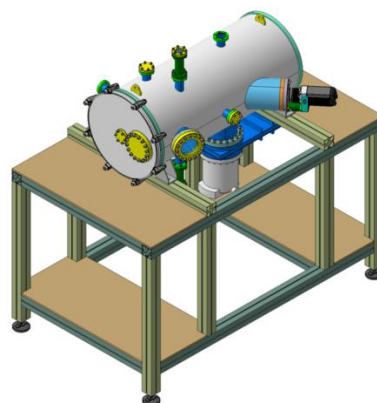


Fig. 2.1.5 Isometric view of the Cs Oven test bed to be installed at PRIMA site

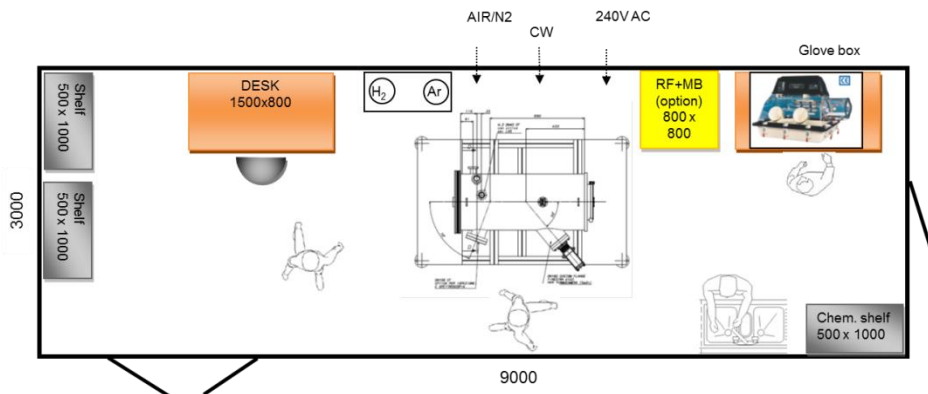


Fig. 2.1.6 Plan view of the Cs Oven test bed room to be installed at PRIMA site inside Building 1

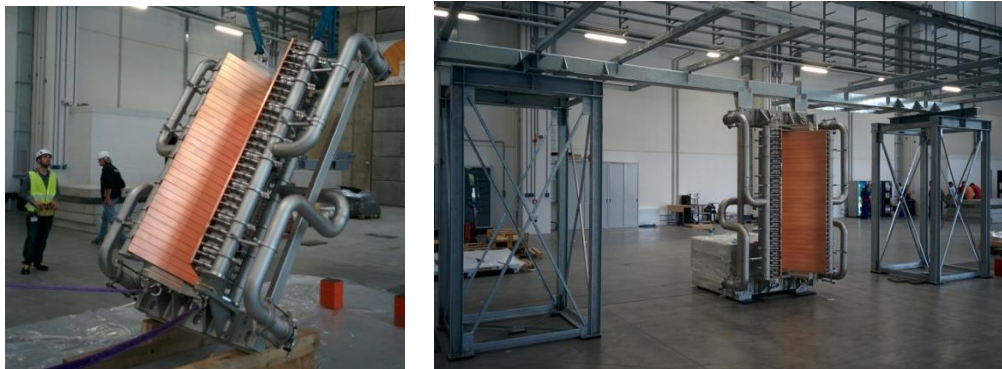


Fig. 2.1.7 Pictures of the Beam Dump during installation inside Building 1.

support by RFX workshop.

2.1.1.5 SPIDER power supplies

In 2016, the realization of the SPIDER Power Supply (PS) system has made a huge progress. Just to remind the main components, SPIDER PS includes the Ion Source Power Supply (ISEPS), hosted in a Faraday cage - called HVD - air insulated with

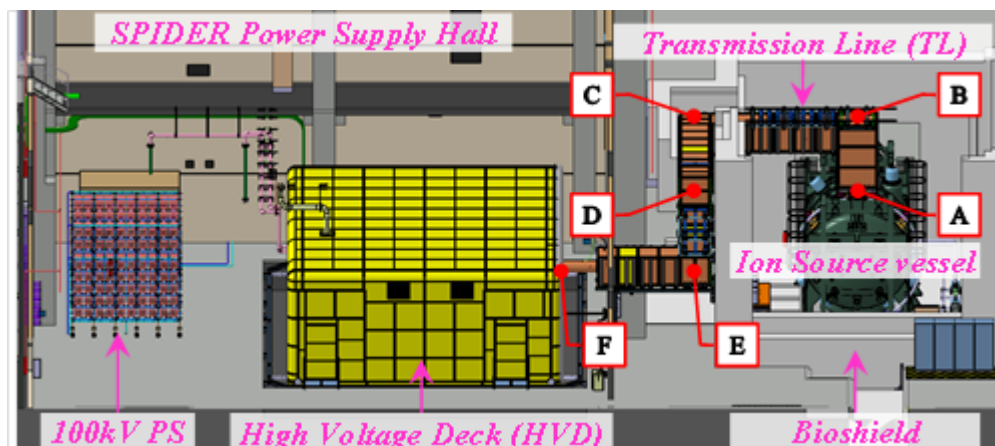


Fig. 2.1.8 3D view of SPIDER layout

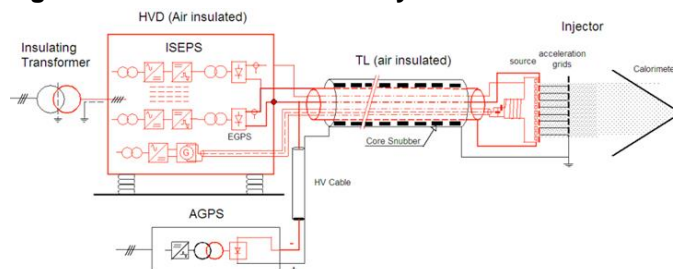


Table 3 - ISEPS and AGPS main data ratings

ISEPS	Output ratings
Extraction (EGPS)	-12.8 kV 140 A
Radiofrequency (RFPS)	4 units, 200 kW each f=1 MHz 50Ω load
Bias (BPS)	±30 V 600 A
PG filter (PGFPS)	15 V 5 kA
AGPS	(-96kV) DC 71A DC

Fig. 2.1.9 Conceptual scheme of the SPIDER PS and ratings of ISEPS and AGPS

respect to ground for -100 kV and the Acceleration Grid Power Supply (AGPS). A 3D

view of the SPIDER layout is shown in Fig. 2.1.8. The conceptual scheme of the whole SPIDER PS and the main rating data of the ISEPS and AGPS are summarized in Fig. 2.1.9. AGPS is procured by INDA, all the other SPIDER PSs and all the other plants, necessary to operate SPIDER, are procured by F4E; the technical follow-up activity by NBTF Team for F4E procurements and the support to the INDA installations on Site have been very intense.

Ion Source and Extraction Power Supply system

The Ion Source and Extraction Power Supplies procurement continued in 2016 with the successful completion of the Site Commissioning and Acceptance Tests in September; Fig. 2.1.10 shows the SPIDER ISEPS in the final installation condition.

The ISEPS system is a heterogeneous set of power supplies. It was the first PS system to be tested in the PRIMA facility; to proceed in parallel, a temporary Medium Voltage and Cooling systems have been set-up since the final ones were not available yet.

The site commissioning started in late 2015 and the large number of functional tests was performed in January 2016 when the first energization of the ISEPS insulating transformer was carried out. A wide-range power test plan was carried out²; it included tests on individual power supplies and a set of special tests which goal was to check the integration of the ISEPS subsystems in the foreseen operational conditions of the SPIDER experiment. All the site activities have been supported and closely supervised by Consorzio RFX personnel; this has permitted an efficient



Fig. 2.1.10 SPIDER ISEPS in the final installation condition

² A. Zamengo et al., "Installation and site testing of the SPIDER Ion Source and Extraction Power Supplies", presented at 29th SOFT, Sep. 2016.

technical exchange with the Supplier and sub-suppliers during all the testing stages. ISEPS was also the first PS system that has been interfaced to the control system CODAS: the exchange of thousands of digital and analogue signals and commands has been verified and operational sequences and fault conditions have been tested. As a result of the final acceptance tests, it was proved that the whole ISEPS system can be controlled remotely in accordance with the SPIDER State Machine. Fig. 2.1.11 shows the ISEPS pulse #506 performed on September 2016 where three ISEPS subsystems, named ISEG, ISPG and ISRF4, were remotely controlled by CODAS. The pulse was performed at low power with the goal of checking simultaneous operation of different subunits; in particular, ISEG applied 2 kV on a 360 Ω load, ISPG 100 A on a short circuit, while RF4 was connected on a mismatched load and provided 5 kW.

Acceleration Grid Power Supply (AGPS)

In the first half of 2016 NBTF Team strongly supported the Indian Domestic Agency (INDA) in predisposing the yard for installation of SPIDER AGPS. The call for tender was issued by INDA in March; during this phase, NBTF Team liaised with Italian bidders to clarify issues relevant to the preparation of the offers. In parallel, the definition on interfaces and logistics prosecuted; in particular, NBTF Team reviewed the 3D model of AGPS, identifying some inconsistencies. Strong support has been

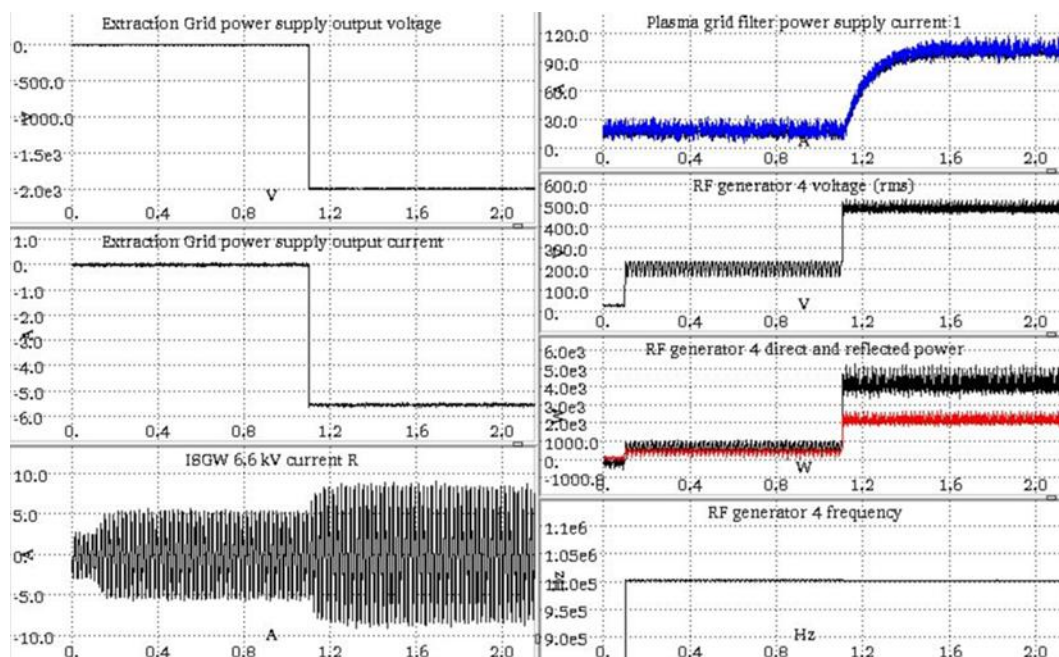


Fig. 2.1.11 Example of remote control of SPIDER ISEPS: pulse #506 with ISEG applying 2 kV on a 360 Ω load, ISPG feeding 100 A on a short circuit and RF4 connected on a mismatched load and providing 5 kW

given for the downloading and storage activities of the AGPS components after delivery at NBTf Site. In agreement with the interface requirements, some adaptations of the buildings have been performed: the completion of the transformer pits with raised basements, the provision of the rails for the transformer wheels, the realization of the three cut-outs in the South wall of Building 6 and the design and procurement of the corresponding three supporting structures for the 45 feedthroughs (Fig. 2.1.12).

The installation activities started in July and prosecuted for all the year. The three transformers have been assembled, moved on the pits, together with their bellows and ducts (Fig. 2.1.13); the transformer flanges have been fixed to the wall and welded with the bellows. After transformers installation, insulation tests have been performed on the machines and all the cable trays have been installed according to the agreed routings. The high voltage racks, which contain series-parallel connection of power supply units to form the 100 kV – 40 A accelerator power supply, have been fixed in the agreed position and the DC switches have been installed. All the power, auxiliary and signal cables have been laid and terminated. It was necessary to find a solution to re-establish the fire barrier in correspondence to the cable feedthroughs; a special test has been carried out to assess the suitability of an intumescent tape placed around the cables at 100 kV, but the result was not satisfactory due to partial discharges. An alternative solution which foresees the filling of the feedthroughs with foam is still under investigation.

In November, the tests on the control system have started and the fire-suppression



Fig. 2.1.12 Supporting structure for AGPS cable feedthroughs



Fig. 2.1.13 Placement of transformers in the pits



Fig. 2.1.14 Test of fire-suppression system



Fig. 2.1.15 General overview of SPIDER AGPS in December 2016

system for the transformers has been procured and successfully tested (Fig. 2.1.14). The first tests on the water cooling system of AGPS have been performed, highlighting the weakness of some pipes, which need to be substituted. Within 2016 year the installation phase is expected to be completed and the commissioning phase started; Fig. 2.1.15 gives an overview of the SPIDER AGPS in the present installation condition.

High Voltage Deck and Transmission Line

As above mentioned, the ISEPS system and the associated diagnostics are hosted inside a -100kVdc air-insulated Faraday cage, called High Voltage Deck (HVD); a High Voltage Transmission Line (TL) carries the power and signal conductors from the ISEPS to the Ion Source (see Fig. 2.1.9 Fig. 2.1.8

To satisfy all the special requirements, TL has been conceived as an original air insulated tri-axial line, consisting of a large (0.5 m diameter) High Voltage (HV) Inner Conductor, hosting ISEPS diagnostic and power cables (RF lines, busbars, power

and signal cables, optic fibers, etc.), included inside a double screened square structure (Outer Conductor 1.2 x 1.2 m²) aimed at assuring suitable EMI protection. A Core Snubber (CS), distributed along the TL high voltage inner inductor, was developed as an additional countermeasure for EMI reduction³ (Fig. 2.1.16).

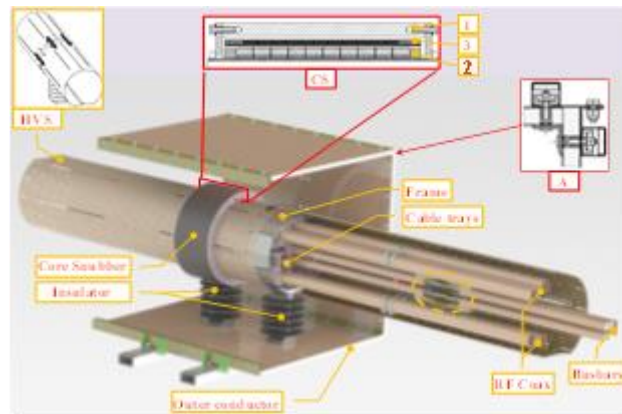


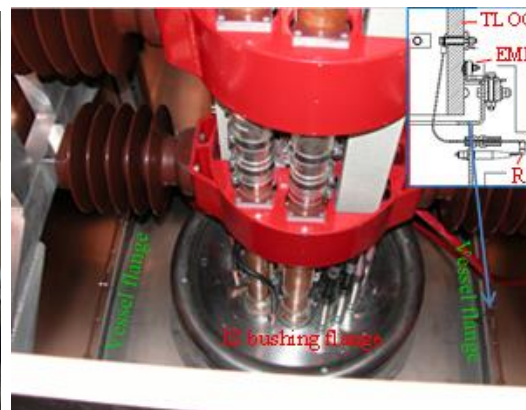
Fig. 2.1.16 TL construction details

The HVD installation was finished in 2015, while the TL installation has been started beginning 2016. Fig. 2.1.17 a) shows part of the installed TL between the building hosting the HVD (left side) and the SPIDER bunker hosting the Ion Source (right side). Fig. 2.1.17 b) shows the TL interface with the SPIDER Ion Source (IS) vessel; each TL cable/conductor is connected to its corresponding feedthrough, embedded on the metallic flange of the IS electric bushing.

On-site, tests have been performed after the completion of the installation: among them, a water leakage test of the overall TL circuit and voltage withstand tests on ISEPS conductors. The most challenging test was the main insulation test in the final installation condition, with the ISEPS equipment inside the HVD and the Ion Source vessel in vacuum. The test itself consisted in the application for 3 hours of -120kV_{dc} between HVD (internally connected to HVS) and ground (to which the TL Outer Conductor was connected). The test was preceded by a preliminary gradual voltage



a)



b)

Fig. 2.1.17 a) part of installed TL,

b) TL Interface with the IS vessel

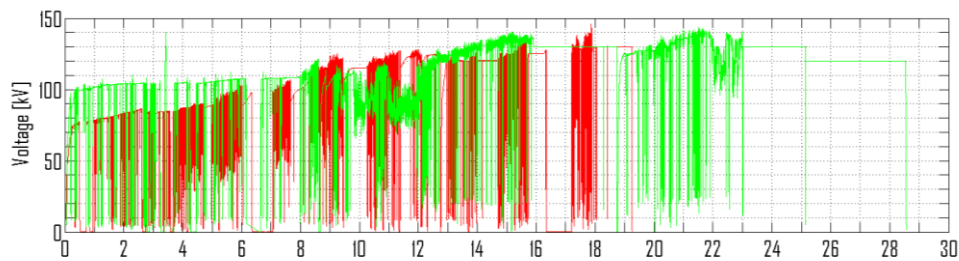


Fig. 2.1.18 Voltage profiles during TL insulating tests

application lasting many hours to condition the vacuum insulation inside the vessel and reach stable voltage withstand conditions at the TL test voltage level.

2.1.1.6 SPIDER & MITICA electric fast transient modellings

In the past years, this activity was addressed to support and verify the integrated design of the passive protection components for SPIDER Power Supply system; an integrated model has been developed at this purpose and has been updated against the real parameters derived from the built-to-print drawings and the actual installation of the sub-systems.

In 2016, this work evolved with also the development of specific models aimed at understanding the results of some site tests; just to give an example, the operation of the ISEPS RF generator when connected to a capacitive unmatched load showed an unexpected behaviour with respect to what recorded during the execution of the same test in factory. The development of a suitable model of the RF generator

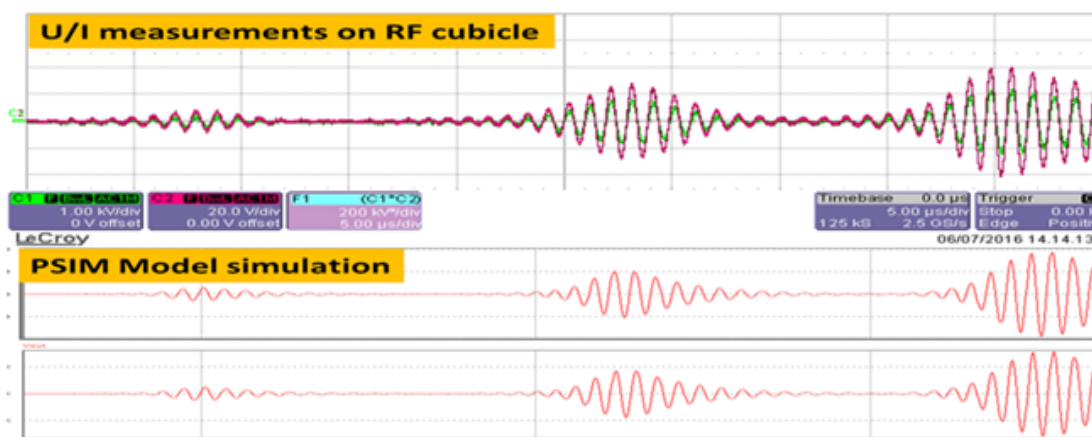


Fig. 2.1.19 measured and simulated waveforms of the RF generator output current and voltage during the start-up phase with capacitive dummy load

allowed understanding the reason and identifying a solution. Fig. 2.1.20 (upper plot) shows the unexpected RF power modulation of the output which, in certain load conditions and at a certain power level, drives the RF generator to unstable operation. The capability to reproduce by numerical simulation the same behaviour (lower plot) also allowed identifying a solution, then confirmed and implemented by the Supplier.

2.1.1.7 SPIDER & MITICA diagnostics

In 2016 the focus has been on design finalization, R&D activities and manufacturing of almost all SPIDER diagnostics⁴, mainly under the Fusion for Energy procurement contract, while development of MITICA diagnostics and of the remaining part of SPIDER systems progressed under the F4E NBTF Work Programme. A first procurement contract with Fusion for Energy includes all diagnostics required at beginning of SPIDER operation (vacuum windows, thermocouples, emission and laser spectroscopy, electrostatic probes, visible and IR imaging) and components of other diagnostics that need R&D (instrumented calorimeter STRIKE, neutron, tomography). The contract started in July 2015 and has been extended till end of 2017, to cover the full installation of the first set of diagnostics before the commissioning of the beam source, and includes the final set of tiles for STRIKE (diagnostic calorimeter) which could require long delivery time. The remaining

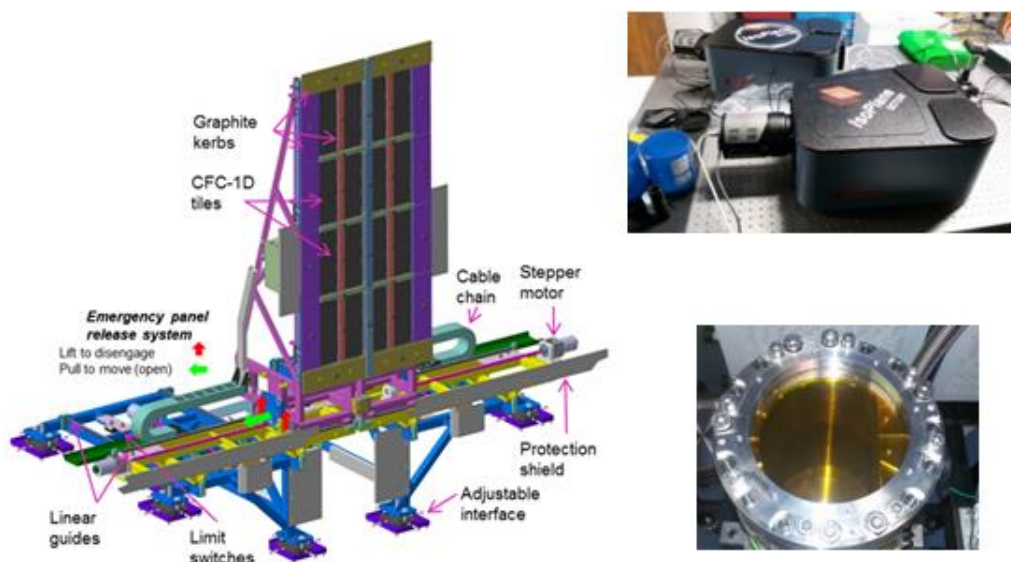


Fig. 2.1.20 Examples of SPIDER diagnostic components: STRIKE in-vacuum support and positioning structure (left), imaging Isoplane spectrometers with Pixis spectroscopic cameras (right top), ZnSe vacuum window for IR camera under vacuum test (right bottom)

SPIDER diagnostics will be completed within a second contract, starting in 2017. The procurement phase of diagnostic components occupied most of 2016, following the approach that assembly, integration and commissioning of each diagnostic system is carried out by the internal diagnostic team with the support of the consorzio technical services. The commercial components have been purchased on the market and the custom ones are designed and manufactured by the local drawing office and the mechanical workshop. At the end of 2016 most procurements have been completed, in particular (see examples in

Fig. 2.1.20): vacuum windows, thermocouples^{5,6}, visible and IR imaging are ready for installation, spectroscopy is missing only minor components and has been assembled and configured, a prototype linear camera suitable for tomography has been developed, the neutron detector box has been manufactured, the electrostatic probes conditioning electronics is starting manufacturing, the STRIKE in-vacuum supporting frame will be completed in January⁷ and CFC-1D prototype tiles have been manufactured and tested both with a focused CO₂ laser beam⁸ on the high power beam of GLADIS, surviving up to 10 MW/m² for 3 seconds. Following evaluation of this result, it will be decided if to continue with CFC-1D tiles or revert to mechanically machined castellated graphite tiles⁹.

For all diagnostics, integration with CODAS is progressing both on layout interfaces, e.g. cubicles and cabling, and on the development of the MDSplus software to centrally manage control and acquisition. Both R&D prototypes - e.g. tomography cameras - and full chains from sensor to acquisition system - e.g. for thermocouples and IR cameras - have been tested in the NIO1 test facility. For some diagnostics, analysis programs have been developed either starting from predictive models, e.g.

⁵ M. Brombin, M. Dalla Palma, R. Pasqualotto, N. Pomaro, "Final design of SPIDER thermal diagnostic system", *Rev. Sci. Instrum.* 87, 11D433 (2016)

⁶ M. Brombin, R. Ghirdelli, F. Molon, G. Serianni, R. Pasqualotto, "Design and Test of Readout Electronics for Thermocouples on Ion Beam Sources", *IEEE Transactions on Plasma Science* 44, 1619-1624 (2016)

⁷ A. Rizzolo, M. Tollin, M. Brombin, V. Cervaro, M. Dalla Palma, M. De Muri, D. Fasolo, L. Franchin, S. Peruzzo, A. Pimazzoni, R. Pasqualotto, G. Serianni, "Final design of the diagnostic calorimeter for the negative ion source SPIDER", submitted to *Fusion Engineering and Design*

⁸ G. Serianni, A. Pimazzoni, A. Canton, M. Dalla Palma, R. Delogu, D. Fasolo, L. Franchin, R. Pasqualotto, S. Peruzzo, M. Tollin, "Test of 1D carbon-carbon composite prototype tiles for the SPIDER diagnostic calorimeter", submitted to *AIP Conference Proceedings*

⁹ S. Peruzzo, V. Cervaro, M. Dalla Palma, R. Delogu, M. De Muri, D. Fasolo, L. Franchin, R. Pasqualotto, A. Pimazzoni, A. Rizzolo, M. Tollin, L. Zampieri and G. Serianni, "Castellated tiles as the beam-facing components for the diagnostic calorimeter of the negative ion source SPIDER", *Rev. Sci. Instrum.* 87, 02B925 (2016)

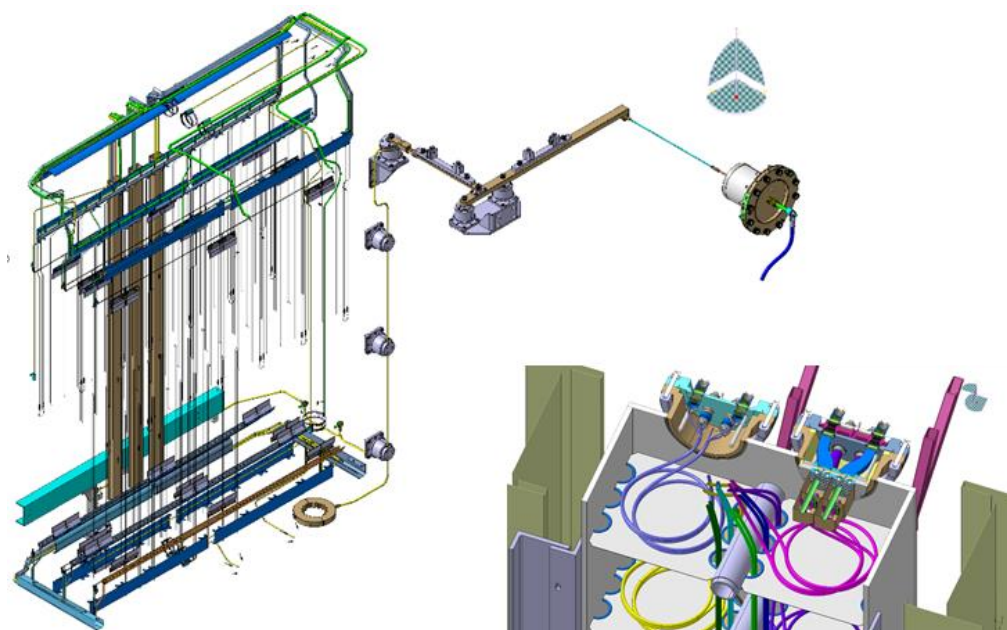


Fig. 2.1.21 CAD model of ERID electrical supply and instrumentation (left) and cross section with details of the standard and ITER-like feedthrough flanges (right)

for beam intensity profile from beam dump thermocouples¹⁰ or using also experimental measurements, on ELISE for beam emission spectroscopy and on NIFS and JAEA neutral beam test beds for a small scale version of STRIKE.

The development of the neutron diagnostic - nGEM detector - and the design of MITICA diagnostics progressed within the F4E NBTF Work Programme. The final nGEM detector to be installed on SPIDER has been completed¹¹, the model for assessment of diagnostic performance in MITICA was further optimized¹² and measurements of the neutron emission rate were performed in ELISE to investigate the adsorption dynamics of deuterium on the beam dump¹³. The sensors, fastening and cable routing of diagnostics embedded in the MITICA beam line components,

¹⁰ M. Zaupa, M. Dalla Palma, E. Sartori, M. Brombin, R. Pasqualotto, "SPIDER beam dump as diagnostic of the particle beam", *Rev. Sci. Instrum.* 87, 11D415 (2016)

¹¹ A. Muraro, G. Croci, G. Albani, G. Claps, M. Cavenago, C. Cazzaniga, M. Dalla Palma, G. Grosso, F. Murtas, R. Pasqualotto, E. Perelli Cippo, M. Rebai, M. Tardocchi, M. Tollin, G. Gorini, "Performance of the Full Size nGEM detector for the SPIDER experiment", *Nucl. Instr. And Meth. In Physics Research A* 813 (2016) 147-152

¹² M. Rebai, G. Croci, G. Grosso, A. Muraro, E. Perelli Cippo, M. Tardocchi, M. Dalla Palma, R. Pasqualotto, M. Tollin, F. Murtas, M. Cavenago, and G. Gorini, "Conceptual design of a neutron diagnostic for 2-D deuterium power density map reconstruction in MITICA" submitted to JINST

¹³ M. Nocente, S. Feng, D. Wunderlich, F. Bonomo, G. Croci, U. Fantz, B. Heinemann, W. Kraus, R. Pasqualotto, M. Tardocchi, and G. Gorini, "Experimental investigation of beam-target neutron emission at the ELISE neutral beam test facility", submitted to *Fusion Engineering and Design*

were further detailed to produce instruction for the installation of these diagnostics by the manufacturer of the beamline components (Fig. 2.1.21 CAD model of ERID electrical supply and instrumentation (left) and cross section with details of the standard and ITER-like feedthrough flanges (right))¹⁴. Electrostatic sensors to be installed in the neutralizer and in the ERID have been designed and integrated in the CAD model¹⁵. A new diagnostic to derive the beam intensity profile at the beam dump, based on the secondary electron emission from the swirl tubes panel, has been conceptually developed¹⁶.

2.1.1.8 NBTF Control and Interlock

In 2016 the activities in the field of the NBTF control, interlock, and safety have been executed under the Fusion for Energy contracts.

The extensive, intense, and comprehensive activities have covered a large number of items including:

- Follow up of procurement contracts of NBTF control and interlock components;
- Follow up of procurement contracts of major SPIDER/MITICA machine components as far as I&C (Instrumentation and Control) are concerned;
- Construction, commissioning and acceptance tests of SPIDER Central CODAS (Control and Data Acquisition System);
- Construction, commissioning and acceptance tests of SPIDER Plant System CODAS;
- Construction, commissioning and acceptance tests of PRIMA/SPIDER I&C infrastructure;
- Construction, commissioning and acceptance tests of the SPIDER Central Interlock System;
- Design of PRIMA and SPIDER Central Safety Systems.

Comprehensive as the activity outcome has been the installation, testing and acceptance of SPIDER Central CODAS, priority SPIDER Plant System CODAS,

14 M. Dalla Palma, R. Pasqualotto, E. Sartori, S. Spagnolo, M. Spolaore, P. Veltri, "Design of in-vacuum sensors for the beamline components of the ITER neutral beam test facility", Rev. Sci. Instrum. 87, 11D417 (2016)

15 S. Spagnolo, M. Spolaore, M. Dalla Palma, R. Pasqualotto, E. Sartori, G. Serianni, P. Veltri, "Preliminary design of electrostatic sensors for MITICA beam line components", Rev. Sci. Instrum. 87, 02B931 (2016)

16 E. Sartori, A. Panasenkov, P. Veltri, G. Serianni, R. Pasqualotto, "Study of a high power hydrogen beam diagnostic based on secondary electron emission", Rev. Sci. Instrum. 87, 11D438 (2016)

SPIDER miniCODAS, PRIMA/SPIDER I&C infrastructure, and SPIDER Central Interlock including all interface with plant systems.

SPIDER Central CODAS

SPIDER computers and data storage equipment have been finally installed along with the SPIDER data networks, including the plant operation network (conventional control), the data acquisition network (data streaming fast network), the time communication network (sub μ s synchronization of distributed systems), and the offline network (conventional IT).

Control software was also produced and tested, including: pulse scheduling (supervisory control); human machine interface (HMI); system configuration; data acquisition, storage and access; alarm and message handling. All software that has been produced is maintained in the CODAS software versioning system (Apache Subversion). Fig. 2.1.22 shows the SPIDER computers system and network star center, respectively

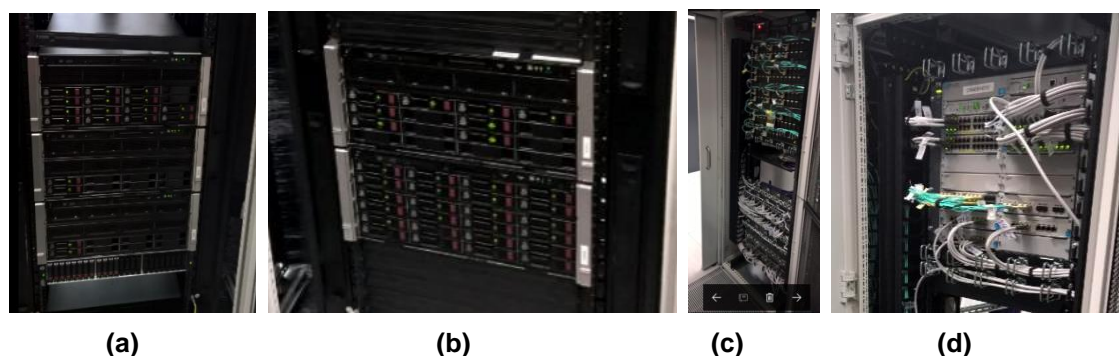


Fig. 2.1.22 SPIDER CODAS (a) online and (b) offline computer system. Online computer system is based on a redundant VMware cluster and RAID6 disks. Offline computer system is equipped with 100 TB storage memory (raw) for data archiving. SPIDER CODAS (c) and (d) active network equipment. Plant Operation, Data Acquisition and Offline Networks are implemented as VLAN.

SPIDER Plant System CODAS

SPIDER Plant System CODAS includes the I&C needed to interface the plant systems to Central CODAS, comprising programmable controllers, fast controllers, and analog and digital I/O boards. The power supply plant system, interfacing ISEPS, AGPS and partly the plasma light source spectroscopy signals, has been completely installed and tested. Part of the Injector, Interlock and PRIMA plant systems interface I&C has been also installed and tested, including:

-
- The source, vessel and beam dump thermocouple data acquisition system along with the fast controller of the Injector plant system;
 - The thermal protection unit to protect the source and beam dump against over temperature has been also installed and tested.
 - The fast data acquisition unit and CODAS Interlock interface have been installed and tested for the Interlock plant system. The fast data acquisition unit allows for > MHz sampling rate of the Central Interlock input/output signals and, thus, for fast diagnosis on the Central Interlock System behavior;
 - The HMI of the SPIDER and PRIMA Gas and Vacuum System.

Fig. 2.1.23 shows (a) the layout of one of the CODAS I&C cubicles to manage the power supply plant system; (b) one of the CODAS HMI panel of the SPIDER Gas and Vacuum System.

SPIDER miniCODAS

SPIDER miniCODAS has been developed to allow for plant unit site acceptance tests. It is a mobile - on wheels - system that can adapt to different plant system I&C interfaces. It has been used extensively in 2016 during the ISEPS and SPIDER Gas and Vacuum System site acceptance tests.

Fig. 2.1.24 shows a front view of miniCODAS along with a few figures taken from the SPIDER ISEPS site acceptance test report ¹⁷.

PRIMA/SPIDER Infrastructure

Fifteen I&C cubicles have been installed on site and tested to host the SPIDER CODAS I&C. The PRIMA/SPIDER data center has been also installed and accepted. This consists of six IT cubicles arranged in a closed enclosure to optimize heat removal from computers. The IT cubicles host the servers, central network I&C, and data storage equipment. CODAS cable trays have been installed and cabling has been installed and tested. **Fig. 2.1.25** shows: (a) two I&C cubicles that have been installed in the SPIDER High Voltage Deck; (b) the computer data center installed in PRIMA Computer Room

SPIDER Central Interlock System

¹⁷ V. Parafati, ISEPS of SPIDER - Site Test Report (UT-RP-0197), F4E-IDM 257YRA v3.1, 5 Dec. 2016

SPIDER Central Interlock System has been installed, commissioned and accepted. The system, which is devoted to SPIDER plant investment protection, includes a

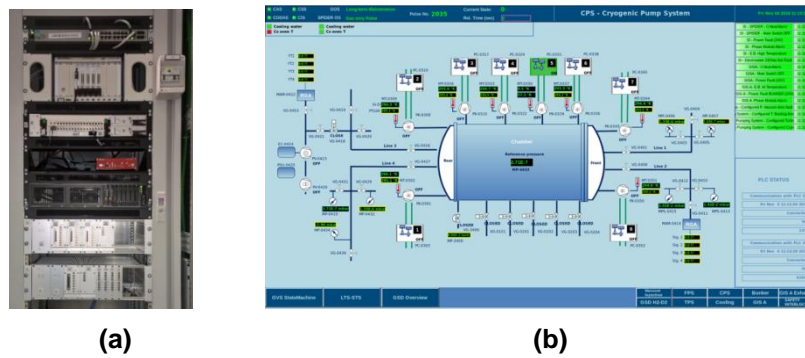


Fig. 2.1.23 SPIDER Plant System CODAS – (a) Power Supply Plant System I&C – SPIDER CODAS interface with SPIDER ISEPS and AGPS. (b) One panel of the human machine interface of the SPIDER gas and vacuum system.

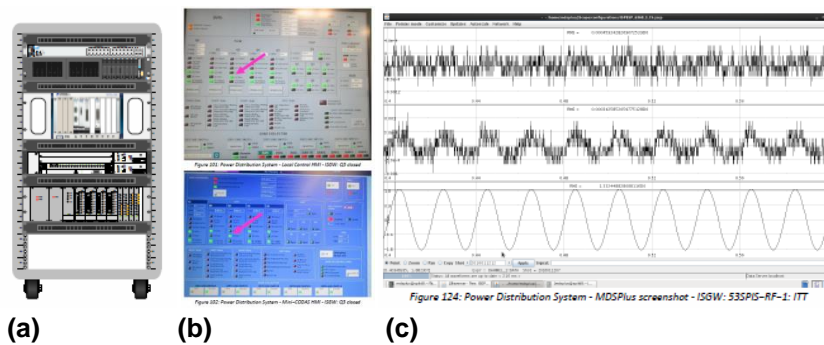


Fig. 2.1.24 SPIDER miniCODAS: (a) system front view; (b) comparison between ISEPS and miniCODAS HMI showing that the same information is displayed on both local and remote HMI; (c) ISEPS signals acquired and stored through miniCODAS during site acceptance tests.

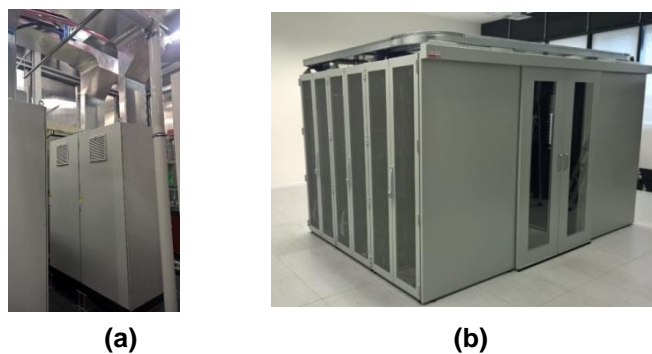


Fig. 2.1.25 CODAS I&C cubicles – (a) HVD ground insulated cubicles for ion source thermocouples and Caesium ovens control; (b) Computer data center.)

2.1.2 MITICA

2.1.2.1 MITICA Vacuum Vessel

The technical follow-up of procurement contract for MITICA Vacuum Vessel (VV) was regularly carried out by the NBTF Team. During the first quarter 2016 a big effort was dedicated to revise the manufacturing drawings and technical documents released by the supplier, including participation to regular weekly and progress meetings among supplier, Fusion for Energy, NBTF Team and Iter Organization. A significant effort was devoted to prepare and revise documents for a number of changes proposed by the different stakeholders. Interfaces for cryopumps installed into the vessel required a number of meetings and verification activities with dedicated structural analyses

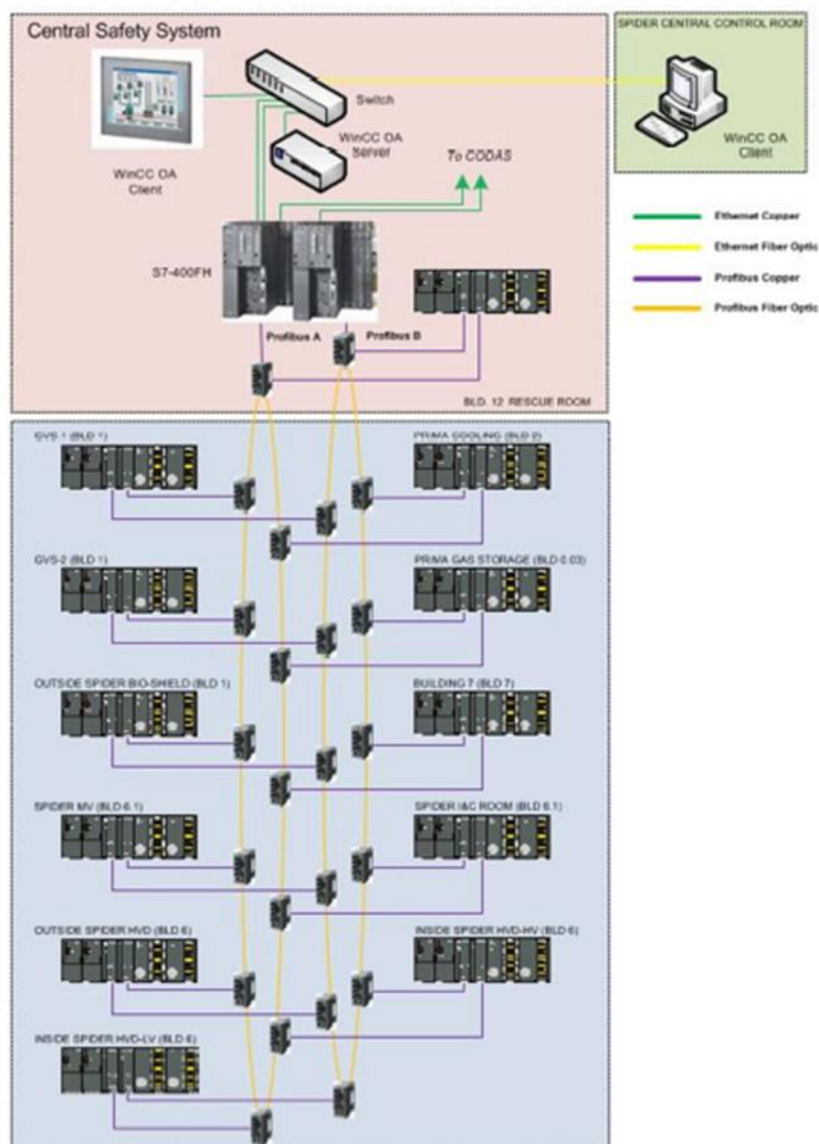


Fig. 2.1.29 Redundant-plc architecture of SPIDER Central Safety System



Fig. 2.1.30 Pictures of the Beam Source and Beam Line Vessels during manufacturing and verifications.

Furthermore the schedule of VV procurement has been discussed and optimized for proper integration with all the other MITICA installation activities on-site.

Manufacturing and installation of Beam Source Vessel – one of the two parts in which the vessel is divided - are on the critical line for MITICA assembly and tests schedule.

The Vessel is under manufacturing phase with high priority for Beam Source Vessel (see Fig. 2.1.30). The installation of the vessel support structure inside MITICA neutron shield is foreseen in January 2017.

On-site meetings and inspections were held in November 2016 to prepare the on-site installation activities for the vacuum vessel and relevant support structure, also involving the metrology team at Consorzio RFX for precise positioning and controls on-site, with reference to specific requirements and data targets inside MITICA Neutron Shield.

2.1.2.2 MITICA beam source

The design of the MITICA Beam Source was completed in middle 2015 and the tender was issued in December 2015. Support was provided to Fusion for Energy during 2016 in the evaluation of the documentation provided by the bidders. Framework contracts for phase 1 of the procurement were signed by Fusion for Energy in July 2016 with three companies and the kick of meeting was held in August 2016. The procurement strategy decided by Fusion for Energy consists in a framework contract divided in three specific stages: stage 1 is the baseline design review, stage 2 is the MITICA Beam Source procurement and stage 3 is ITER Beam Source procurement. Stage 1 involves three companies in parallel, in charge for the revision of the design details, 3D CAD model, 2D drawings and the technical specifications. In this phase follow-up activities by RFX were carried out with several

meetings occurring, both in person at suppliers' premises and in videoconference. A large effort was required since the beginning of this contract to manage and answer to several technical queries and proposals raised in parallel by the three different suppliers, with very tight time for discussions and response preparation.

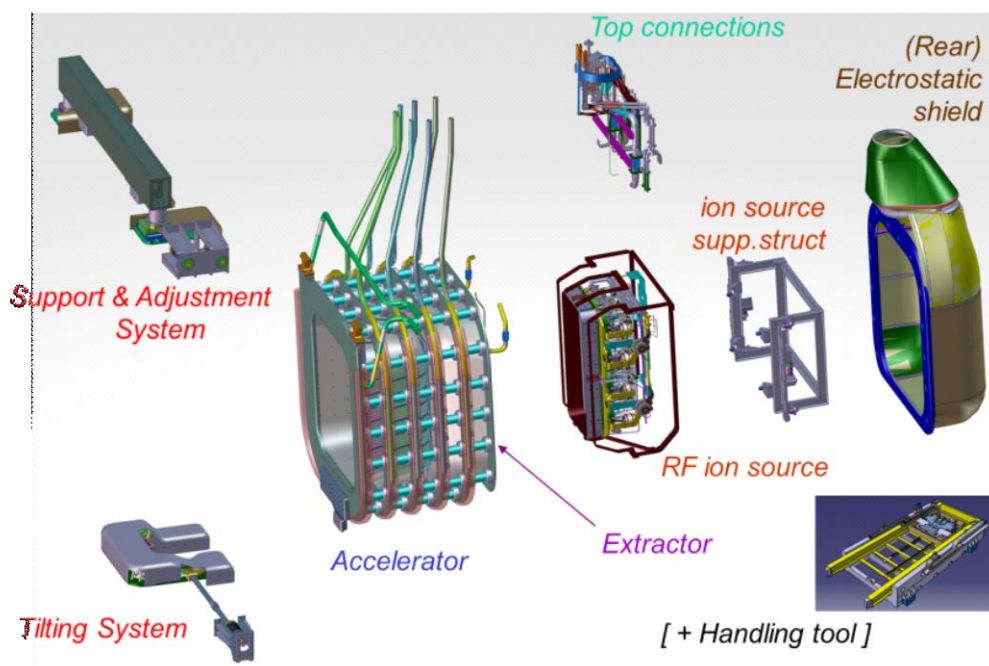


Fig. 2.1.31 Exploded view of the MITICA Beam Source under procurement.

2.1.2.3 MITICA Beam Line Components

The CAD, drawings and tech spec of Beam Line Components (BLCs) were fully completed, checked and finally sent to F4E as deliverables in the first quarter 2016. Limited further activities for finalization of the set of verifications (in particular thermo-mechanical analyses and fatigue verifications of ERID Beam Stopping Elements) were completed in middle 2016. Later, in parallel to the support of tender documents preparation, some additional design activities were necessary to revise a few details, as a consequence of the review phase of tech specs and design by Iter, Fusion for Energy and an external consultant.

A final strong effort from NBTF Team was dedicated during last quarter 2016 to prepare the full set of technical documents updated which reflects the Fusion for Energy procurement strategy, decided to be identical to the one foreseen for MITICA Beam Source.

2.1.2.4 MITICA Cryopumps

The NBTF Team activities for MITICA Cryopumps were limited in 2016 to the support for preparation of Call for Tender documentation. Checks and integration of the technical documents were performed by the NBTF Team in the first quarter 2016, mainly focusing on all the interfaces with Vessel, diagnostics and Cryogenic Plant. Additional thermal shields are necessary to limit the heat loads applied to the cryopumps edges and first pumping sections due to post accelerated electrons exiting from the Beam Source. Thermal analyses on these shields were completed by NBTF Team in middle 2016.

A specific procurement contract was launched in 2016 by F4E for “The design, the prototyping and the manufacturing of Johnston Couplings for the MITICA Cryopump and cryoplant”. These are connection elements between Cryopumps and Cryogenic Plant, to be specifically customized for this application. After a negotiation and Call for Tender phase lasting about five months the contract for Johnston couplings procurement was finally awarded in December 2016.

2.1.2.5 MITICA Cryogenic Plant

The main functions of the Cryogenic Plant for MITICA experiment are:

- to produce supercritical Helium (ScHe) at 4.6 K and gaseous Helium (GHe) at 81 K and to feed these cryogens to the cryopump placed inside the MITICA Vacuum Vessel;
- to supply the needed refrigeration power to remove the heat loads on the Cryopump during different experimental scenarios, while maintaining the cryopump panels at the correct operational temperatures.

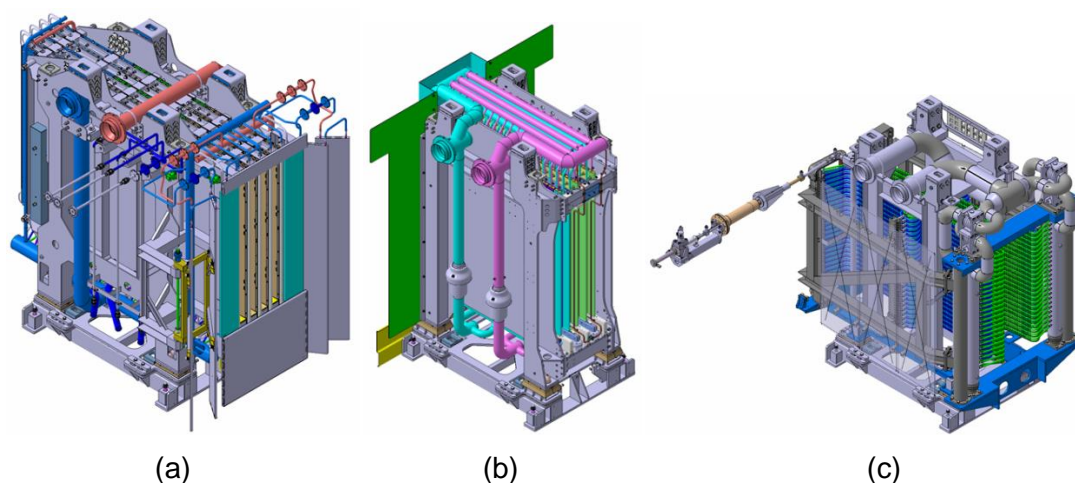


Fig. 2.1.32 Isometric views of the MITICA Beam Line Components.

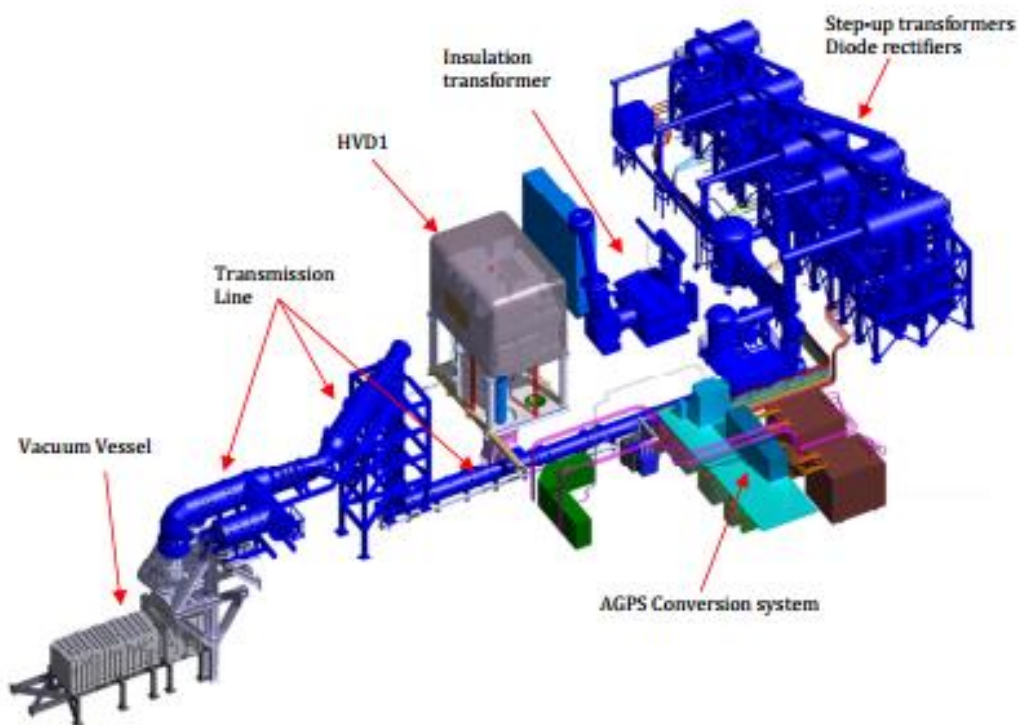


Fig. 2.1.33 - 3D view of the MITICA Power Supply system

The procurement of MITICA Cryogenic Plant was launched by F4E in September 2016 after a long negotiation phase with two bidders.

The NBTF Team gave the foreseen technical support to F4E during the negotiation, call for tender and awarding phases. Specific aspects regarding the integration of the plant on PRIMA site and relevant main design choices have been mainly addressed, transferring the information to the bidders and then to the Supplier.

The contract was finally awarded and the kick-off meeting was held on 30 September 2016.

The activities for technical follow-up of MITICA Cryogenic Plant procurement were then carried out by NBTF Team during last quarter 2016 with regular activities and frequent meetings for technical support and documents review.

Electrical and control aspects were faced since the very beginning of this contract to allow a smooth and correct development of these parts, requiring several interactions with the supplier and possible sub-suppliers during the design development phase.

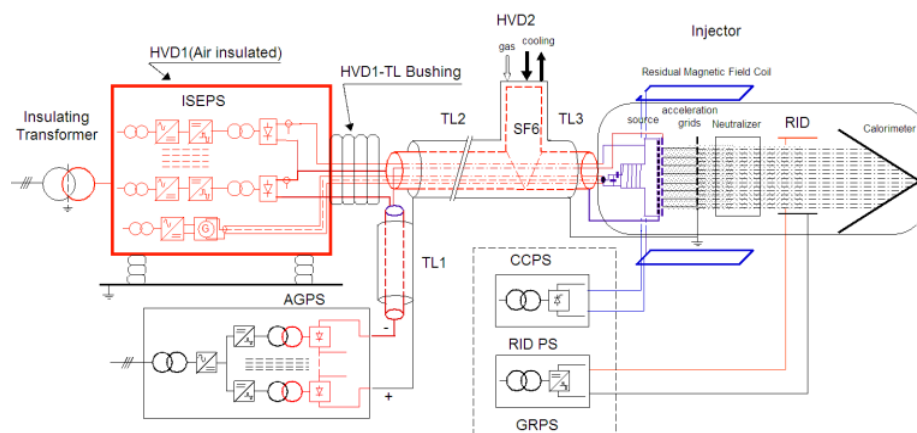


Fig. 2.1.34 Conceptual scheme of the MITICA PS and ratings of AGPS

2.1.2.6 MITICA power supply systems

Significant progress has been achieved on the procurement of the Power Supply (PS) system for MITICA. The MITICA PS system is a very complex; a 3D view and a conceptual scheme of it are given in Fig. 2.1.33 and Fig. 2.1.34 respectively. The main subsystems are:

- the Acceleration Grid Power Supply (AGPS) producing the 1MV dc voltage, in five stages, 200kV each, to accelerate the ion beam. AGPS is divided into two parts: the AGPS Conversion system (AGPS-CS) and the AGPS DC Generator (AGPS-DCG).
- the Ion Source PS to feed the Ion Source, similar to the one for SPIDER ISEPS (see 2.1.1.5)
- the Residual Ion Dump PS feeding the electric panel of the E-RID.

ISEPS and AGPS PS are connected to the loads inside the vacuum vessel through a special High Voltage SF₆ gas insulated Transmission Line (TL), 100m long.

The HV components, including step-up transformers and diode rectifiers of AGPS, TL and 1 MV insulating transformer of ISEPS, are provided by JADA (parts in blue in Fig. 2.1.34) all the other PS components by F4E.

Ion Source and Extraction Power Supply system (ISEPS)

In 2016, the activity was limited to the ISEPS design revision, based on the findings from the commissioning and acceptance tests of the ISEPS for SPIDER. Effort was devoted to further explore the possibility to implement a solution based on solid state technology instead of tetrods for the RF generators, but contractual constraints force F4E to prevent in proceeding to this direction.

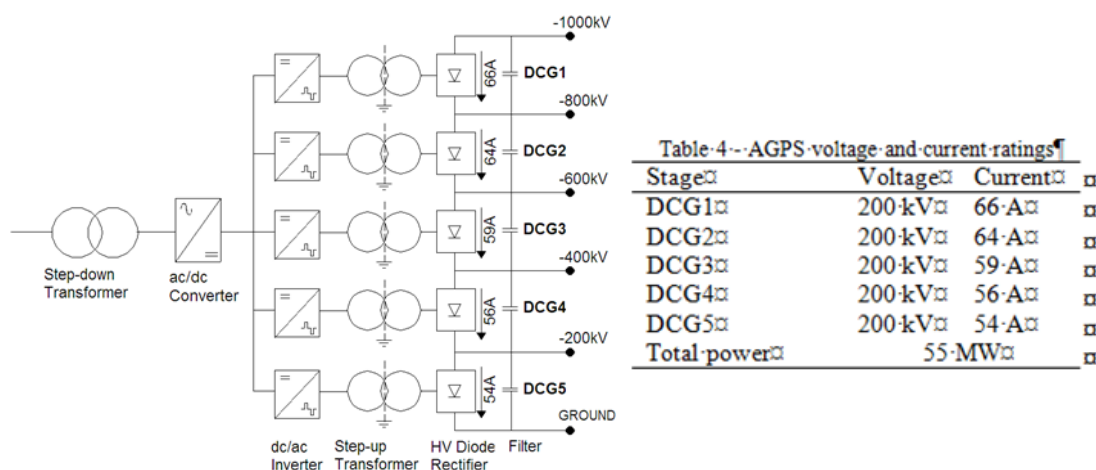


Fig. 2.1.35 AGPS conceptual scheme

Acceleration Grid Power Supply (AGPS)

The AGPS is a special conversion system feeding around 56 MW at -1MV dc to the acceleration grids, and able to interrupt the power delivery in some tens of microseconds in case of grid breakdown, which is a condition expected to occur rather frequently during a pulse. The ITER AGPS reference scheme, shown in Fig. 2.1.35 consists of an ac/dc stage feeding five three-phase inverters, each connected to a step-up transformer feeding a diode rectifier and a DC filter. The rectifiers are connected in series at the output side to obtain the nominal acceleration voltage of -1 MV dc, with availability of the intermediate potentials.

Acceleration Grid Power Supply Conversion system (AGPS-CS)

The AGPS-CS is the low voltage conversion system part of the power supply and includes the step-down transformer, the ac/dc converter and the dc/ac inverters (left side of the scheme in Fig. 2.1.35) and the control system. The activity in 2016 focused on the close monitoring of the manufacturer working on the detailed design of the AGPS-CS. During this development phase, particular attention was addressed to the most critical components, the Neutral Point Clamped (NPC) inverters, based on 6.5 kV Integrated Gate Commutated Thyristors (IGCTs), which must comply with severe conditions in case of internal faults, due to the large amount of energy stored in the system¹⁸. The demanding requirements in terms of power and dynamic

¹⁸ L. Zanotto et al., “Final design of the Acceleration Grid Power Supply Conversion System of the MITICA Neutral Beam Injector”, presented at 29th SOFT, Sep. 2016 and submitted for publication in FED.

performances, called for a custom design of the AGPS-CS. R&D activities, with respect to presently available industrial solutions, have been necessary especially on the NPC inverters. In particular, the special requirements more impacting on the design are the high voltage and current ratings and the need of quickly cut-off the power in case of breakdowns, in order to avoid damages to the acceleration grids. Since the breakdown is equivalent to a short-

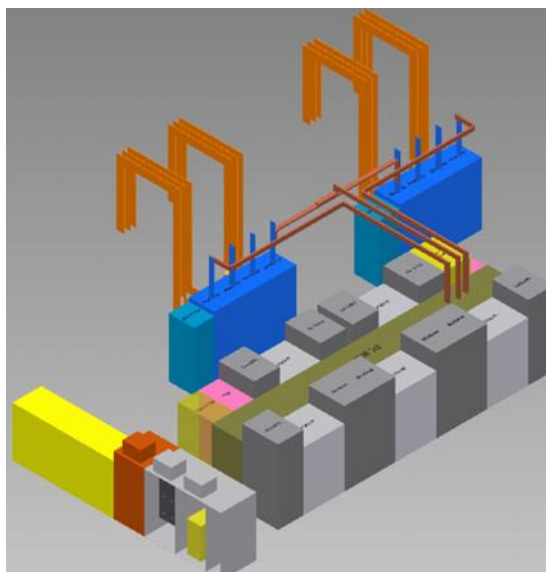


Fig. 2.1.36 Layout of the AGPS-CS

circuit of the load, the inverter switches have been designed to turn-off a high current (about 6kA) within short times (less than 150 μ s). The development of the detailed design has been continuously monitored by the NBTF Team; specific analyses and numerical simulations were in particular carried out to evaluate different options to protect the inverters in case of internal faults and for verifying the final choice proposed by the supplier. The definition of AGPS-CS control system architecture was another design task requiring a huge amount of joint work to help the supplier in understanding the specific functional and interface requirements of an application so different from the industrial ones. Further work was also devoted to the assessment of the interfaces, in particular those with AGPS-DCG, including the issue related to the signal transmission for the step-up transformers protection. The layout of the system in the MITICA facility is shown in Fig. 2.1.36; step-down transformers and cable trays have not been represented for the sake of clarity. The group of inverter cubicles is colored in grey. The ac/dc converter cubicles are shown in blue; two groups, each with two 6-pulse rectifier units are connected in series through dc busbars. The ac busbars from the step-down transformers (installed outdoor) comes from a penetration into the walls placed at the top of the hall.

Acceleration Grid Power Supply – DC Generator (AGPS-DCG)

The delivery on Site of JADA HV components started in December 2015 with the first three step-up transformers: DCG5 (-200kV), DCG4 (-400kV) and DCG3 (-600kV). In June 2016 were delivered DCG2 (-800kV) and DCG1 (-1000kV); this challenging

installation, requiring preloading of the interested areas and special solutions for the alignment of the parts, is now completed (Fig. 2.1.37).

The Transmission Line (TL), starting from initial section nearby DCGs (indicated as TL1) was installed during 2016 inside the pit (Fig. 2.1.38 left side), then the TL enters inside Building 8 (where TL is indicated as TL2 after connection with the European



Fig. 2.1.37 DC Generators (DCGs)



Fig. 2.1.38 TL in the pit indoor Building 8 - TL2 vertical section in between Building 8 (on the left) and Building 1 (on the right)

HV Bushing, collecting the cables of ISEPS hosted inside the HVD1), then it exits from Building 8 and climbs towards Building 1 supported by its tower (Fig. 2.1.38,,



Fig. 2.1.39 High Voltage *Bushing of the -1MV Insulating Transformer*

right side). The -1MV insulating transformer to feed ISEPS inside HVD1 was delivered to PRIMA site in September 2016 with the machine separated from its HV Bushing: the Bushing was assembled at site, then erected and coupled together with the transformer through a delicate operation due to the stringent mechanical tolerances of the coupling (Fig. 2.1.39).

Strong support has been given by NBTf Team to the installation of JADA components. The activities were performed under the supervision of QST (ex JAEA) laboratory of Naka and Hitachi experts, with specific contributions of Consorzio RFX to finalize solutions for different issues encountered during daily operations.

High Voltage Deck and Transmission Line

The HVD1 is a unique device, consisting of a two-floors metallic box hosting the ISEPS, operating as a Faraday cage, air insulated to ground for -1 MV dc by means of post insulators. The external size of the HVD1 is 12 m × 8 m × 10 m (L×W×H). The post insulators are around 6.5 m high. The ISEPS outputs are connected to the TL via an air to SF₆ gas HV Bushing Assembly (HVBA), installed under the HVD1. It has an overall height of about 12m and a total weight of 19t. The chosen layout foresees the installation of the HVBA in a pit underneath the HVD1, with the HVBA base

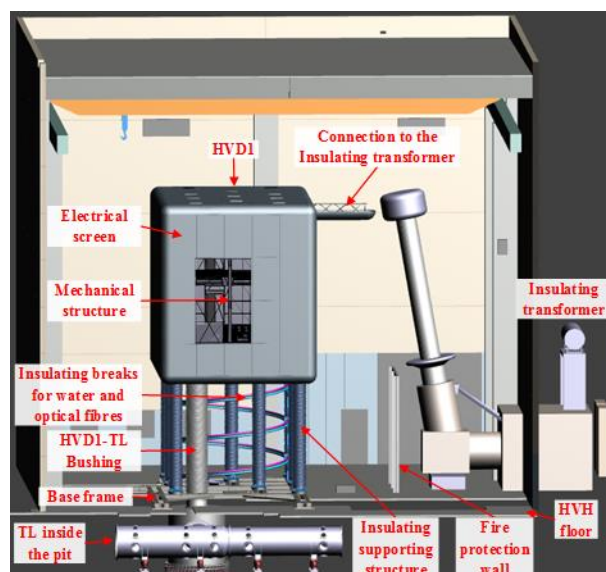


Fig. 2.1.40-. Layout of main components inside the MITICA High Voltage Hall

(Interface Box) aside of the TL. The layout of main components inside the High Voltage Hall is shown in Fig. 2.1.40.

The design phase¹⁹ of the HVD1 and HVBA, closely monitored by the NBTf Team, was completed in June 2016; special effort was devoted to the definition of the HVD1 layout and relevant interfaces with the building and with the ISEPS system; which



Fig. 2.1.41 (left) HVD1 mock-up inside HSP laboratory for Insulation tests, (right) HVBA during assembly for pressure tests

¹⁹ M. Boldrin et al., "Final design of the HV deck1 and bushing for the ITER Neutral Beam Injector", presented at 29th SOFT, Sep. 2016 and submitted for publication in FED.

has reached a sufficient assessment level. On the contrary, the challenging interface between the HVBA and the TL, delivered by JA Domestic Agency, needs to be still further discussed to solve a few open issues. In the second semester, the phases of manufacturing design and factory tests were started. A 1:5 scaled-down mock-up of the HVD1 was realized and tested at 1.2 MV for 5 hours; (Fig. 2.1.41 left side) shows the set-up for the long-duration dc voltage withstand test, executed in July. The pressure test on the HVBA (Fig. 2.1.41, right side), according to the INAIL (Italian National Authority against Worker Accident) requirements, has been carried out in June and October. In November 2016 the cantilever test, internal pressure test and tightness tests have been successfully carried out and the electric and temperature rise tests are scheduled at beginning of January 2017. The follow-up activities continued and have been particularly addressed to the monitoring of the manufacturing design, the revision of control plan and test plans, participation in factory testing and analysis of relevant results.

Ground related Power Supplies (GRPS)

The kick-off-meeting for GRPS procurement was in January 2016. The initial work of NBTf Team was mainly addressed to review the technical offer with particular effort on the layout integration with the support of 3D models. The follow-up of the contractual activities prosecuted with special attention to the layout, MV instrumentation and cooling system design. A possible route of the output cable of the Residual Ion Dump Power Supplies (RIDPS) for MITICA has been proposed by NBTf Team and included in the overall 3D model of the facility. In August, the Supplier provided a draft of the Preliminary

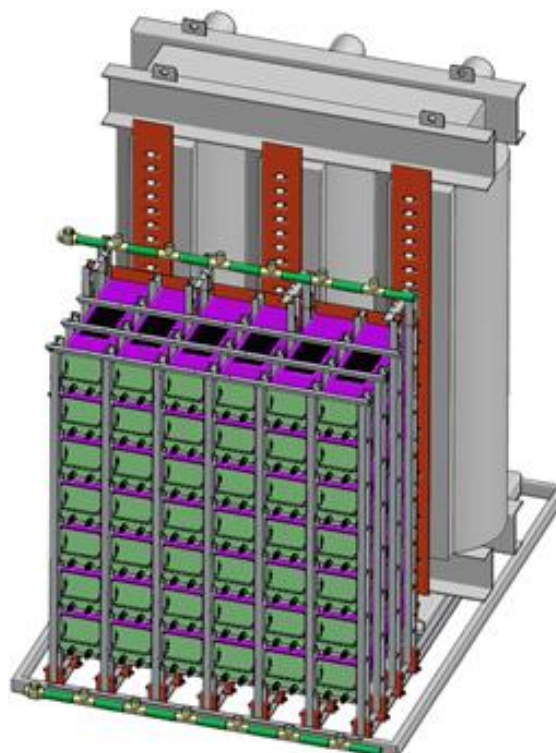


Fig. 2.1.42 RIDPS mechanical layout

First Design Report for MITICA RIDPS. The document has been deeply reviewed by NBTf Team; a set of technical clarifications have been required and obtained from

the Supplier and a list of comments (jointly with F4E) has been prepared and discussed. A paper has been written on the design of the RIDPS and presented at the SOFT conference in September²⁰.

Further checks have been performed on the auxiliaries and services available in the area where the installation is foreseen (Building 3). In November the Supplier issued the draft of the First Design Report, that was been further revised before

its submission to a review panel in view of the Design Review Meeting held on December 15th and successfully concluded with the green light for starting the manufacturing phase.



Fig. 2.1.43 - Installation of a concrete slab of the MITICA bio-shield roof

2.1.3 *PRIMA buildings and plants*

2.1.3.1 Buildings and auxiliaries

The NBTF building construction, including auxiliary conventional plants, started in September 2012, was finished in 2015. The building supplier, ITER Coop company and its subcontractors, has dismantled the yard in 2016, meanwhile, it is performing commissioning in order to release the different auxiliary systems to Consorzio RFX. In parallel, verification of all documents and certification required by the testing committee is in progress.

Further supplies in reinforced concrete have been done under different contracts to complete the Facility; in particular:

- realization and installation of MITICA bio-shield made of concrete beams,;
- the concrete slab supporting the high voltage transmission line and the core snubber;
- the realization of a fire protection concrete wall in the external area hosting the high voltage transformers.

²⁰ A. Ferro et al., "The design of the Residual Ion Dump Power Supply for ITER Neutral Beam Injector", presented at 29th SOFT, Sep. 2016 and submitted for publication in FED.

Finally, activities of adaptation of the buildings and auxiliaries have been done in order to integrate experimental plants to the site; the more significant are:

- building adaptations to host INDA's power supplies, including restoration of REIfire resistance around holes in the wall for the crossing of power cables;
- partial disassembly and reassembly of west side wall of main building in order to install the high voltage core snubber of the transmission line;
- removal and restoration of the main gate and part of its supports of the CNR research Area, in order to transit the large isolation transformer;
- installation of a foam fire-fighting system around multi-winding transformers of the SPIDER power conversion system;
- installation of mechanical fences to protect against access to the SPIDER transformer area.

2.1.3.2 Cooling Plant for SPIDER and MITICA



Fig. 2.1.44 Cooling Plant equipment installed on the roof and inside Building 2

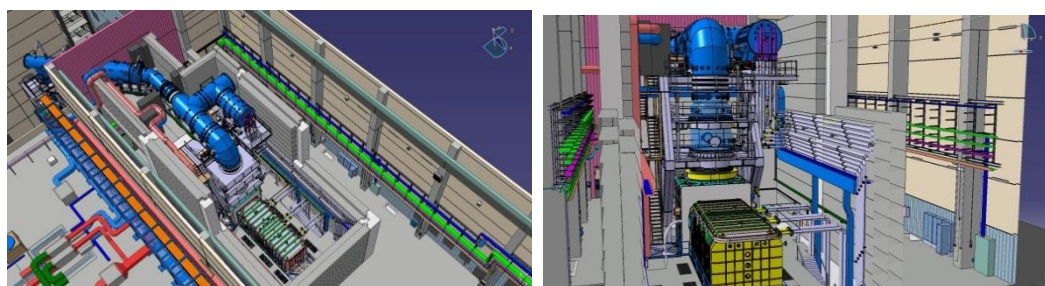


Fig. 2.1.45 CAD layout of MITICA Cooling Plant Unit inside and outside MITICA Neutron Shield

The on-site assembly of SPIDER Cooling Plant was almost completed during 2016 and NBTf Team gave continuous technical support with follow-up activities aiming to verify the correct installation, to help the Supplier's operators if needed and to solve the problems due to integration issues and compatibility with all the other on-going activities and plants on PRIMA site. Overall views of pipes, pumps, heat exchangers,

air coolers and cooling towers inside and on the roof of Building 2 are shown in Fig. 2.1.44.

The commissioning and site acceptance tests of the SPIDER Plant Unit were carried out starting from pressure tests on primary, secondary e tertiary circuits.

Power supply, monitoring and control equipment were set up and are planned to be completed within January 2017 to allow the complete commissioning and acceptance tests of SPIDER and Shared Plant Units within April 2017.

In parallel the detailed design of MITICA Plant Unit was completed by the Supplier with continuous support and verification by NBTF Team.

The full 3D CAD model of cooling circuits was continuously updated by Consorzio RFX to allow careful integration checks and to give support to the supplier in the preparation of the detailed drawings of the cooling circuits (see Fig. 2.1.45).

2.1.3.3 Vacuum, gas injection and gas storage for SPIDER and MITICA

During 2016 the activities for the procurement of the Gas and Vacuum System (GVS) continued up to the completion of the installation of the gas storage and distribution plant (namely GSD-Shared Plant Unit, which serves both SPIDER and MITICA) and of the SPIDER Plant Unit, which includes the vacuum system, the gas injection system and their control system. The NBTF team has carried out the technical follow-up during the installation and site acceptance tests; the activity is still in progress due to an issue on the cryopumps arose during the on-site test which has to be solved. In parallel to the SPIDER related activities, starting from the second half of the year the review of part of the MITICA gas injection and vacuum system detailed design has been performed aimed to start, as soon as possible in 2017, with the installation of the MITICA GVS Plant Unit and, no less important, to freeze the information necessary for the integration of buildings with conventional and experimental plants.



Fig. 2.1.46 SPIDER GVS components: pumping system inside the bioshield (left, middle) and gas injection cabinet GIS-A (right).



Fig. 2.1.47 – Medium Voltage board

2.1.3.4 Medium voltage

The NBTf experiments require a dedicated power distribution system to deliver power from the existing 400/21.6 kV substation to SPIDER and MITICA.

The procurement of the NBTf power distribution system is split in two main contracts:

- Procurement of the medium voltage lines and associated civil infrastructure
- Procurement of the medium voltage distribution boards.

The Call for Tender of the medium voltage lines procurement has been launched in September 2016 and the provisional contract awarded in November. Work under this contract is expected to commence in January 2017, with planned completion in line with the requirements of MITICA. In the meanwhile, the power needs of the SPIDER power supply and integrated commissioning phases are being met by a temporary power line from RFX-mod power distribution system. The arrangement has been in place since Autumn 2015 and has ensured smooth commissioning of the SPIDER Ion Source and Extraction Power Supplies (ISEPS) in 2016.

The contract for the medium voltage distribution board has been signed at the end of 2015 and work has started in February 2016. The Supplier's design phase has been followed closely by monitoring and reviewing all proposed materials and manufacturing drawings. The SPIDER medium voltage distribution board has been successfully factory tested at the end of July and installed on site at the beginning of

September. The auxiliary supply rectifiers, procured under the same contract, became available at end of November, which has finally allowed energisation of the SPIDER medium voltage distribution board at the beginning of December. With the SPIDER distribution board in service, electric power can be distributed to the SPIDER power supplies as required to perform the SPIDER integrated commissioning. The two remaining distribution boards supplied under the contract are less critical in terms of schedule of the NBTF project and have been successfully factory tested in December. These distribution boards, required for the commissioning of the MITICA power supplies, will become operational after the completion of the medium voltage lines installation.

2.1.3.5 PRIMA Safety

The PRIMA safety is to be considered as the set of measures, procedures, tools, hardware, software and risk analyses that, as a whole, are devoted to prevent dangerous event in the NBTF facility (see). During 2016 the design of the Central Safety System (CSS), which is the system implementing and executing the safety functions, besides the monitoring of the whole site safety, has been completed as well as the technical specifications for its procurement.

In parallel, the implementation of the SGSA (Sistema Gestione della Sicurezza Antincendio – System for the Management of the Fire Safety) has started being a prescription of the fire brigade Responsible Officer. The risks analysis upgrade has been also performed together with the definition of the actions aimed to mitigate as much as possible the identified risks; a third party has been involved to assess the SIL/SIF analysis performed by the Consorzio RFX safety team.

The interfaces between the safety system, the conventional plants (as the fire

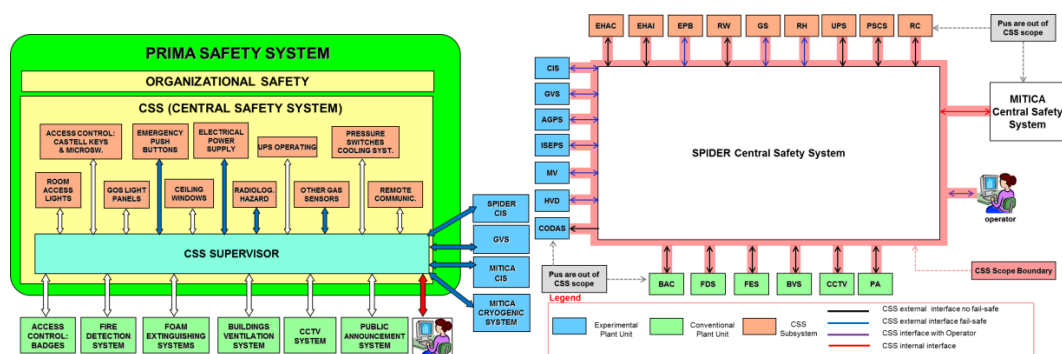


Fig. 2.1.48 Safety overall scheme for PRIMA (left) and for SPIDER CSS with interfaces (right)

system) and experimental plants have been better defined: further analyses will be necessary in the near future for the integration of the upcoming plant procurements (as the cryoplant) for which only a preliminary design of the interfaces has been developed in 2016.

2.1.4 *Host Supporting Activities*

During 2016 significant resources were invested on the activities for construction supervision and coordination, both concerning buildings construction completion with their auxiliary systems and the installation of the experimental plants.

Particular effort was required to manage interfaces between buildings and experimental plants: in fact, most of the latter are now fully assembled and tested or in advanced procurement phase. Also the management of the interfaces between plants themselves required large effort: specifically to this end the interface management structure, run by RFX personnel, worked in a coordinate way with the aim of reducing as much as possible clashes during installation of plants and to be able to define in real-time the modifications required in any of the plants.

The support to Fusion for Energy and the other Domestic Agencies for the management of the Construction-Erection All Risks insurance contract for the NBTF, activated middle 2014 and directly managed by Consorzio RFX, continued.

The NBTF-site management, with reference to Titolo IV of D.Lgs. 81/08 (Health and Safety on site), whose structure had been set up through the Implementation Agreement, continued in 2016: the Responsible of Work and the Safety Coordinator continuously monitored and periodically reported the state of the site. Significant resources were spent to assist F4E, in particular, by the Safety Coordinator who is in charge for the issue of all the Plans for Safety and Coordination (called PSC documents), being the latter an essential part for both the procurement call for tenders and contracts management. RFX personnel (contract Liaison Officer-LO and Deputy Liaison Officer-DLO) closely collaborated with the Safety Coordinator to this end.

With the support of the Coordinator of the Directors of Works (called CDL) the baseline schedule for MITICA on-site activities was prepared and discussed among Consorzio RFX and all involved Domestic Agencies during the second half of the year: it has not been frozen yet because of uncertainties on some procurement contracts. Furthermore, as a coordination method, 44 weekly Site Progress Coordination Meeting (SPCM) have been held, and the minutes distributed and uploaded in F4E IDM.

Several site inspections were performed by nearly all of the Companies and Domestic Agencies that were operating.

General follow up activities were performed for all the companies working on site and all the companies related to the Balance of Plant procurements. Further working activities come from the companies involved into the three signed Framework Contracts (CODAS-Interlock-Safety, Diagnostics, Assembly).

A very large effort has been given to INDA and its suppliers by the NBTF team concerning the SPIDER AGPS installation works: in particular, the interactions with companies involved in the materials transportation and downloading required a strong support up to the on-site download and positioning of several components (both inside building and outdoor).

As for the Licence to operate the two experiments:

- for SPIDER the licence (Nulla Osta) category A (art.28 D.Lgs.230/95 e s.m.i.) arrived in November 2015 with some prescriptions. The latter were discussed with the local Fire Brigades officer and comments have been sent back within 30 days to the Ministry of Economic Development (“Ministero dello Sviluppo Economico”), as required in the “Nulla Osta” letter. Following this, the final “Nulla Osta” with prescriptions for SPIDER has been obtained on 15/07/2016 allowing the operation of the test bed.
- for MITICA the preparation of all the necessary documents to be sent to the Italian Authorities progressed, with priority given to the radioprotection technical report that is now almost finalized.

Furthermore, metrology on-site activities were performed mainly devoted to the definition of the SPIDER, MITICA and PRIMA networks. CAD-related metrological activities, complementary to the on-site ones, have been also carried out. The full metrology survey of the PRIMA site areas has been completed preparing, for example, the information (absolute coordinate system, reference coordinate systems and reference fiducial points) to be given to the companies “as reference” or “starting point” for the installation/positioning of different components.

Periodical measurements of the positions of the fiducial points were performed to check the motion of the buildings both during their settlement period and during preloading phase (as for transformers areas). In addition, Consorzio RFX metrology team gave large and frequent support to the personnel of the main contractors in charge for metrology activities, or performed activities on behalf of them.

2.1.5 RFR&D

The main RF R&D activity is the characterization of dielectric strength of low pressure gasses when subjected to RF electric field, with the final aim of the verification of the electrical insulation design of the RF coils of the drivers of SPIDER and MITICA.

The operating conditions of the ion source coils are reproduced in a dedicated test facility called High Voltage Radio Frequency Test Facility (HVRFTF) in terms of voltage (magnitude and frequency), gas species, pressure, materials.

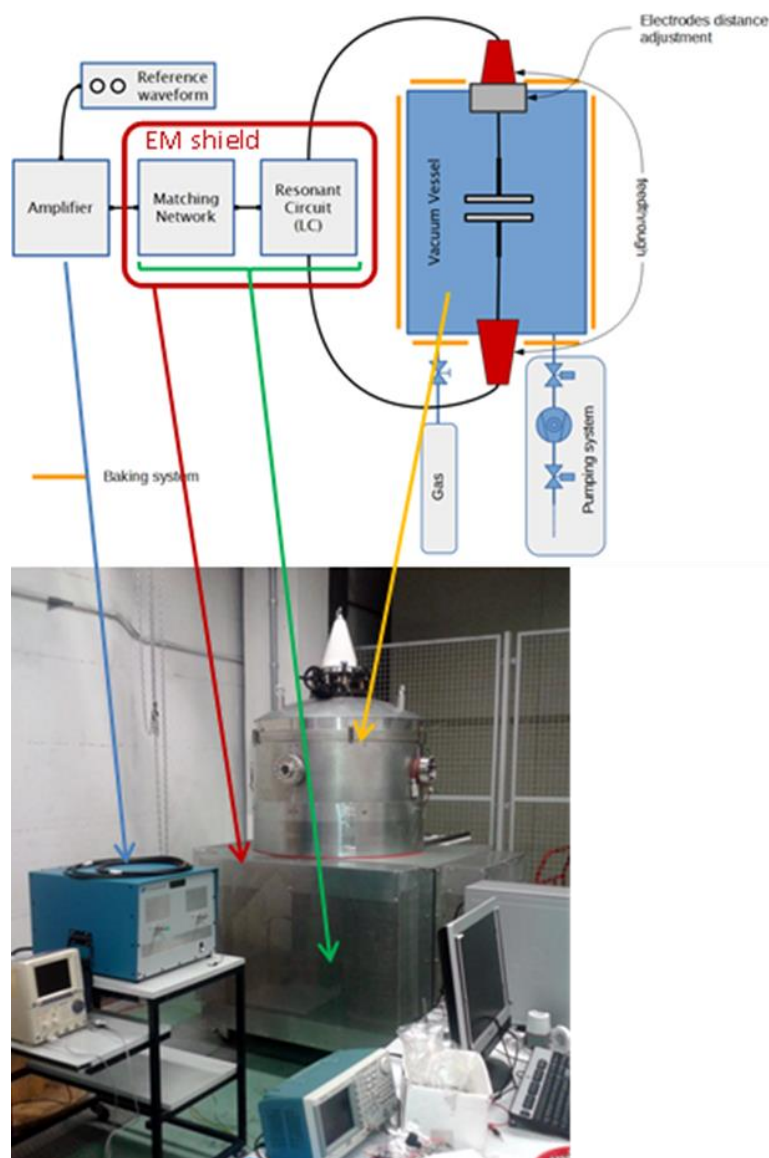


Fig. 2.1.49 Final set up of the High Voltage Radio Frequency Test Facility (HVRFTF)

During 2016 the setup of the HVRFTF proceeded with preparation of plants and systems required for its operation, in particular:

- The RF circuit used to produce the high voltage has been developed, and in particular the inductor has been designed, wound and then characterized to verify its design.
- The EM shield has been designed, installed and its effectiveness has been proved with dedicated test campaigns with an external expert.
- The pumping system has been installed on the Vacuum Vessel (VV).
- The gas injection system has been designed, procured and installed on the VV.
- The low voltage distribution system has been designed and installed.

The final set up of the HVRF (Fig. 2.1.49) was presented at the ²¹; the integrated commissioning was successfully performed in September with the contemporary operation of the vacuum systems (pumping and gas injection) and the RF circuit able to reach 9,5 kV. After, the first commissioning tests were performed with Argon from 10-5 mbar to 10-2 mbar and first Paschen curve was derived. A main issue was found: the discharge was not between electrodes but between the high voltage electrode and the Vacuum Vessel. A possible solution has been identified and will be tested in 2017.

2.1.6 Development of flux-gate magnetic sensor

The development of a radiation-hard magnetic sensors suitable to be installed in the neutral beam injector area of ITER for the feedback control of the magnetic field compensating coils (ACCC) has been continued, with additional experimental activities. The sensor is based on the well know flux-gate concept (Fig. 2.1.50), however, it is designed to provide a measurement range about one order of magnitude larger than the commercial flux-gate sensors.

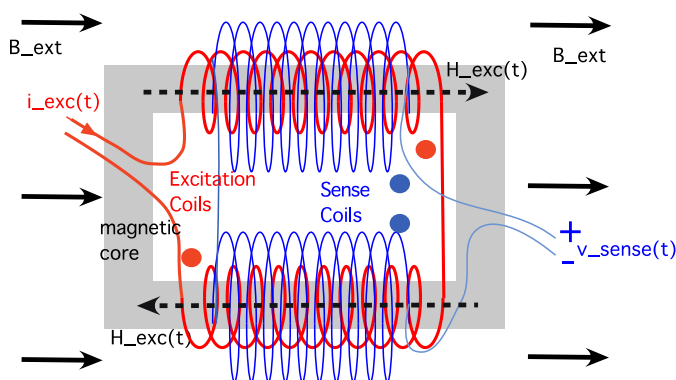


Fig. 2.1.50 conceptual scheme of a flux-gate sensor

..

²¹ A. Maistrello et al., "High Voltage Radio Frequency Test Facility for the characterization of the dielectric strength in vacuum of RF drivers for Neutral Beam Injectors Ion Sources", presented at the 2016 IEEE Power Modulator and High Voltage Conference.

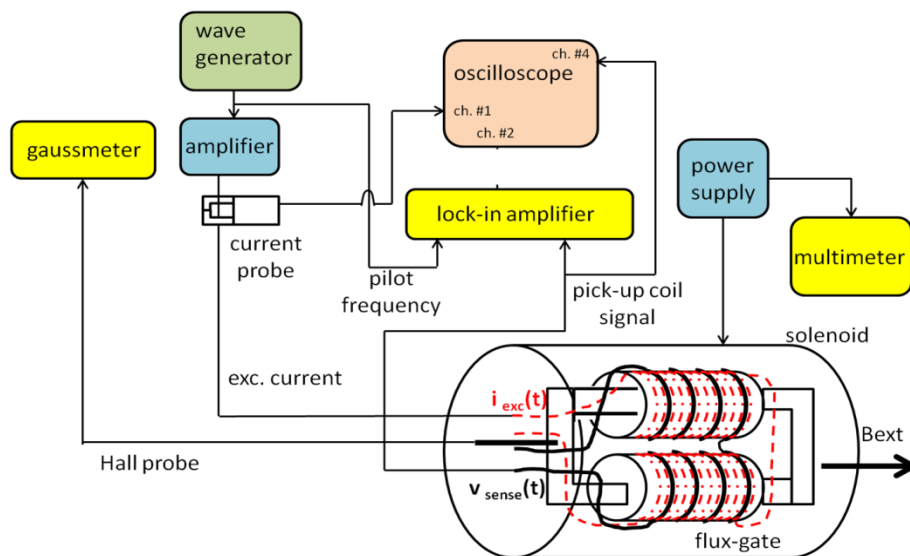


Fig. 2.1.51 scheme and experimental setup for the characterization of the flux gate sensor prototype

The experiments have been carried out using the same prototype built by Consorzio RFX during 2015, however in a new measurement set-up, with new reference gaussmeter and a new lock-in amplifier (Fig. 2.1.51).

The results have shown that the sensor output can be affected by a non-negligible measurement offset under some conditions. However, a procedure for the compensation of this offset has been developed and tested successfully. The delay time necessary for the completion of this procedure could marginally affect the

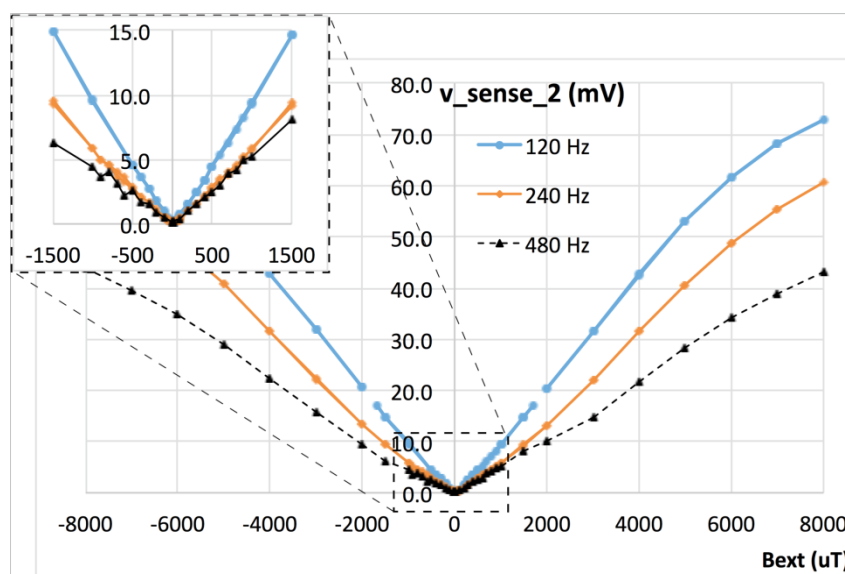


Fig. 2.1.52 flux-gate sensor output voltage v_{sense_2} as a function of the externally applied magnetic field B_{ext} , for 3 different operating frequencies.

measurement rate of the sensor, but this seems to be acceptable with respect to the required bandwidth

If the compensation procedure is applied, the sensor behaviour appears to be very satisfactory, the calibration curves are linear until ~5 mT and anyway regular up to over 8 mT, as shown in Fig. 2.1.52. The calibration curves are very well repeatable (within less than 0.1 mV), corresponding to a measurement accuracy of about 10 μ T. The sensor sensitivity is of the order of about 10 mV/mT, at 120 Hz.

Therefore the Flux-gate sensors are a good candidate of magnetic sensors for measuring the field inside the NBI vessel and feedback controlling the ACCC, because their high simplicity, accuracy and intrinsic radiation hardness.

The prototype sensor development activities are described in a paper by M. Ichikawa presented at SOFT2016 [22].

2.2 ITER NBI Physics activities

The numerical simulations of the beam physics in the accelerator and along the beam line continued in 2016 in parallel to the construction of the SPIDER and MITICA beam sources. The activities were dedicated to the benchmark of the codes versus experimental data and to the analysis of the expected conditions at the beginning of SPIDER operations particularly in terms of the diagnostic performances of the STRIKE calorimeter and of SPIDER beam dump. The benchmark of the codes is dealt with in section 3.4. Concerning the expected early operation of SPIDER ²³, using the beam simulations performed in the past for the expected first operational conditions of SPIDER at perveance match without caesium (10% of the nominal current and correspondingly 22.4 keV particle energy), the calculated heat load was used as input for a COMSOL heat transfer finite element model to determine the temperature map measured by the STRIKE calorimeter in correspondence to the different segments of the acceleration grids. From such calculations beamlets are expected to be clearly distinguishable and the low temperatures involved suggest that the duty cycle may be enlarged. A finite element code was customized in order to allow non-linear analyses in flow boiling conditions and examine the sensitivity of the SPIDER beam dump as diagnostic device. It was found that reducing the mass

²² G. Chitarin, D. Aprile, M. Brombin, N. Marconato, L. Svensson, "Feasibility study of a flux-gate magnetic field sensor suitable for ITER Neutral Beam Injectors" presented at 29th SOFT 2016, Sept 5-9 2016, Prague, Czech Republic, Proc. to be published in Fus Eng. and Design

²³ G. Serianni et al., Neutralisation and transport of negative ion beams: physics and diagnostics, to be submitted to New J. Phys..

flow rate for one panel is expected to allow a significant improvement of the beamlet detection capabilities of the beam dump.

The development of handy codes will be investigated for the everyday use in the control room during SPIDER experimental campaigns. These codes must be validated by comparison with experimental measurements. Comparison of the numerical codes with experimental data allows to identify possible areas of improvement, like the effect of possible non-uniformities of the current density at the meniscus, as discussed in section 3.4. Numerical simulations were devoted to prepare a model of the caesium atoms exiting a caesium oven and a model of the flow measurement by a surface ionization detector²⁴. The caesium flow is simulated as atoms pass through a controlled valve, the evaporation ducts and injection nozzle, and the angular distribution of the emitted cesium atoms was obtained. The atom flow hitting the ionization filament and the trajectories of emitted cesium ions were calculated to identify the fraction of charges collected by the collector filament. The models were applied to the cesium oven developed for the ITER neutral beam injector.

The measurement of the plasma potential and of the energy spectrum of secondary particles in the drift region of a negative ion beam offers an insight into beam-induced plasma formation and beam transport in low pressure gasses. The simulation of the properties of the plasma was performed for NIO1 and for the NIFS test stand and represented the basis for the design of a 4-grids Retarding Field Energy Analyzer²⁵, which was later built and operated in the NIFS test stand together with the mini-STRIKE.

2.3 ITER Core Thomson Scattering

The activity of RFX in the design of the ITER core Thomson Scattering (TS) system continued in 2016. At first a set of simulations aimed to assess the performance of the new design, based on the conventional approach, has been carried out in an informal collaboration with Iter Organization. The purpose of this simulation was to contribute to solve some of the chits raised in the 2015 Conceptual Design Review (CDR). These simulations included a study of polarimetric Thomson scattering as a

²⁴ E. Sartori et al., Modeling the cesium flow from a dispenser oven and the measurement by a surface ionization detector, under preparation.

²⁵ E. Sartori et al., Development of an Energy Analyzer as Diagnostic of Beam-Generated Plasma in Negative Ion Beam Systems, 5th International Symposium on Negative Ions, Beams and Sources 12-16 September 2016, Oxford, UK, poster MonP3; submitted to AIP Conf. Proc..

possible technique to overcome the limitations of the TS system in the high T_e range^{26,27,28} and the development of a detailed model for the calculation of the plasma light background based on realistic plasma profiles. Then in June 2016 Iter Organization issued a call for an update of the core plasma Thomson scattering design (SQES83) to which Consorzio RFX answered positively and a contract was awarded to RFX. Objective of this contract, whose duration is one year, is to review and advance, together with the TS teams of CCFE (UK) and IPP Prague (CR), the design of the ITER core Thomson scattering system (CPTS). Main responsibilities of RFX team in this contract are the calibration methods and the simulations of the system performance. The work for this contract started in July 2016 and continued throughout the year, and will end in June 2017. In addition in 2016 we have carried out a test in RFX of a self-calibrating, dual laser, TS technique. This method is of high interest for ITER and so far was never tested experimentally. Although in RFX the conditions for the application of this advanced technique were not optimal, the experiment was carried out successfully and gave meaningful results²⁹. Finally, during the last JET campaign, in collaboration with the TS team of JET, an experiment has been carried out to measure the depolarization effect of TS radiation in the HRTS system of JET. Data have been collected in a set of high TE JET discharges and are presently under analysis.

²⁶ L. Giudicotti, M. Bassan, F.P. Orsitto, R. Pasqualotto, K. Kempenaars and J. Flanagan, "Conceptual design of a polarimetric Thomson scattering diagnostic in ITER", JINST 11 C01071 (2016).

²⁷ L. Giudicotti, R. Pasqualotto and O. McCormack, "Extending the T_e range of the ITER core Thomson scattering system by detection of the unpolarized scattering radiation", Contributed paper to HTPD, the High Temperature Plasma Diagnostics, Madison, 5 - 9 June, 2016

²⁸ L. Giudicotti and R. Pasqualotto "A polarimetric Thomson scattering diagnostic in ITER", Communication to the 102 SIF Conference, 26-30 September, 2016

²⁹ O. McCormack, L. Giudicotti, A. Fassina and R. Pasqualotto, "Dual-laser, self-calibrating Thomson scattering measurements in RFX-mod". Submitted to Plasma Physics and Controlled Fusion

3 EUROfusion Programme

3.1 RFX-mod: experimental, modeling activities and upgrades

In January 2016 an international panel established in order to scientifically evaluate the RFX-mod upgrade proposal met in Padova to discuss the scientific motivations and perspectives of the proposed modifications (the upgraded RFX-mod device will be dubbed RFX-mod2 in the following). These were described in a specific document formerly distributed among the panel members. After requiring some additional clarification to the document, the panel produced an extremely positive report. The conclusions of such document are here reported:

“In summary, the Panel enthusiastically endorses the proposed upgrades. There is a high probability that the upgrades will create substantially improved plasma conditions that are important for the assessment of the RFP as well as for the development of fusion science more broadly. The RFX program has demonstrated scientific leadership in a number of research topics. This is evidenced by a strong and consistent publication record that includes papers in the world’s most prominent journals for physics and fusion research. The plan and preliminary designs for the upgrades appear sound, but given the limits of our panel’s expertise, we recommend an independent external technical review by suitable experts. We make this recommendation only to ensure that the upgrade proceeds robustly and expeditiously. The panel would like to thank the RFX team for organizing our meeting and generous hospitality during our short visit. We look forward to exciting new research enabled by the upgrade.”

In 2016 the design activities progressed (sec. 3.1.6) in view of the technical review suggested by the scientific panel.

3.1.1 *Analysis of experiments in RFP configuration*

3.1.1.1 Plasma-wall interaction

In the last experimental campaigns, different tiles were exposed to the plasma and tested by power loads up to tens of MW/m². In 2016, after the extraction, the behaviour of graphite with various shaping and thermal conductivity properties, with and without the application of tungsten films has been investigated³⁰. The power load has been reconstructed by a dedicated code combined with the measurements performed by an IR camera. The microscopic analysis of the retrieved samples has

³⁰ A. Canton et al., 43rd EPS Conference on Plasma Physics, P5.012, July 2016, Leuven, Belgium

shown that thin films (1-3 μm) of tungsten over the same high conductivity graphite with properly smoothed surface can survive to the worst PWI conditions. An example is shown in Fig. 3.1.1, where no damage of the W coating is visible. Moreover, the damages were strongly reduced in tiles whose shape features a reduced flat central surface connected by rounded surface to the edges (which is a smoother shaping with respect to the RFX-mod tiles). These results are part of the decision for the wall material in RFX-mod2.

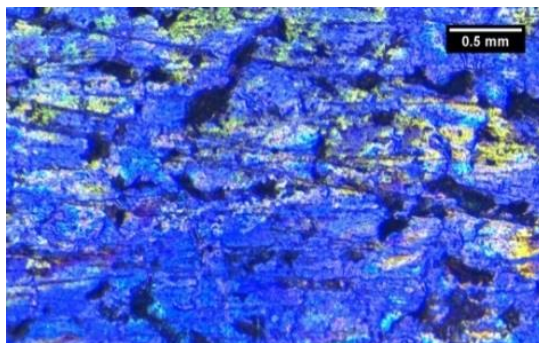


Fig. 3.1.1 Microscopic analysis of a 1 μm tungsten film on a high conductivity graphite tile exposed to RFX-mod plasmas. No damage of the metal film is seen.

For the first time in RFX-mod, the edge transport has been analyzed and modelled exploiting thermography measurements combined with the edge fluid code SOLEDGE2D-EIRENE³¹. The measurements confirmed the presence of increased heat flux in the direction of the electron drift side, in agreement with previous RFP findings, with the novelty of the identification of a density threshold above which the asymmetry disappears, comparable to that observed for the achievement of SHAx states. The modelling has shown that transport is drastically reduced in the SOL region compared to the edge one. The resulting very short heat flux decay length has important consequences on the PWI, increasing the peak power on edges of wall tiles as mentioned before

3.1.1.2 Transport barriers and isotopic effect

Data analysis of helical states, where thermal transport barriers (ITBs) develop and high temperature gradients encompass a hot plasma core, have been advanced. It has been found that the width of the ITBs features an increasing trend with the dominant mode amplitude. Such a trend is continuous and smooth. A key role on the barrier radial extension is played by the level of increased stabilization of secondary modes occurring as the dominant one increases [R. Lorenzini et al., Phys. rev. Lett. 116,185002 (2016)]

Studies on the isotopic effect in 3D plasmas have also progressed, aiming at contributing to the understanding of this still unresolved issue by the exploration of a

³¹ P. Innocente et al., P454, 22nd PSI Conference, June 2016, Rome, Italy, to be published in Jour. Nucl. Mat.

space of plasma parameters complementary to those of tokamaks and stellarators. In RFX-mod first comparisons of hydrogen and deuterium plasmas showed a clear isotope effect on the magnetohydrodynamic properties of RFP plasmas: increasing the mass of the main gas (Mi) induces a stabilizing effect on tearing modes, resulting in longer SHAx states, more monochromatic and more resilient to weak sawtoothing³². The measured electron temperature is higher in deuterium than in hydrogen in a significant fraction of the plasma volume ($r/a < 0.9$) and the energy confinement time scales $\sim Mi^{0.3}$, while the particle confinement time shows a scaling $\sim Mi^{0.45}$. Such effect on confinement has been mainly associated to the mitigation of transport at the edge, internally to the scrape-off layer where long range correlations have been detected^{33,34}.

In 2016 the effect of Mi in presence of 3D magnetic fields has been characterized on a statistical basis. Only a slight effect of such perturbations has been observed on the confinement properties, as shown in Fig. 3.1.2, where the core electron temperature T_e and the estimated energy confinement time τ_E are shown as a function of the normalized amplitude of the applied 3D field for the two isotopes. Such behaviour has been numerically investigated by the Hamiltonian guiding center code ORBIT, with attention to the magnetic topology in plasmas with and without the application of 3D fields on deuterium and hydrogen test ions transport. In agreement with experimental estimates, numerical studies show that particle transport is reduced in deuterium plasmas but not significantly affected by the application of helical boundary conditions.

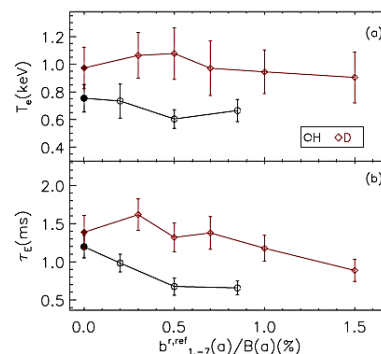


Fig. 3.1.2 (a) Average core T_e vs. normalized $b_{1,-7}$ amplitude in H (black) and D (red) plasmas. (b) Average energy confinement time τ_E .

Such behaviour has been numerically investigated by the Hamiltonian guiding center code ORBIT, with attention to the magnetic topology in plasmas with and without the application of 3D fields on deuterium and hydrogen test ions transport. In agreement with experimental estimates, numerical studies show that particle transport is reduced in deuterium plasmas but not significantly affected by the application of helical boundary conditions.

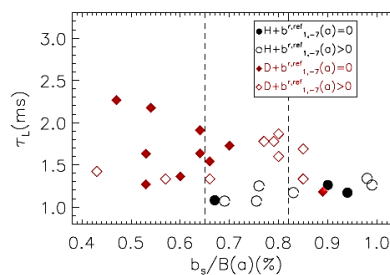


Fig. 3.1.3 Helical loss time vs. secondary mode amplitude in standard (full symbols) and induced (empty symbols) helical deuterium (red diamonds)/hydrogen (black circles) discharges

³² M.E. Puiatti et al., Nucl. Fusion **55**, 104012 (2015)
³³ R. Lorenzini et al., Nucl. Fusion **55**, 043012 (2015)
³⁴ M. Gobbin et al., Plasma Phys. Control. Fusion **57**, 095004 (2015)

This result is summarized in Fig. 3.1.3, where the estimated helical loss times are reported as a function of the normalized amplitude of the secondary modes³⁵.

3.1.1.3 Impurities

The analysis of Ne doped D₂ cryogenic pellet injection confirmed the past experimental evidence of impurity outward convection in RFX-mod helical states³⁶. Similar diffusion coefficient and outward convection resulted from the impurity transport analysis of all the impurity species, without strong dependence on mass/charge.

The 1-D collisional radiative code usually applied to interpret the impurity behavior in RFX-mod has been updated in order to deal with helical shaped plasmas, enlighting the differences between a cylindrical and a helical modeling approach. The comparison between simulations in cylindrical and helical geometry, for the typical shape and values of diffusion and convection of RFX-mod scenarios, shows a small difference between

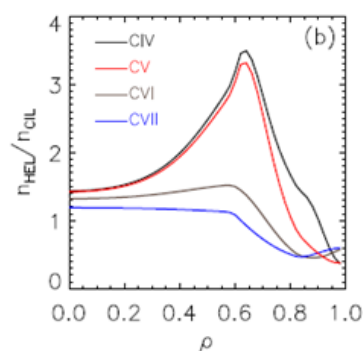


Fig. 3.1.4 ratio between carbon ion populations in helical and cylindrical geometry

carbon ion populations in the two cases, mainly affecting the ionization levels of CV and C/V whose densities increase with the helical geometry (see an example in Fig. 3.1.4). However, the slightly more penetrating impurity profile found in the helical geometry affects the reconstruction of SXR brightnesses, and should therefore be taken into account³⁷.

3.1.1.4 Edge studies and turbulence

Detailed studies, deepening the description of the kinetic response of the edge plasma to 3D magnetic fields with different helicities, have been performed, both in RFP and Tokamak configuration (see sec. 3.1.2.2 for the latter). It has been found that in the presence of rotating Magnetic Perturbations (MP), the profiles of electrostatic particle and energy flux mainly follow the symmetry of the dominant imposed perturbation. The electrostatic turbulence induced flux is observed to be modulated by the underlying topology, with an enhancement close to the O-point and

³⁵ M. Zuin et al., 26th IAEA Fusion Energy Conference Kyoto, Japan 17–22 October 2016, paper OV/P-2, submitted to Nucl. Fus.

³⁶ T.Barbui et al., Plasma Phys. Control. Fusion **57**, 025006 (2015)

³⁷ M. Gobbin et al., submitted to Plasma Phys. Contr. Fusion

a reduction at the X-point of the magnetic island. In terms of transport relevant k , an analysis of the spectra of the fluxes reveals that the transport contribution is due to fluctuations propagating in the electron diamagnetic drift direction peaked at $k_{\text{perp}}\rho_i \sim 0.1$ as is shown in Fig. 3.1.6, where the k -resolved spectra of the electrostatic particle flux is shown.

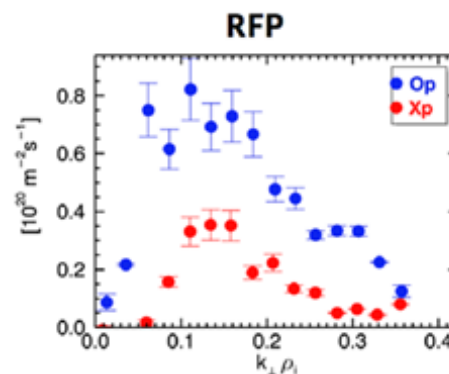


Fig. 3.1.6: k -resolved particle flux; blue and red points refer to data on O-point and X-point respectively (RFP plasmas)

Moreover, the detailed behaviour of edge floating potential V_f and electron pressure P_e along the poloidal direction in presence of different MPs has been studied exploiting measurements from the Thermal Helium Beam diagnostic (P_e) and the internal array of electrostatic sensors for the floating potential (V_f)³⁸. The considered perturbations had an $m=1$ poloidal periodicity. However, it has been found that the Connection Length at the wall of the magnetic field (L_{cw}) has a more

complex structure, and, due to the interaction of both $m=1$ and $m=0$ modes shows a non monochromatic behaviour along the poloidal angle (Fig. 3.1.5). This L_{cw} structure is responsible for the not pure $m=1$ behaviour of the plasma wall interaction of the floating potential and of the electron pressure. The floating potential and toroidal flow have been characterized along the whole poloidal angle, highlighting that their structure is a mix between $m=1$ and $m=0$; the measurements of electron

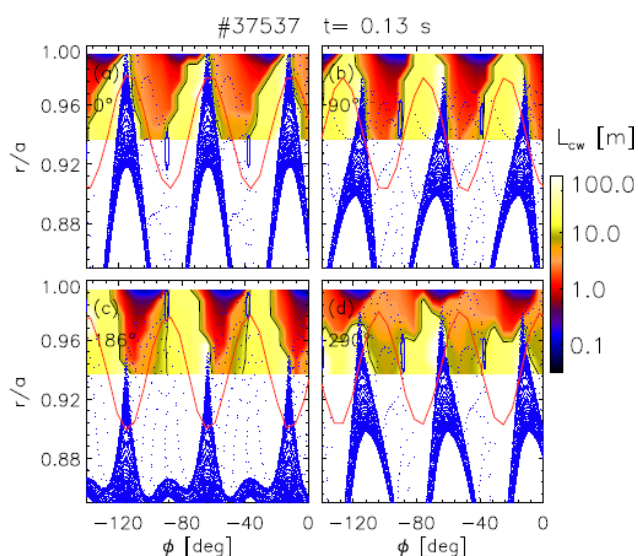


Fig. 3.1.5 Contour plot of L_{cw} as a function of the toroidal angle ϕ and radial coordinate for four poloidal angles: $\theta = 0^\circ, 90^\circ, 186^\circ, 290^\circ$. Blue points: Poincaré plot; red curve: (1,-7) component of MP. Small conserved structures at $0.92 < r/a < 0.99$ are the O-points of the $m=0$ island; large structures at $r/a < 0.92$ corresponds to the O-point of (1,-7) islands

³⁸ M. Agostini et al., 26th IAEA Fusion Energy Conference Kyoto, Japan 17–22 October 2016, paper EX/P5-310, submitted to Nucl. Fus.

pressure at $\theta = 0^\circ$ and $\theta = 90^\circ$ confirm this behaviour, together with the CCD image of the plasma wall interaction.

The characterization of transport in the RFP edge has been deepened by the application of the ORBIT code where an analytical model for the plasma potential has been implemented to analyse the ambipolar flow. It has been found that both ion and electron dominated transport regimes can exist³⁹.

Studies on the relation between particle dynamics and reconnection events, where magnetic energy is converted into kinetic one, have also progressed. The analysis shows that the current sheet observed when reconnections occur are subject to fragmentation, with an energy transfer from the largest to the smallest scales⁴⁰.

3.1.1.5 MHD control with different actuator configurations

An effort to summarize and integrate the techniques used to optimize the output magnetic field of the feedback control system has been done, in order to provide a fast, reliable and benchmarked modelling tool. In particular, the activity has been focused on the actuator-sensor decoupling and D-matrix technique aiming at reducing spurious harmonics (e.g. in presence of failed saddle coils in RFX-mod)⁴¹.

3.1.1.6 Plasma spontaneous rotation

Experiments in the last RFX-mod campaigns demonstrated the possibility to recover the tearing modes fast rotation by lowering the plasma current under a certain threshold around 120 kA, corresponding to a low enough mode amplitude⁴². The analysis of such experiments by the RFXLOCKING has shown that the feedback allows the recovery of the fast rotation with no hysteresis when reducing mode amplitude. This evidence changes the standard paradigm valid in the absence of feedback, which considers the transition from fast rotation to wall-locked condition a substantially irreversible process. Given the agreement between simulations and experiments, the code has been applied to evaluate the current threshold for mode

³⁹ G. Spizzo et al., "The electrostatic response to edge islands: a comparison between the Reversed Field Pinch and the Tokamak" invited talk at 21st EU-US Transport Task force meeting, Leysin, September 2016

⁴⁰ L. Cordero et al., 43rd EPS Conference on Plasma Physics, P5.015, July 2016, Leuven, Belgium

⁴¹ L. Pigatto et al., "Control system optimisation techniques for real-time applications in fusion plasmas: the RFX-mod experience", 20th Real Time Conference, Padova June 2016

⁴² P. Innocente et al., Nucl. Fusion **54**, 122001 (2014)

unlocking expected in RFX-mod2, which has been found to increase up to 375-625 kA⁴³.

3.1.1.7 Fast particle dynamics

Electron and ion temperatures are found to be of the same order in RFX-mod, their ratio approaching 1 at high density. However, measurements by a charge exchange NPA diagnostic show that a non Maxwellian high energy tail is present in the ion distribution function (Fig. 3.1.7). In addition, the presence of self-generated fast particle population is indicated by the observed Alfvén eigenmodes. The fast ion tails are well correlated with cyclic magnetic reconnection events: as shown in Fig. 3.1.8, at reconnection, the high energy component of flux is increased before the low energy component, thus indicating an acceleration process⁴⁴. At reconnection, an increase of DD neutron production rate, as detected by a neutron detector, is also observed. Interestingly, as clearly shown by MST device results, fast ions are well confined in the RFP⁴⁵, since the condition for island overlapping is different (milder superposition) for ion guiding centre with respect to magnetic field lines. This different behavior might be important in a reactor perspective.

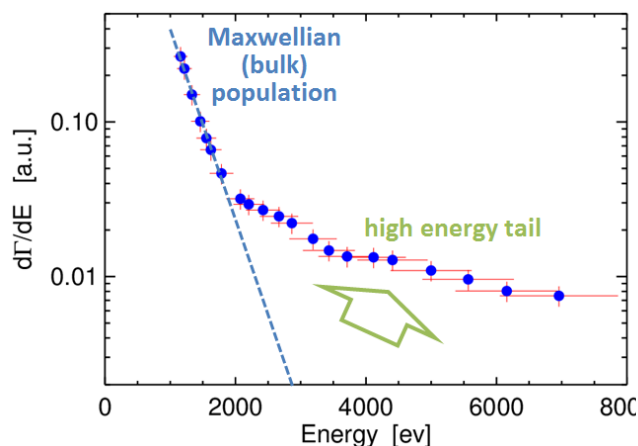


Fig. 3.1.7 Ion distribution function in RFX-mod, from charge-exchange NPA

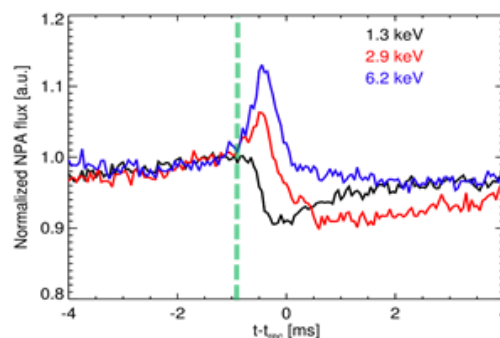


Fig. 3.1.8 Different energy flux components corresponding to a reconnection event

⁴³ M.E. Puiatti et al., 26th IAEA Fusion Energy Conference Kyoto, Japan 17–22 October 2016, paper EX/P5-23

⁴⁴ M. Zuin et al., “Neutron production and fast particle dynamics in Reversed Field Pinch Plasmas for FFH”, presented at 2nd Int. Conf. on fusion-fission sub-critical systems for waste management and safety, Frascati 26-28 October 2016

⁴⁵ J. S. Sarff et al, Nucl. Fusion **55**, 104006 (2015)

3.1.1.8 3D magnetic surface reconstruction

Helical equilibria in the RFP configuration are routinely reconstructed using V3FIT/VMEC with diagnostics information in RFX-mod ⁴⁶. In the past the MHD dynamo electric field and potential from such equilibria were never calculated. Instead in 2016 we applied to RFP plasmas a procedure developed for 3D tokamak equilibria to estimate the effective loop voltage able to produce a helical core.

Once a 3D equilibrium is available, it is possible to obtain the MHD dynamo e.m.f. by balancing Ohm's law over its helical flux surfaces. In general for the RFP (in a purely ohmic condition) one can write under stationary conditions $\mathbf{E}_{loop} - \nabla\phi = \eta\mathbf{j} - \mathbf{v} \times \mathbf{B}$, where ϕ is the electrostatic potential, \mathbf{j} the total current from V3FIT. Taking the part parallel to the magnetic field, one can obtain an equation for the potential.

The result of the computation is shown in Fig. 3.1.9, which starting from the left shows the contour plot of the potential (in Volts) over-plotted to flux surfaces. In the central panel the $\mathbf{E} \times \mathbf{B}$ velocity field produced by the interaction of the dynamo field with the magnetic field is shown, and on the right the effective V_{loop} computed by taking the flux surface average of the dynamo potential over axi-symmetric surfaces (i.e. $n=0$ loop voltage) is reported. This can be compared to the loop voltage of at least 20 V that is measured in a typical RFP discharge during helical states.

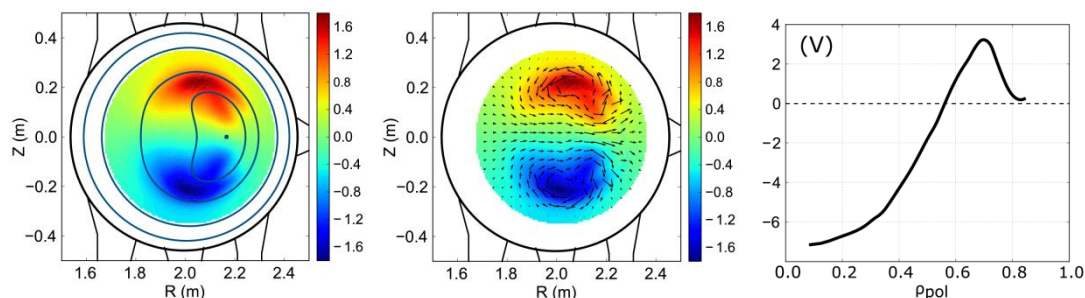


Fig. 3.1.9: electrostatic potential over flux surfaces (left), velocity field (cente) and effective V_{loop} due to MHD dynamo.

This result is well in agreement with what expected from theoretical models. It is worth mentioning that, since some approximations are adopted to treat resonances, this activity will be refined next year.

Anyway, the full 3D reconstruction by the VMEC+V3FIT code can require long computational time. An additional approach to calculate the last closed magnetic surface (LCMS) has been proposed. Such approach relies just on the information

⁴⁶ D. Terranova, L. Marrelli, J.D. Hanson, S.P. Hirshman, M. Cianciosa and P. Franz, *Nucl. Fusion* **53** (2013) 113014

coming from the magnetic diagnostic system and does not use additional information coming from the MHD model (as the equilibrium hypothesis) to obtain the solution. The approach is divided in three steps: (i) identification of an equivalent 3D plasma current; (ii) reconstruction of a set of magnetic surfaces; (iii) selection of the LCMS. The application to RFX-mod plasmas has shown a good agreement with the arising MHD modes of the device⁴⁷.

3.1.1.9 The RFP as a neutron source for a hybrid system

Studies on the advantages and issues related to the use of a RFP as a neutron source in a hybrid reactor have been recently presented at FUNFI2, in Frascati⁴⁸. In particular, assuming the temperature vs. current scaling of RFX-mod extrapolated to a 15 MA device (possible with presently available technologies) with major and minor radii twice the RFX-mod major/minor radii and under the hypothesis of half plasma volume in helical state, the fusion power and neutron production rate have been calculated. The fusion power has been estimated $\approx 19\text{MW}$, with a neutron production rate $\approx 7 \cdot 10^{18}\text{s}^{-1}$ and a neutron wall loading $\approx 0.1 \text{ MW/m}^2$. The RFP as a neutron source could work with ohmic heating only, with no need of neutral beams and with low toroidal field at the coils (i.e. without the requirement of large superconducting coils), therefore resulting in a simple, robust and relatively cheap device.

3.1.2 Analysis of experiments in Tokamak configuration

In the last part of the experimental activity the RFX-mod device has been operated in Tokamak configuration for some weeks. In the following sections data analysis from such last tokamak plasmas are summarized.

3.1.2.1 L-H transitions induced by an electrode:

Enhanced confinement regimes have been obtained exploiting a polarized graphite electrode, inserted inside the last closed flux surface (LCFS) from the bottom of the device by a manipulator. The applied voltage has been varied between -800V to +350V, in order to stimulate electric fields with both signs. Transition to improved confinement regimes were obtained both in circular and Single Null plasmas with

⁴⁷ P. Bettini et al., "3D magnetic surface reconstruction in RFX-mod", presented at 29th Symposium on Fusion Technologies, Prague 5-9 September 2016.

⁴⁸ R. Piovan et al., "The RFP as a neutron source for Fusion-fission Hybrid system: strengths and issues", presented at 2nd Int. Conf. on fusion-fission sub-critical systems for waste management and safety, Frascati 26-28 October 2016

negative polarization of the electrode⁴⁹. An example is shown in Fig. 3.1.10: when the applied voltage exceeds a threshold, the electron density increases without any puffing applied, the H α signal decreases and the toroidal rotation becomes faster. The transition phases can also be characterized by an oscillating behavior between low and high confinement: such oscillations seem to be associated to the onset of

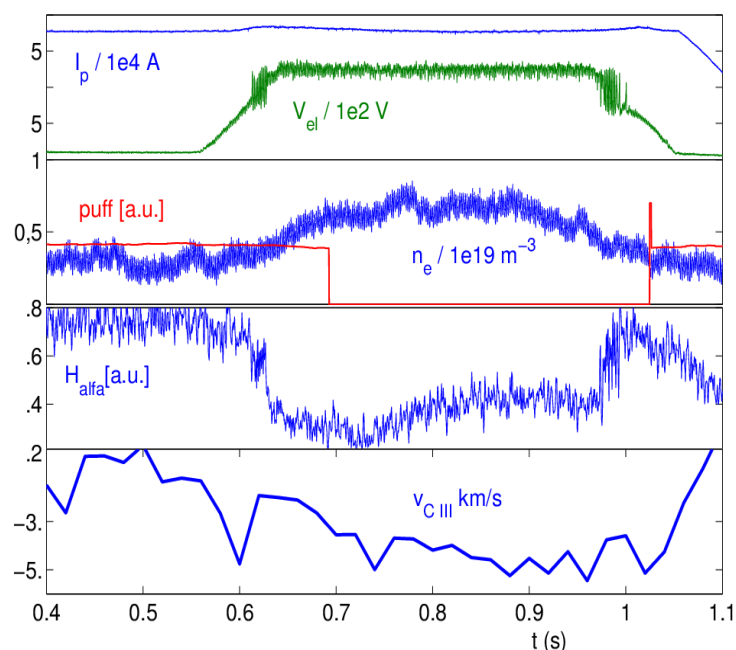


Fig. 3.1.10 RFX-mod tokamak discharge, from top to bottom: plasma current and electrode voltage; electron density and puffing pulse; H α signal; toroidal rotation from C III

MHD activity⁵⁰. Floating potential, edge temperature and density were measured by an insertable probe on various radial position. Data analysis shows that during the enhanced confinement phases a strong radial electric field builds up inside the LCFS (few cm). The radial profile of saturation current, linearly depending on the electron density, steepens, thus indicating that a local transport barrier is established, sustained by the polarized electrode.

3.1.2.2 Edge turbulence and topology.

The characterization of the kinetic response of the edge plasma to a 3D magnetic field, has been extended to RFX-mod in tokamak configuration. The main result, found for the RFP and reported in sec.3.1.1.4, is that in the presence of rotating

⁴⁹ M. Spolaore et al., 26th IAEA Fusion Energy Conference Kyoto, Japan 17–22 October 2016, paper EX/P5-24

⁵⁰ L. Carraro et al., 43rd EPS Conference on Plasma Physics, P5.014, July 2016, Leuven, Belgium

magnetic perturbations the profiles of electrostatic particle and energy flux at the edge follow the symmetry of the dominant imposed perturbation is also true for the tokamak: the modulation of flux profiles manifests itself with an increase around the O-point of the outermost resonating island and a reduction in the X-point region due to the fluctuation level and not due to the relative phase between electron density and electric field fluctuations. The spectra show that fluctuations propagating in the electron diamagnetic drift direction peak at $k_{\perp}\rho_i \sim 0.06$ (Fig. 3.1.11).

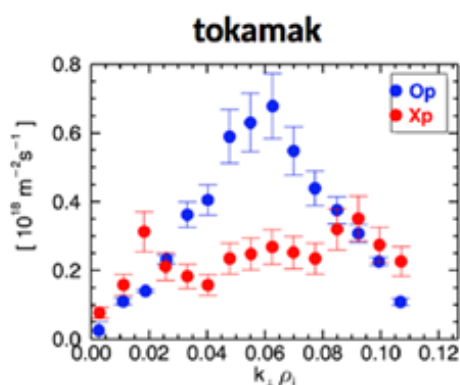


Fig. 3.1.11 k-resolved particle flux; blue and red points refer to data on O-point and X-point respectively (Tokamak plasmas)

3.1.2.3 Runaway electron studies

The analysis of experiments carried out in RFX-mod exploiting Magnetic Perturbations (MP) with different modal numbers to deconfine Runaway Electrons (RE) has been completed. Statistical studies over more than one hundred discharges show that REs are observed at densities below 10^{19} m^{-3} and at a toroidal electric field greater than 0.03 V m^{-1} . Fig. 3.1.12 shows that a $m=2, n=1$ MP is effective in reducing the high energy portion of the gamma ray spectrum; this is true both in $q(a) < 2$ and in

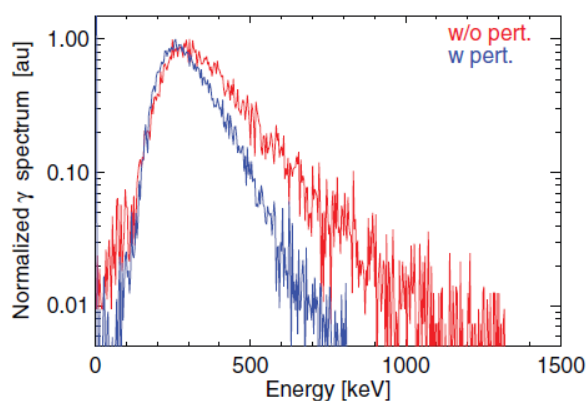


Fig. 3.1.12: gamma ray spectra with (blue) and without (red) MP in a RFX-mod tokamak plasma

q(a) >2 discharges. The ORBIT code has been upgraded to a relativistic version and used to interpret the mechanism generating RE and the effect of MPs. It has been found that RE enhanced losses are associated with an increased level of stochasticity, the effect being more pronounced when the MP amplitude is higher and internally resonant.

3.1.2.4 Magnetic equilibrium reconstruction

Equilibrium reconstruction of tokamak plasmas are currently obtained in axisymmetric configuration using MaxFea as well as V3FIT/VMEC. These two codes use different approaches to solve the inverse problem of equilibrium reconstruction; in particular MaxFea exploits only magnetic measurements while V3FIT can also constrain the reconstruction with some kinetic measurements such as SXR emissivity, electron temperature profile (from Thomson scattering) and plasma density (from the interferometer).

When operating the non axisymmetric saddle coils, it is necessary to use a 3D approach and in this respect V3FIT/VMEC is the more appropriate tool. As no internal measurement of magnetic quantities is available in RFX-mod, the reconstruction proved to be quite tricky, with the additional issue of the high degeneracy of equilibria with circular cross section. This has not been completely resolved using kinetic measurements that clearly show evidence of a 3D helical structure in the core, differently from the RFP case. A possible improvement might be obtained by different parametrizations for q or toroidal current profiles, however this will be matter of investigation for next year.

3.1.2.5 Modelling of beam penetration

In RFX-mod2, a neutral beam will be applied, already available at Consorzio RFX (25 keV, 50 A) and originally developed at AIST (Japan), in order to make more robust and reliable the transition to H-mode. The duration of the beam pulse, when operated at 25 keV, is limited to 30ms, which should be sufficient to induce the L-H transition, but could be too short to perform RMP experiments for ELM control. However, if operated at 15 keV the pulse duration can be extended to 100 ms. Simulations by the METIS code have been done showing that with a beam energy of 15 keV in the density parameter range of RFX-mod tokamak the losses (shine-through + orbit

losses) are below 50% and scenarios with enhanced temperature and $T_i/T_e > 1$ can be explored⁵¹.

3.1.3 Analysis of experiments in ultra-low-q configuration

Experimental and modelling efforts carried out to study the physics of the density limit in the RFP in last years enlightened the crucial role of the magnetic topology, and in particular of the edge $m=0$ islands, in producing toroidally localized edge density accumulation as a result of due to an $E \times B$ convective cells arising as an ambipolar response of the plasma to the presence of the island fixed points⁵². The analysis of high density ultra low q (Ulq) discharges, whose equilibrium mainly differs from the RFP because of the absence of any $m=0$ resonance in the plasma, has been done in 2016. Results are summarized in Fig. 3.1.13. In RFP configuration, when $n > 0.5n_G$, the power radiated locally inside the MARFE greatly exceeds the local input power (red dots in Fig. 3.1.13 (a)), even if globally $P_{\text{rad}}/P_{\text{Ohm}} < 0.5$ (open, black dots in Fig. 3.1.13 (a)). Instead, in Ulq discharges (Fig. 3.1.13 (b)), the fraction of radiated power smoothly increases with n/n_G , with no localized radiative structure, with $P_{\text{rad}}/P_{\text{Ohm}} \sim 0.6$ when $n/n_G = 1.0$. Extrapolating the curve, the balance $P_{\text{rad}} = P_{\text{Ohm}}$ is obtained for $n/n_G \sim 1.5$, which is a value 3 times larger than the critical value for MARFE onset in

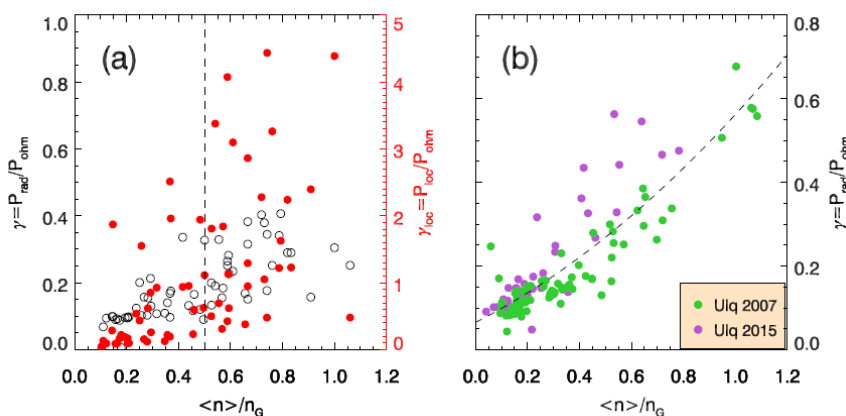


Fig. 3.1.13 $P_{\text{rad}}/P_{\text{Ohm}}$ ratio as a function of normalized density: a) RFP case, b) Ulq plasmas. In a) black points refer to global values, red ones to values from a local balance along the toroidal angle

⁵¹ M. Vallar et al., "Requirements and modelling of fast particle injection in RFX-mod tokamak plasmas", presented at 29th Symposium on Fusion Technologies, Prague 5-9 September 2016, submitted Fusion Eng. Des.

⁵² G. Spizzo et al, Nucl. Fusion **55** 043007 (2015)

the RFP⁵³.

3.1.4 3-D modelling of RFP helical states

The numerical investigation on the effect of external magnetic perturbations in 3D MHD modelling of the RFP culminated in a systematic comparison of stimulated helical RFP states with different dominant helicities. Helical RFP states were found to be characterized by different equilibrium and topological properties depending on their

dominant helicity⁵⁴. In particular, helical states with non-resonant $n=6$ dominant mode were confirmed to be the most resilient to magnetic chaos originated by remnant secondary modes, as shown in Fig. 3.1.14. Moreover, the numerical $n=6$ helical state was found to have the best confinement properties in terms of both diffusion coefficient of magnetic field lines and robustness of Cantori. The latter are partial barriers to field-line transport, detected with an advanced technique based on the computation of finite-time Lyapunov exponents⁵⁵.

A remarkable outcome of this modelling activity was the validation of the MHD model with respect to experimental observations. Indeed, the comparison with experiments carried out in RFX-mod confirmed the MHD prediction about stimulated helical states with applied MPs⁵⁶. As for example shown in Fig. 3.1.15 a good quantitative agreement was obtained between numerical modelling and RFX-mod experiments as far as the dynamics of MHD modes is concerned. Electron temperature profiles for $n=6$ stimulated helical states obtained in RFX-mod are characterized by somewhat broader hot central regions than spontaneous $n=7$ helical states. This experimental

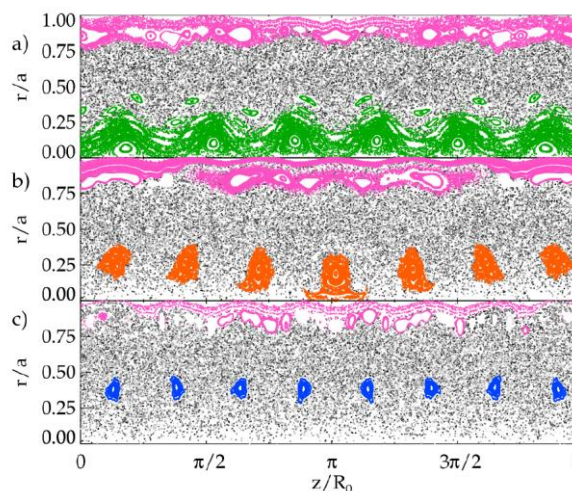


Fig. 3.1.14 Magnetic field topology for helical RFP states with a) $n=6$, b) $n=7$ and c) $n=8$ dominant mode.

⁵³ M. Zuin et al., 26th IAEA Fusion Energy Conference Kyoto, Japan 17–22 October 2016, paper OV/P-2, submitted to Nucl. Fus.

⁵⁴ D. Bonfiglio, S. Cappello, M. Veranda, et al., Proc. IAEA-FEC, TH/P3-35 (2016).

⁵⁵ G. Rubino, D. Borgogno, M. Veranda, et al., PPCF 57, 085004 (2015).

⁵⁶ M. Veranda, D. Bonfiglio, S. Cappello et. al., submitted to PRL (2016).

finding appears to be consistent with the modelling prediction of best magnetic order in the $n=6$ state.

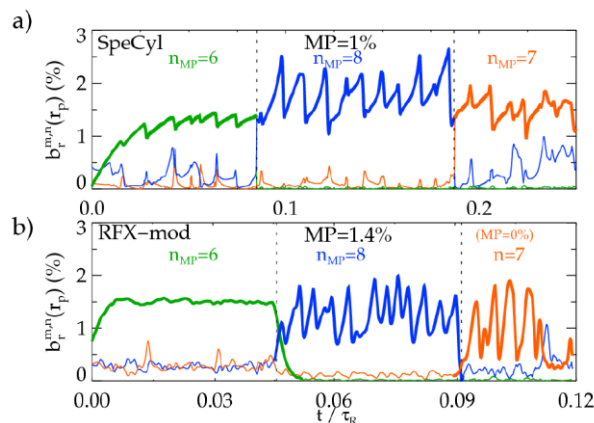


Fig. 3.1.15 Validation of MHD modelling: a) simulations b) RFX-mod experiments.

A further notable result of MHD modelling with applied MPs is the demonstration of a common fundamental physical basis of RFP and tokamak plasmas. Indeed, in both configurations the spontaneous sawtooth dynamics can be mitigated (e.g., made more frequent and less intense) with MPs. Moreover, a stationary helical state can be stimulated (similarly to what obtained without MPs by increasing the visco-resistive dissipation⁵⁷) when the external perturbation amplitude is above a given threshold⁵⁸. The sawtooth mitigation effect predicted by MHD simulations in both RFP and tokamak configuration was experimentally confirmed. This effect, already observed in the past for both RFP and tokamak RFX-mod discharges⁵⁹, has now been also demonstrated in the DIII-D tokamak device⁶⁰. An additional important observation of the common physics of RFP and tokamak plasmas regards the MHD dynamo. This effect, crucial for the sustainment of the RFP configuration, has been found to be also essential to sustain tokamak equilibria with a helical core, in both MHD simulations and experiments⁶¹.

3.1.5 Transport studies

3.1.5.1 Transport in presence of multiple magnetic axes

⁵⁷ D. Bonfiglio, L. Chacón and S. Cappello, *Physics of Plasmas* 17, 082501 (2010).

⁵⁸ D. Bonfiglio, invited talk at the 43rd EPS conference on Plasma Physics (Leuven, 2016); see also D. Bonfiglio, M. Veranda, S. Cappello et al., *PPCF* 59, 014032 (2017) and D. Bonfiglio, M. Veranda, S. Cappello et al., *PPCF* 57, 044001 (2015).

⁵⁹ P. Piovesan, D. Bonfiglio et al, *Physics of Plasmas* 20, 056112 (2013).

⁶⁰ C. Piron et al, *Nucl. Fusion* 56, 106012 (2016)

⁶¹ P. Piovesan, D. Bonfiglio et al., *Proc. IAEA-FEC, EX/1-1* (2016).

The development of a code able to describe energy and particle transport in presence of magnetic islands, started in 2015, has progressed in 2016. More specifically, the multiple axis solver (MAxS), based on a Multiple Domain Scheme (MDS) has been successfully used to interpret RFP plasmas in both double axis (DAX) and SHAx states in RFX-mod (an example is given in Fig. 3.1.16, showing the heat diffusivity profile obtained for a Double Axis case). The code has been also applied to model transport properties of the Large Helical Device (LHD) and TJ-II Helic plasmas⁶².

3.1.5.2 First principle model for the density limit

Tokamaks and Reversed Field Pinches share the same density limit (the empirical Greenwald limit), while in Stellarators the density is limited by the Sudo scaling. A theoretical and simple model providing a unified explanation of the three limits has been developed, based on the thermal balance equation and Ohm's law computed at a single position, the plasma center⁶³. Such new model gives predictions in fair agreement with experimental observations from all three configurations. The dependence of the density limit on the energy transport is found to be weak for a pure Ohmic configuration, while the scaling of the density limit depends on the density radial profile, indicating that a fully self-consistent approach to the problem should include a model for the particle transport.

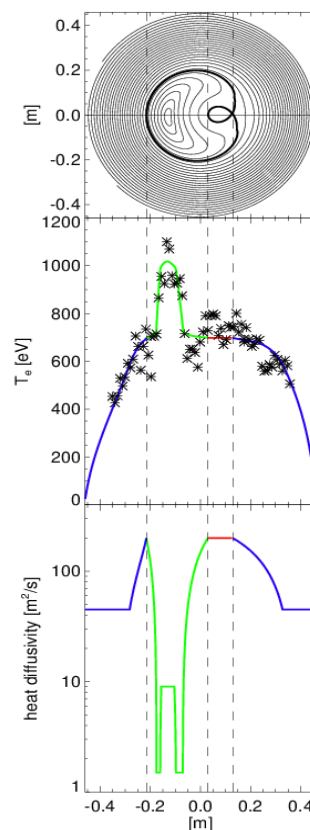


Fig. 3.1.16: From the top: flux surface reconstruction for a DAX plasma; electron temperature profile (dots experimental values, solid line reconstructed profile); heat diffusivity profile computed by MAxS. Different colors refer to different domains considered in the analysis.

⁶² R. Lorenzini et al., 26th IAEA Fusion Energy Conference Kyoto, Japan 17–22 October 2016, paper EX/P5-26; F. Auriemma et al., to be submitted

⁶³ P. Zanca et al., submitted to Nucl. Fus.

3.1.6 *RFX-mod upgrade*

3.1.6.1 The Load Assembly

As anticipated in Section 3.1, during 2016 the design activity of machine upgrades for the RFX-mod experiment had been progressing up to an advanced conceptual level presented at the 29th Symposium on Fusion Technology⁶⁴.

The scientific objective is the improvement of 3D physics studies through a more robust transition to higher confinement regimes in both RFP and Tokamak configuration obtained thanks to an advanced system for the active control of MHD instabilities.

The main design driver requirements for this machine upgrade are the removal of the present resistive Vacuum Vessel (VV) and the enhancement of the 'shell-plasma proximity', to reduce the deformation of the last close magnetic surface and to improve the self-organized helical plasma regimes.

The fulfillment of these requirements implies a major change of the internal components of the machine such as:

- the replacement of the whole First Wall (FW);
- the change of the support system of the Passive Stabilizing Shell (PSS);
- the modification of the present Toroidal Support Structure (TSS) to provide the function of vacuum barrier (VTSS).

Fig. 3.1.17 shows the cross section of RFX-mod2 compared to the present RFX-mod and the enhancement of shell/plasma proximity that can be obtained with the removal of the present VV and the reconfiguration of the main components of the load assembly indicated in Fig. 3.1.18 Rendering of the new components of the load assembly (FW, PSS, VTSS)

The most critical aspects of the new torus assembly are the development of reliable and effective solutions for:

- the equatorial and poloidal joints of the VTSS, in order to guarantee the vacuum boundary and the penetration of electro-magnetic fields within the plasma chamber;
- the compensation of the expected magnetic error fields generated by the PSS poloidal gaps, which could be obtained by means of a dedicated active control system of local magnetic field or relying on the possibility overlapping the

⁶⁴ S.Peruzzo, et al., oral presentation at 29th SOFT Symposium on Fusion Technology, Prague, Czech Republic, 5-9 September 2016, submitted to Fusion Engineering and Design

insulated gaps of the PSS, as adopted in RFX-mod configuration, but with the new complication of the vacuum environment.

Extensive thermo-mechanical and electro-magnetic analyses had been carried out to define the most viable solution, complying with the geometrical constraints of existing components that make this approach rather challenging. The preliminary design of the modifications had been reviewed with some potential industrial contributors. The design has been considered feasible, for the significant but not radical change of the existing components, and challenging, for the potential innovations proposed for some particular technological solutions.

The detailed design is expected to be completed in the first half of 2017, with the definition of the open issues still to be solved regarding the critical aspects mentioned above.

3.1.6.2 Glow Discharge Cleaning system

The analysis of data from dedicated experimental sessions performed before the disassembly of the RFX-mod device has proven that the efficiency of the cleaning procedure is not significantly affected if the electrodes are flush with the first wall, instead that being placed in the centre of the vacuum chamber (as in RFX-mod). This result is important to design the new GDC system for RFX-mod2, which will be likely based on a larger number of electrodes (2 in RFX-mod), still object of investigation.

3.1.6.3 Magnetic and electrostatic sensors

The new configuration of magnetic sensors for RFX-mod2 has been studied. The number of poloidal sensors will be increased. In fact the present number of poloidal and radial measures is quite adequate to determine the plasma horizontal and vertical position in circular discharges, with the magnetic equilibrium reconstructed by

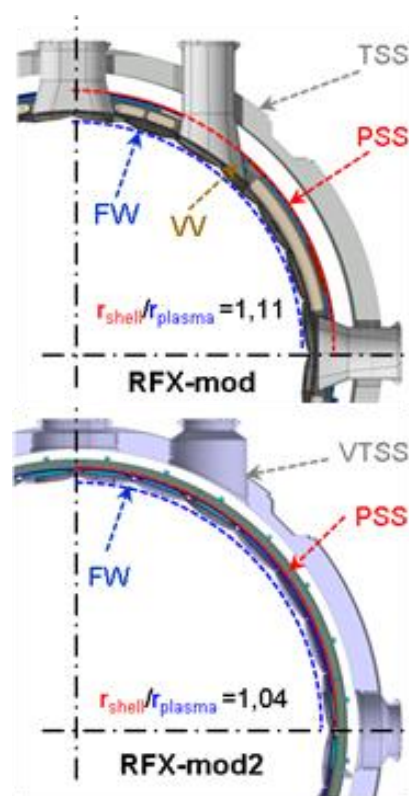


Fig. 3.1.17 Enhancement of shell/plasma proximity obtained with removal of present VV

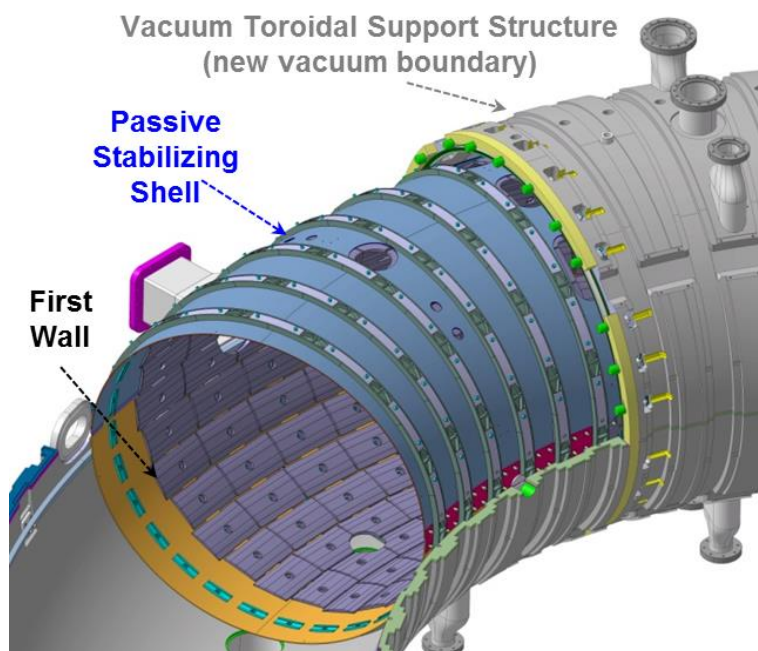


Fig. 3.1.18 Rendering of the new components of the load assembly (FW, PSS, VTSS)

a fully model-based approach⁶⁵. Instead, in shaped discharges, the contribution of higher order harmonics is not negligible and has to be numerically evaluated. Their direct calculation is limited by the present 4 (toroidal) x 8 (poloidal) array of probes. Considering the presence of 28 tiles, an array of 12 (toroidal) x 14 (poloidal) sensors has been identified as the minimum requirement for a measurement-based and reliable equilibrium reconstruction. This magnetic diagnostic improvement will allow a strong enhancement in the control of magnetic equilibrium and plasma shape, thus increasing the flexibility in the position of the X-point; also negative triangularity shaping will be tested.

The possibility to improve the poloidal resolution of electrostatic sensors, for a better characterisation of the plasma edge, is instead still under investigation.

3.1.6.4 Upgrade of the Thermal Helium Beam diagnostic

Laboratory tests have been performed (and are still in progress) to upgrade the detectors used for this diagnostic, exploiting solid state photomultipliers less sensitive to the magnetic field than the standard ones and which can be therefore placed close to the machine, thus avoiding long optical fibres and improving the signal level. In

⁶⁵ G. Marchiori et al., Fusion Eng. Des. 108 (2016) 81-91

addition, to improve the precision of temperature and density measurements, an investigation is in progress to add a fourth He I line to the three presently measured. This requires both a rearrangement of the diagnostic and the development of a new analysis tool with updated atomic physics (foreseen as an activity for next year).

3.1.6.5 Upgrade of Thomson scattering system

A modification of the Thomson scattering diagnostic is in the design phase, aiming at improving the signal-to-noise ratio by modifying the present system (which provides temperature and density profiles on 84 radial points with 10 ms repetition rate) in order to allow a double-pass of the laser beam. This will be useful in particular for measurements in tokamak configuration, where signal is low due to the rather low density.

3.1.6.6 Reflectometry

A new reflectometry system has been designed, based on three reflectometers located in three poloidal positions at the same toroidal angle: two on the equatorial plane, on the Low Field Side (LFS) and on the High Field Side (HFS), the third one on the upper side. In RFP configuration, working in the O-mode, the covered density range is $3\text{-}8 \cdot 10^{18} \text{ m}^{-3}$, allowing detailed measurements of the edge density profile and, in particular, a direct probing of the HFS/LFS asymmetries and a deeper characterisation of the $m=0$ islands. In tokamak configuration, the upper X-mode cutoff frequency will be exploited to probe the edge density both on the HFS and on the LFS; this condition is also suitable for measurements in the upper position. Main aim of the diagnostic configured with three reflectometers is the real-time control of plasma position, which is a critical issue for future devices, where the use of magnetic sensors will be limited by high neutron fluxes. For this reason a specific work package has been set-up for DEMO by the EUROfusion Consortium. Indeed a full reflectometry based plasma position control has never been conceived up to now, so that RFX-mod2 will be an excellent test bench for this kind of diagnostic.

3.2 Medium Size Tokamaks and JET

Significant has been the participation of Consorzio RFX to the Eurofusion program with, in particular, 10 Scientific Coordinators of experiments within JET and ITER-Physics work-packages, one Task Force Leader, one Deputy Head in the PMU for JET and an overall assignment of more than 13 ppy.

Below a brief description of some of the relevant scientific contributions to the JET and ITER-Physics work-packages.

3.2.1 Activities on JET

Impact of ELM's on High Z impurities transport

Limited by various faults of the JET plant, the experiment consisted in probing the penetration of medium and heavy impurities into the edge of JET plasmas in various conditions in order to understand the relative role of ELM and inter-ELM phases in controlling the impurity content. The question is of relevance to ITER, whereby heavy impurities are expected to be kept outside by favourable kinetic gradients at the edge, but where it is not clear to what extent a non neoclassical diffusive component of transport during and in between ELM's could allow some impurity inflow. The analysis is still ongoing however certain conclusions regarding the low power part of the experiments can be drawn as also exemplified in Fig. 3.2.1: a) ELM's expel impurities in the same way regardless of their masses (Ne to W) b) Spontaneous and kicks paced ELM's have same impact c) SXR can be used to analyze impact of single ELM and try to discriminate between diffusive and convective nature of ELM transport. A few high power discharges have been performed at the end of the JET campaign and will be compared to the low power cases to highlight the impact of the pedestal region, in particular of the edge ion transport barrier, in the way heavy impurities are affected.

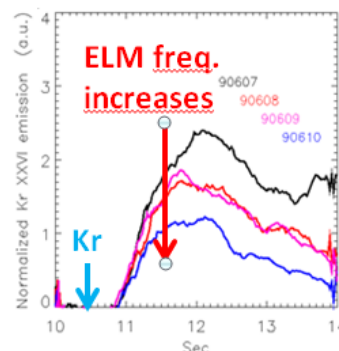


Fig. 3.2.1 Kr density after injection, The Kr content decreases with increasing ELM frequency. The pink and red curves refer to cases with same ELM frequency but different origin: spontaneous and kick induced respectively

Isotope effect on impurity transport

Several injections of Mo have been performed during the hydrogen campaign at JET in order to build a database to investigate the isotope effect on impurity transport. Preliminary considerations seem to exclude that there are important differences between the behaviour of impurities in H and in D plasmas that are not connected to the the different in the pedestal that is typically established for the same level of gas refuelling.

Disruption prevention and avoidance

A scenario depending relation matrix has been established between the alarms and the suitable recovery actions in terms of disruption avoidance or disruption mitigation.

M15-20 Seeding to maximum f_{rad} towards high P_{sep}/R

The aim of the experiment was the study of the possibility to reach the 90-95 % of the power radiated which will be required in DEMO. In this experiment in particular the influence of flux expansion and recycling on the radiation distribution and X-Point peak has been studied. An increase of the flux expansion has been obtained by the presence of a second null in the divertor region. The preliminary analysis of a few pulses with flux expansion has shown a shift of the radiation towards the target and an increase of the pedestal radiation, ELM frequency. Confinement has also increased. Modelling of the configurations without and with flux expansion is underway by means of the EDGE2-EIRENE and SOLEDGE2-EIRENE codes.

Isotope effect: heat and particle core transport analysis.

The M15-26 (Deuterium) and H16-01 (Hydrogen) have been performed at JET in 2015-2016 to specifically address the effect of different main gas isotopes on plasma properties. A large database (about 50 plasma setup) has been built and the TRANSP code has been exploited to study the core heat and particle transport properties, by means of interpretative runs. The comparison of the results with predictive runs of JETTO is ongoing.

3.2.2 *European Medium Size Tokamak studies*

Decorrelation of runaway electrons

This activity began in 2015 and has been completed during this year. The main aim was to test methods to de-correlate Runaway Electrons (RE) either during the RE avalanche or afterwards, when the RE beam is fully formed, by applying magnetic perturbations. Application of properly designed 3D magnetic fields in fact can act as a mitigation mechanism. In particular, in ASDEX Upgrade discharges, the application of $n=1$ Resonant Magnetic Perturbations (RMPs) by means of the B-coils before and during the disruption resulted in a longer current quench time together with a lower RE current in the post-disruption phase. The efficacy in the reduction of the final RE current has been found to be dependent on the upper-to-lower B-coils phasing i.e. on the poloidal spectrum of the RMPs. In fact, when the $n=1$ radial field, resonant with edge q profile, was maximum, the post-disruption runaway beam was reduced or

suppressed and measurements from scintillator diagnostic showed a clear decrease of the hard-x-rays (HXR) signal associated to runaway electrons. Moreover, RMPs have been found to affect also the resulting HXR energy spectrum with a large depression at values greater than 300keV.

Experiments performed in TCV during 2016 have been mainly dedicated to the generation and

control of runaway electron post-disruption beams and to the observation of the effects related to the spontaneous MHD activity. Disruption-generated RE have been obtained through small injections of high-Z impurities (Ne) in low-density inner limiter circular plasmas by means of the disruption mitigation valve. A dedicated controller for RE suppression has been implemented in the digital plasma control system which detects the current quench (CQ) phase and the RE plateau onset; then, a new plasma current reference, ramping-down to zero with a pre-selectable rate, replaces

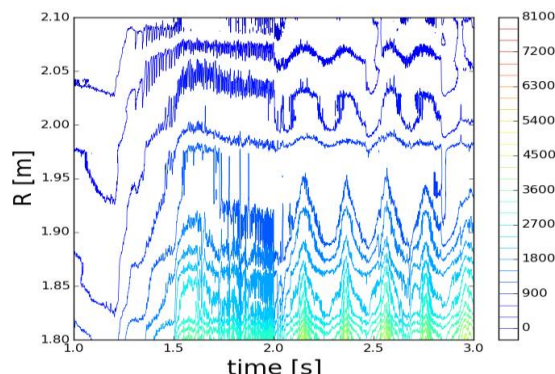


Fig. 3.2.3 ECE (filtered at 1 KHz) radial contours vs. time. RMP at 5Hz is applied t=2 s. Mode entrainment is demonstrated by the wide plasma radial region affected by the ECE oscillations.

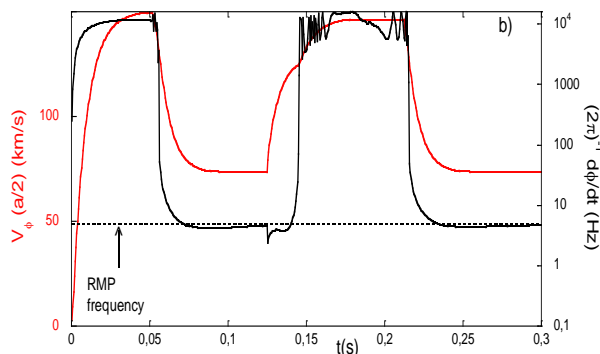


Fig. 3.2.2 Simulated toroidal flow velocity at $r=a/2$ (red) and mode phase velocity in logarithmic scale (black). β_N is varied during the simulation. Mode is entrained to the RMP only at high β_N , which implies high NTV.

the standard reference.

Disruption avoidance via applied magnetic perturbation

The entrainment of the $m=2$, $n=1$ tearing mode to a slowly rotating (5-10Hz) external magnetic perturbation (RMP) has been realized in ASDEX Upgrade experiments, in

high beta conditions ($\beta_{N\sim 2-3}$)⁶⁶ (see Fig. 3.2.3). This technique is expected to prevent, or at least delay, the disruption induced by a growing amplitude $m=2$, $n=1$ mode, by avoiding the strict locking of this mode to the wall. In this respect, the results have not been conclusive, since the disruption was prevented only for not too large NBI power ($P_{\text{NBI}} < 10\text{MW}$). The experiments gave also the opportunity to study the coupling between plasma and RMP, both in terms of magnetic perturbation amplitude and flow velocity. Simulations performed with a cylindrical code (RFXlocking), enriched by pressure and neo-classical physics, indicate the importance of the neo-classical toroidal viscosity (NTV) in determining the locking/unlocking dynamic (see Fig. 3.2.2).

Detachment optimization in snowflake configuration

On TCV experiments have been executed in Snowflake (SF) configuration to assess the potential advantage in detached conditions of SF configuration with respect the standard Single Null (SN) configuration. Various elements have been considered: the definition of the optimal snowflake configuration (SF+, SF-) which minimise target heat load in attached conditions the possibility to access detached condition at lower density and/or lower core radiation and the effects on confinement. Detachment has been obtained both increasing density and by impurity seeding (N2). Experimentally it was confirmed the ability of SF configuration to split the power over the four strike points with the ratio controlled by the distance between the two nulls, the access to the detachment was found similar to those in SN but a more pronounced detachment was possible in SF. In seeded discharges it confirmed the possibility to localize steadily the radiation in the region between the two nulls, a possibility previously foreseen in EMC3 simulations.

Modelling of the experiments with 2D fluid code SOLEDGE2D-EIRENE has started in order to see if the code is able to reproduce the experimental results in attached and detached condition in terms of strike point heat loads and radiation distribution.

Filamentary Transport Studies

An experimental activity on filamentary transport studies in high density regimes has been carried out on AUG and TCV.

⁶⁶ R. Paccagnella *et al*, 43th EPS Conference on Plasma Physics, Leuven, Belgium (2016), P.1027

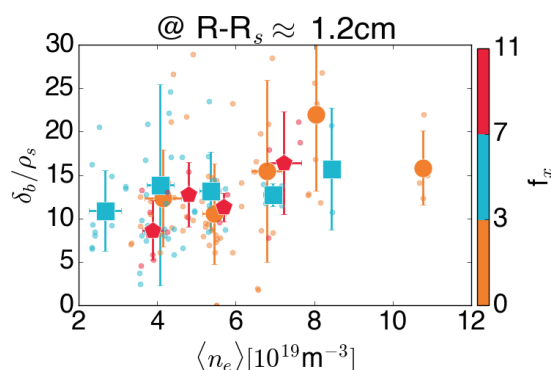


Fig. 3.2.4 Blob size normalized to local ion sound gyroradius as a function of line average density. The color code indicates classes in flux expansion

In AUG the development of the Scrape Off Layer (SOL) density profile shoulder, observed in L-Mode plasma whenever density is increased⁶⁷, has been investigated in moderate H-Mode as well. It has been found that in H-Mode the appearance of the shoulder is related not only to the divertor normalized collisionality Λ , but also to the level of gas fueling⁶⁸. Similar investigation has been performed on TCV, focusing on the role played by the parallel connection length variation in L-Mode ohmically heated plasmas. Variation of parallel connection length has been obtained by varying the flux expansion f_x and repeating similar density ramps to check the modification of SOL profiles with line average density. It has been found that despite the large variation of divertor normalized collisionality Λ , which linearly depends on parallel connection length, at the same level of density upstream profiles, remain unchanged. This suggests indeed that Λ is not the key ingredient in describing SOL profile saturation but, as in the case of the AUG H-Mode, a certain level of fueling is indeed mandatory to provide consistent modification of the upstream profiles. As to the modification of the filament properties it has been proved that the filament size increases almost linearly with line average density, without substantial distinction in classes of flux expansion as shown in Fig. 3.2.4.

Impact of external 3D fields on high-beta hybrid tokamak plasmas

Experiments performed in ASDEX Upgrade and DIII-D studied the impact of external 3D fields on high-beta tokamak plasmas operated in the so-called hybrid scenario, a promising steady-state operational scenario for ITER. This effort was led by Consorzio RFX scientists in collaboration with a wide international team and within the MST1-EUROfusion task force. The work showed that external 3D fields, due to

⁶⁷ Carralero D, *et al Nuclear Fusion* **54** 123005 (2014)

⁶⁸ Carralero D, *et al* in Proceedings of the 26th IAEA FEC Conference, Kyoto (2016)

machine error fields or intentionally applied with non-axisymmetric coils, stimulate the formation of a large helical core equilibrium. This new state was characterized with a variety of diagnostics and modelled with state-of-the-art MHD codes, including VMEC, MARS-F/K and M3D-C1. The helical core displacements impact various quantities, in particular kinetic profiles, plasma rotation and impurities. These effects have profound consequences on hybrid tokamak operation if external error fields are not properly controlled, as discussed in a 2016 EPS invited talk and published in [⁶⁹]. The helical core also redistributes the current profile through an MHD dynamo effect similar to that present in helical RFP plasmas. The similarities between continuous MHD dynamo in the tokamak and RFP were discussed in a recent IAEA paper [⁷⁰].

3.3 Contribution to the ITER Physics

3.3.1 *Preparation of Exploitation of JT-60SA*

3.3.1.1 JT-60SA polarimeter design and q profile determination

JT-60SA is the new tokamak device that is being built in Japan under the Broader Approach Satellite Tokamak Program and the Japanese National Program and will operate as a satellite machine for ITER. To provide valuable information for the steady state scenario for ITER and the design of DEMO, a high β_N scenario is included in the program, where the real-time control of the q-profile is needed. In this year we have refined the study of the geometry of the polarimetry chords, based on a true realistic CAD-driven feasibility layout, aiming at an optimization in terms of q-profile reconstruction, using the V3FIT code⁷¹. Some magnetic and kinetic measurements are considered along with the FIR poloidal polarimeter in order to assess the possibility of estimating q in the core with the required accuracy (around 10%) providing a diagnostic for a continuous measurement useful in high density pulses where MSE measurements would not have adequate time resolution.

The conceptual design of a multi-channel polarimeter has shown that this system meets the initial requirements and also that it has a strong potential for machine protection & control.

⁶⁹ P Piovesan et al 2017 Plasma Phys. Control. Fusion 59 014027

⁷⁰ P Piovesan et al 2016 IAEA-Fusion Energy Conference, "Role of MHD dynamo in the formation of 3D equilibria in fusion plasmas" paper EX/1-1

⁷¹ J.D. Hanson, S.P. Hirshman, S.F. Knowlton, L.L. Lao, E.A. Lazarus and J.M. Shields, *Nucl. Fusion* **49** (2009) 075031

The effectiveness of different layouts of polarimetric chords has been evaluated using V3FIT/VMEC (VMEC⁷² was used as the equilibrium solver) addressing the capability of providing reliable information for q profile reconstruction (in particular q-on-axis) considering the use of different subsets of chords as a full diagnostic set-up might not to be available from the beginning.

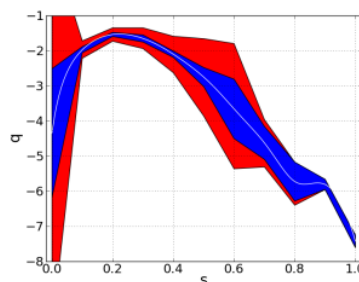


Fig. 3.3.1 Final result of q profile reconstruction using the full system of 12 chords (blue) or just three chords (red).

Fig. 3.3.1 shows the reconstructed q profile for two different configurations: in red 1 vertical chord and two horizontal chords, and in blue the full system of 12 chords (3 vertical and the rest horizontal). The design of the polarimeter proved to be adequate for q profile determination in its full-system configuration (i.e. 12 chords). Error bars (shade areas in figure) are still large for q-on-axis determination, but can clearly provide good information. Any reduction in the system geometry can only lead to a degradation of the result up to a condition where non information can be inferred for q profile (red area in figure).

Additional diagnostics are necessary to compensate for the lack or reduced information in some regions of the plasma. MSE and ECE are being implemented as diagnostics in V3FIT and could be used to re-asses this study possibly with an aim at real-time control of profiles.

The present study provides some indication with a limited number of diagnostics (both magnetic and kinetic). A more realistic description (e.g. without assuming a fixed pressure and density profile) should be considered in addressing q profile reconstruction with the full system of magnetic diagnostics and possibly other diagnostics available at phases of JT-60SA exploitation according to the research plan.

3.3.1.2 Preparation of the JT-60SA Exploitation

In preparation of the JT-60SA exploitation a document has been prepared with a description of the requirements and recommendations for the implementation of a Remote Experiment Centre (REC) in Europe for JT-60SA. The document has been submitted to the EUROfusion leaders to take a decision on the subject and to decide the actions EUROfusion should do in order to be ready when the JT-60SA will start to

⁷² S.P. Hirshman and J.C. Whitson, *Phys. Fluids* **26** (1983) 3554

operate. The document has been prepared by a group of European and USA experts leads by Consorzio RFX. In the document has been described the facilities that should be available at REC, the most important of which is the Remote Experiment Room (RER). For the RER it has been defined available functionalities and roles of researchers when operating remotely JT-60SA.

3.3.1.3 Edge modeling

Modelling of the divertor and wall power load has started with the SOLEDGE2D-EIRENE code. The first simulations of the JT-60SA low density inductive reference scenario have shown too high a temperature and power load at the target. Additional simulation adding deuterium gas-puffing and/or impurity seeding are underway to ascertain to conditions to reach satisfactory conditions at the targets.

3.3.1.4 MHD modeling

Consorzio RFX provided a major effort in 2016 to contribute to the modeling of JT-60SA plasmas and in particular to the study of MHD stability and control in high β_N scenarios. In these operational scenarios, aiming at attaining steady state (fully non inductive) conditions, Resistive Wall Modes (RWM) are found as main MHD limiting instabilities.

RWM stability in JT-60SA is being studied, including both energetic particles and rotation effects, that turn out to be strongly stabilizing, when combined. Kinetic effects have also been included in simulations with the 2D MHD code MARS-F/K⁷³. Original results showing that substantial RWM damping is found with a combination of drift-kinetic effects with plasma rotation, where the former are represented by the precession drift resonance for trapped particles⁷⁴. The 2D map of an m=2 harmonic is shown in Fig. 3.3.2 for the fluid non-rotating case. Further developments include the possibility of studying anisotropic energetic particle distributions and including additional kinetic resonances for a more detailed description of the RWM damping physics.

Active control of the RWM by a specific magnetic coil system will be a key ingredient of these scenarios and is being actively investigated by 3D electromagnetic computations coupled to a realistic representation of the real time control software. The codes CAFE and CARIDDI have been used to characterize the dynamic

⁷³ Y. Liu et al, Phys. Plasmas 15 (2008) 112503

⁷⁴ L. Pigatto et al., Resistive Wall Mode Stability in JT-60SA High β_N Scenarios, 43rd EPS Conf. on Contr. Fusion and Plasma Phys., 2016, P4.078

response of the MHD control system in JT-60SA, in the presence of the 3D conducting structures surrounding the plasma⁷⁵.

The ensemble of these studies should allow designing a comprehensive control strategy to cope with RWM and securing the high beta JT-60SA operational space. Studies performed in Consorzio RFX on this subject were presented at the last IAEA-FEC conference⁷⁶. A proof-of-principle of RWM feedback control was obtained through an eigenvalue study of the closed-loop system, which allowed achieving mode stabilization. The result of this first approach, in which only six out of eighteen active coils have been implemented, is shown in Fig. 3.3.3 as a gain scan. It appears that eigenmodes that are strongly unstable in the open loop case can be stabilized if the appropriate closed loop proportional gain is applied. It is worth mentioning that the plasma description underlying these simulations is purely fluid, therefore not including any kinetic damping.

3.3.2 Exploitation of W7-X and Stellarator optimization

3.3.2.1 MDSplus for control and data acquisition

The activities carried out in 2016 for the support of the usage of MDSplus in W7-X diagnostic data management have been:

- The finalization of the development of the software modules for handling setup and data acquisition of the camera devices that have been used in the first W7-X campaigns.

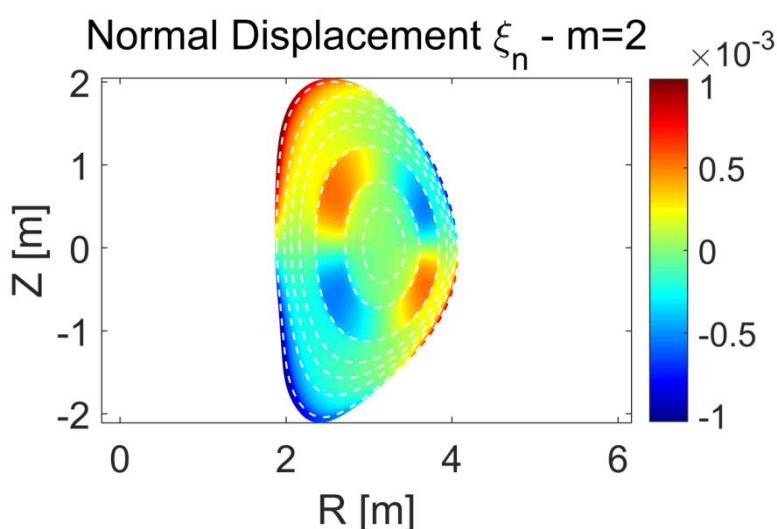


Fig. 3.3.2 RWM computations with the MARS-F code for parameters representative of a high beta reference scenario showing the normal component of the perturbed plasma displacement, m=2 harmonic, in a non-rotating case.

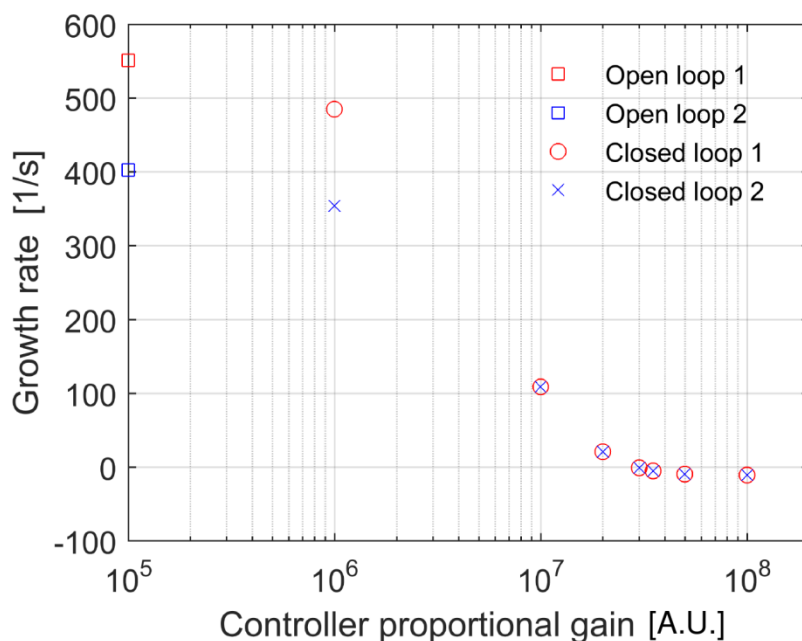


Fig. 3.3.3 Gain scan on the two unstable eigenmodes (labelled 1 and 2) using one out of the three available active coils arrays (six active coils along the toroidal direction used).

- The development of a programmable timing device based on the ZINQ FPGA architecture. This device will be synchronized with the main W7-X timing system and will provide a configurable set of trigger and clock signals.

3.3.2.2 Transport in presence of multiple magnetic axes

A new approach in modelling transport in presence of islands has been developed, dubbed Multiple Domains Scheme (MDS). In the MDS three regions inside the plasma are identified: the first around the main magnetic axis, the second around the island axis and the third includes the outer plasma. The three zones are interfaced by the separatrix that acts as common boundary. In each domain a monotonic radial coordinate can be chosen and the metric elements can be computed accordingly, including the discontinuities arising on the separatrix. This scheme is independent on the equilibrium magnetic configuration hence it can be applied to Tokamaks, Stellarators or Reversed Field Pinches. The MDS has been implemented in a new numerical tool, dubbed Multiple Axis Solver (MAxS). A first application of MAxS to LHD data has been performed: such proof of principle work shows the capability of MAxS of facing both stationary and transient transport analysis in presence of island. A second study has been carried out on the RFX-mod Reversed Field Pinch device where the presence of a large $m=1$ island has a beneficial impact on energy

confinement: e-ITB is established in the island region, the electron temperature profile peaks and temperature gradients reach several keV/m (See Fig. 3.3.4).

3.3.2.3 In vessel optical system for the Gas Puffing Imaging (GPI) diagnostic

A system of 3 lenses and a Flat Mirror (FM) in vacuum and a photographic objective coupled to a bundle of fiber optics in air has been chosen to relay the image of a He cloud generated at the edge of the plasma at a distance of 2m. The total magnification of the optical system is ~ 6 and ~ 10 for objective lenses of $f=85\text{mm}$ and $f=50\text{mm}$ respectively. Given the optical fibers interspace of 0.44mm , the image resolution is about 2.6mm for the 85mm objective lenses and 4.4mm for the 50mm one. Transmission tests have been carried for 8 equidistant positions inside the field of view, for both the 2 objectives and a FM mirror that simulates the geometry expected on W7-X and for two aperture values. With the 50mm objective transmission is about 12% and 22% for $f^\# = 2.8$ and $f^\# = 2$ respectively.

Numerical simulations with the Zemax code (2003 version) and the optics available in its library, different from those used on the optical bench, agree with the experimental tests (blurs of $400\mu\text{m}$ and $600\mu\text{m}$ for the 50 and $f=85\text{mm}$ lenses respectively).

3.3.2.4 High resolution probes

During 2016 the design of the High Resolution Probe head to be installed on the W7-X experiment was designed at Consorzio RFX, in collaboration with the IPP

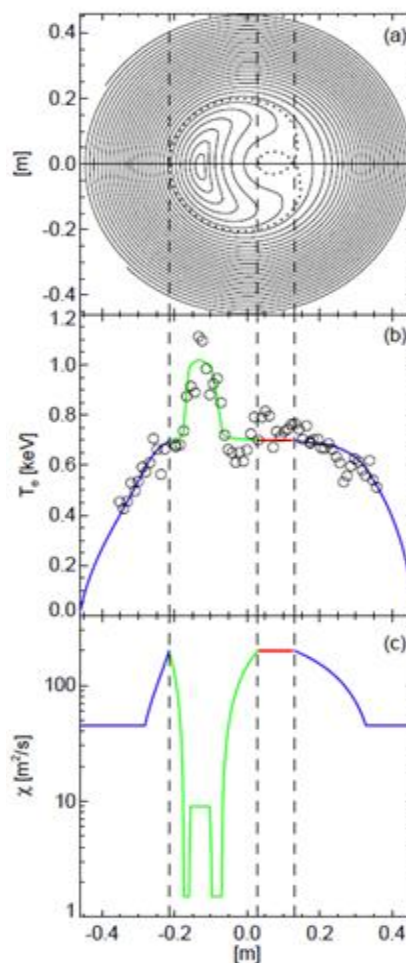


Fig. 3.3.4 Example of MxS simulation: (a) plasma cross section, with separatrix highlighted as dotted line; (b) comparison of experimental (o) and numerical (line) T_e profiles on the equatorial diameter; (c) effective diffusivity profile. The vertical dashed lines are the intersections of the separatrix on the equatorial plane.

Greifswald team. It was decided to operate the probe head predominantly within the OP1.2 phase.

In particular the aim is to provide information on the parallel current density associated to L-mode filamentary turbulent structures as well as on ELM structures in H-mode^{77 78 79 80}. Furthermore the possibility to measure the time evolution of radial profiles of flow was considered as a further interesting part of the study, given the strong interplay expected between the turbulent fluctuation and the average flows.

Special attention was devoted to the design of a shield for the magnetic sensors embedded into the probe head, which would allow the magnetic fluctuation measurements ($f_{\text{meas}} \leq 1$ MHz) and at the same time the shielding from ECRH ($f_{\text{ECRH}}=140\text{GHz}$) used for additional heating.

3.3.3 WP ISA Infrastructure support activities

The activity addressed the development of a new architecture of the Universal

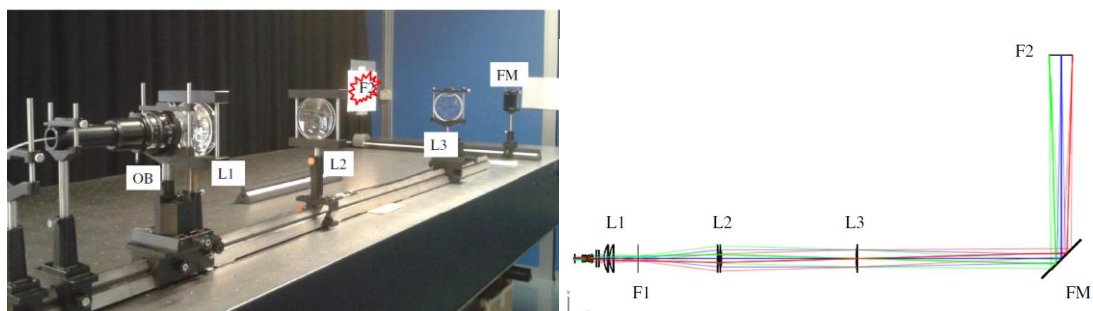


Fig. 3.3.5 Set up for the bench test of the optical and the equivalent Zemax simulation
Access Layer (UAL) to be used for handling data during simulations. The new architecture is based on Object Oriented concepts and is implemented in C++. In addition, the new layer will support the organization foreseen for ITER simulation, requiring a different management of the timebase information for the signals

⁷⁷ M. Spolaore, et al Phys. Rev. Lett. 102, 165001 (2009)

⁷⁸ N. Vianello, M. Spolaore, E. Martines, R. Cavazzana, G. Serianni, M.Zuin, E. Spada, and V. Antoni, Nucl. Fusion 50, 042002 (2010).

⁷⁹ Furno I., Spolaore M., Theiler C., N. Vianello, et al., Phys. Rev. Lett. 106, 245001 (2011).

⁸⁰ M. Spolaore et al. , "Electromagnetic ELM and inter-ELM filaments detected in the COMPASS Scrape-Off Layer", to be publ. on Journ. of Nucl. Mat.

managed during simulation. The integration of the new UAL in simulation workflows is foreseen in 2017.

3.3.4 ITER Modelling and some related support activities

In 2016 the activity on disruption modelling with the M3D code has been focused mainly in code validation using JET data and in disruptions avoidance experiments in ASDEX-U under the MST1 initiative, aimed at understanding, using simplified models, the relevant physics that could describe the plasma complex interaction with an external magnetic field.

Regarding JET some M3D simulations have been presented at the 43th EPS Conference in Leuven and also at the 26th IAEA Conference in Kyoto .

In particular⁸¹ it was shown that during a VDE's the JET equilibria can produce MHD modes and strong horizontal forces. Moreover the observed rotation frequency of the wall force, of few hundred Hz, was in the same range as observed in the experiments at JET. Finally a linear correlation of the toroidal flux and toroidal current asymmetries has been found (see Fig. 3.3.6) in simulations, again similarly to what experimentally measured.

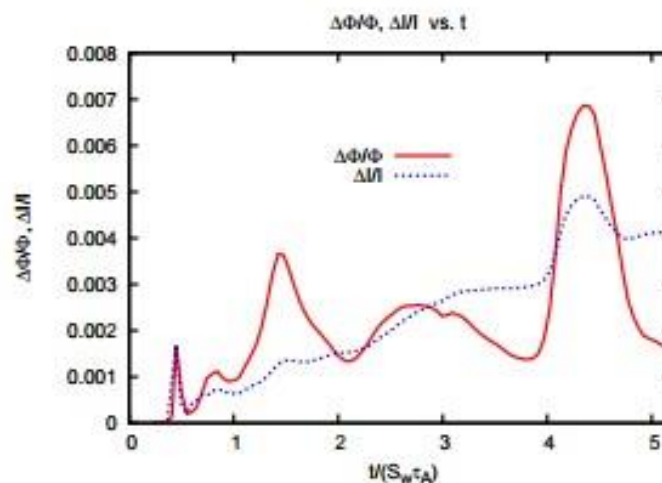


Fig. 3.3.6 Toroidal current and toroidal flux asymmetries vs. normalized time.

In ASDEX-U some experiments dedicated to disruptions avoidance using rotating magnetic perturbations (RMP) have been done. These experiments, that showed a good entrainment of a 2/1 island structure in the plasma to the externally applied

⁸¹ H. Strauss et al, 43rd EPS Conference on Plasma Physics, Leuven, Belgium, 4 - 8 July 2016 – ECA Vol. 40A – P2.012.

slowly rotating (10-20 Hz) RMP, have been interpreted using a model that couples plasma stability, magnetic field penetration through a conducting structure and torque exerted by the RMP on the magnetic island, which has been shown to originate the entrainment.

The results have been published⁸² at the EPS Conference. An interesting observation, that requires further modelling analysis, is that a kink aligned external RMP produces the strongest plasma response, i.e. it couples and excites, with the highest efficiency, a resonant magnetic island structure.

An activity aimed at coupling the M3D and the Cariddi⁸³ codes has been also initiated in 2016. The foreseen coupling is based on an exchange of data between the two codes at selected times. The full current distribution calculated by M3D at a given time according to a toroidal nonlinear plasma dynamical model, will be used as a source for the Cariddi code that could in this way calculate, although not fully self-consistently, the wall currents in complex 3D geometry, that are consistent with the given plasma state. A post processor of the M3D code has been written, although not already tested, that can output the required information as a text file to be read by the Cariddi code.

During year 2016, the study of connections between 3D edge transport in RMP tokamaks to stellarators and RFPs, which is considered to be most informative for ITER ELM mitigation, has been fostered under the ITPA-PEP19 initiative. On the stellarator side, impurity transport with stochastic fields and magnetic islands in the electron and ion root has been investigated, in particular addressing helium exhaust during RMP application in LHD⁸⁴.

Regarding the RFP, a detailed topological study, performed with the guiding centre code ORBIT, of the helical stochastic edge of RFX-mod with a $m/n=1/7$ dominant mode, has revealed the great importance of toroidal sidebands with helicity $m=0$ in determining the kinetic plasma response. Simulations with ORBIT of connection lengths $L_{c,w}$ on all three dimensions (r, θ, ϕ) , reproduce quite well the rather

⁸² R. Paccagnella et al, 43rd EPS Conference on Plasma Physics, Leuven, Belgium, 4 - 8 July 2016 – ECA Vol. 40A – P1.027

⁸³ R. Albanese, E. Coccorrese, R. Martone, G. Rubinacci, IEEE Trans. on Magnetics **29** (1993) 2353.

⁸⁴ O. Schmitz et al., in Fusion Energy Conference (*Proc. 26th Int. Conf. Kyoto, Japan, 17–22 October 2016*) (Vienna: IAEA) EX/1-4

complicated dependence of the edge floating potential on the poloidal and toroidal angles, with a mixed $m=0$ and $m=1$ topology⁸⁵.

Finally, regarding the tokamak, a study of the electrostatic response to edge islands, and its connection with convective cells, has been undertaken in ASDEX-U, using the same tools exploited in a recent work on TEXTOR⁸⁶. In particular, ORBIT has been adapted to the L-mode high density limit scenario of ASDEX, prior to a minor disruption, when it is believed that stochastisation of the magnetic field happens, leading to fast particle and energy loss⁸⁷. An analytic form of the tearing mode eigenfunctions⁸⁸ has been extrapolated to the edge, in order to match amplitude and phases of the pick-up B_θ coil array. The somewhat unexpected result is that, even if a dominant $m=3$ pattern is visible in the coil data, other sidebands are necessary to reproduce measurements: in particular, a large $2/1$ mode (island width ~ 6 cm in the LFS) is necessary, plus smaller $3/1$, $4/1$ and $5/1$ islands. Since high m harmonics are considered, a study of the role of passive structures, such as the poloidal stabilization loop (PSL) has been started. The purpose is to assess the contribution of currents flowing in these structures to harmonics with $m>2$, as partially done in the past⁸⁹.

The importance of toroidal sidebands in ASDEX is reminiscent of the result on RFX-mod, and will be further investigated.

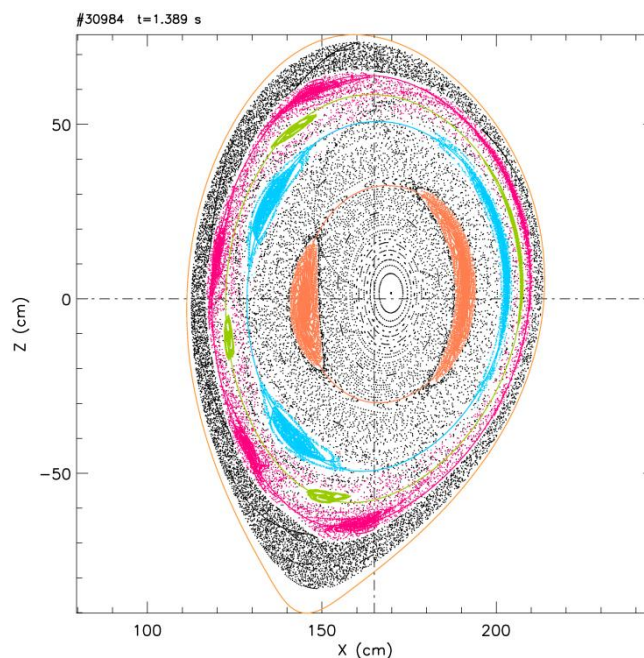


Fig. 3.3.7 Reconstruction of the magnetic topology of a L-mode density limit discharge in ASDEX-U (shot #30984, $t=1.39$ s), prior to a minor disruption ($t=1.4$ s) due to the growth and locking of a large $3/1$ mode. It is evident the contribution of other harmonics, $2/1$, $4/1$ and even $5/1$.

3.3.5 *Divertor Test Tokamak studies (DTT)*

An activity related to the power exhaust modelling has started together with the modelling of the alternative DEMO configurations. The final aim of this activity is to model the power load on the target in the divertor configuration alternative to the standard Single Null Divertor (SND) configuration. In particular the following configurations have been considered: the X Divertor (XD), the Super-X Divertor (SXD), the SnowFlake Divertor (SFD). An analysis of all configurations has been already done with the simplified edge code TECXY and with the more detailed SOLPS code in the SD, SXD and SXD cases. These analyses present

some limitations because a fluid model has been used and SOLPS was impossible to deal with the SF equilibrium. For these reasons together with an improvement of the analysis with the same code, a modelling activity with SOLEDGE2D-EIRENE code has started, which is more flexible in terms of magnetic equilibria.

3.4 NBI Accompanying program

During 216 activities aimed to prepare the Team for the operation of the Test Facility, to improve the understanding of the fundamental processes and to develop new concept in sight of the NBI system for DEMO, have progressed. NIO1 has regularly operated during the year, a novel configuration of magnets has been successfully tested in collaboration with the former JAEA Team in Naka, new measurements of beam transport including charge compensation related processes have been carried out in collaboration with NIFS, the collaboration with other leading laboratories has been pursued. HV holding theory and experiments have contributed to improve the present understanding and progress toward a better comprehension of the underlying processes.

3.4.1 *NIO1 operation*

The NIO1-related activities performed during 2016 can be divided into the following categories: improvements to the plants and experimental operation.

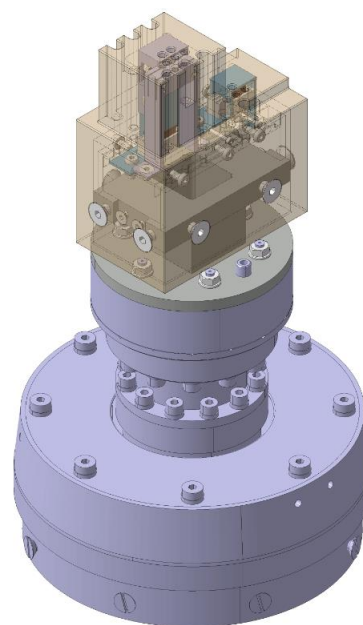


Fig. 3.3.8 3D view of the HRP probe head designed for W7-X fast reciprocating manipulator

The operation was shut off four times for a total down-time of 4 months, including the holiday periods throughout the year. One of the shutdowns was due to air leak after the occurrence of a small crack on the pyrex insulator below the radiofrequency coil; another shutdown was due to the Extraction Grid Power Supply being damaged by the occurrence of large and sudden currents flowing between plasma grid and extraction grid. During these unexpected shutdowns several minor and major improvements were performed as described below, including the modification of the return path of the magnetic circuit, including two more “C”-shaped conductors located on the external surface of the front multipole, so as to increase the region of the source plasma affected by the magnetic filter field.

One more shutdown was devoted to the temporary installation of a Langmuir probe, to characterize the source plasma in different operating conditions; the probe was inserted into the source from the downstream side of the accelerator, so that, when measuring in the vicinity of the plasma grid, the plasma disturbance was minimized. The last shutdown, in December 2016, was dedicated to the removal of the Langmuir probe and to the modification of the magnetic filter field, by changing the configuration of the magnets located in the front multipole so as to provide a magnetic filter field also in the absence of currents flowing through the plasma grid and to increase the overall strength of the filter field itself. During this shutdown, the plasma grid and the bias plate was protected by means of molybdenum liners so that now no copper is exposed to the plasma in the source; the pyrex insulator was also changed, as it exhibited some colouring presumably due to re-deposited particles.

The following improvements to the machine were performed in 2016:

- finalization, installation and test of a fast interlock system to switch the high voltage power supplies off in case of accelerator breakdowns;
- installation and test of a fluxmeter to control the amount of injected gas; however the fluxmeter is not used, because of radiofrequency interference;
- realization of a PID controller for the source pressure, based on the Pirani gauge installed in the source and on the electromagnetic valve used for gas injection;
- finalization of the beam emission spectroscopy diagnostic;
- construction and first test of a Langmuir probe for the characterization of the plasma in the vicinity of the beam in the beam drift region;
- construction of a retarding field analyzer for the characterization of the space charge compensation in the beam drift region;

-
- construction and operation of a Langmuir probe for the characterization of the plasma inside the radiofrequency source;
 - the CFC tile (mini-STRIKE) collecting the beam was insulated from its supporting structure and was moved as close as possible to the beam source;
 - development of distributed measuring systems based on the Raspberry PI microcontroller; correspondingly the front-end circuitry for measuring the current through the post-acceleration electrode, the repeller and the CFC tile was realized;
 - design and realization of new circuitry for thermocouple signals;
 - insulation of the magnetic bias plate from the plasma grid and connection to the electrostatic bias plate; installation of a power supply to polarize the bias plate with respect to either the plasma grid or the source walls;
 - modification of the magnetic circuit, by introducing the “C”-shaped conductors and by use of permanent magnets as already briefly described;
 - design and test of a prototype protection system for the extraction grid power supply in case of breakdowns, involving the use of DIACs, which will allow to attain the nominal performances of the accelerator.

The advances in the Acquisition, Data Retrieval, Interlock and Control Systems are described in ⁹⁰. They include: the realization of a database, based on PostgreSQL, of the measurements averaged over some hundreds ms; the use of Raspberry PI microcontrollers for generation and acquisition of signals.

Concerning NIO1 operation, the main topic of 2016 was the characterization of beam extraction and acceleration; experiments with the following gases were performed: hydrogen, air, oxygen, mixture of oxygen (90%) and argon (10%). The RF power was limited to 1200W to preserve the pyrex insulator ⁹¹.

Depending on gas pressure used, NIO1 was up to now operated with total voltage <25kV for beam extraction, whereas 60kV were applied for insulation tests. The distinction between capacitively coupled plasma (E-mode, consistent with a low electron density plasma) and inductively coupled plasma (H-mode, requiring larger electron density) was clearly related to several experimental signatures, and was confirmed for several gases, when the applied radiofrequency power exceeds a given threshold P_t (which exhibits hysteresis). For hydrogen P_t was <1kW, with a

⁹⁰ G. Serianni et al., Acquisition, Data Retrieval, Interlock and Control Systems for the Negative Ion Source NIO1, 5th International Symposium on Negative Ions, Beams and Sources 12-16 September 2016, Oxford, UK, poster MonP5; submitted to AIP Conf. Proc..

⁹¹ M. Cavenago et al., Improvements of the Versatile Multiaperture Negative Ion Source NIO1, 5th International Symposium on Negative Ions, Beams and Sources 12-16 September 2016, Oxford, UK, oral presentation MonO8; submitted to AIP Conf. Proc..

clean radiofrequency window and molybdenum liners on most of the surfaces exposed to the plasma; for oxygen $P_t \leq 400W$. Beams of H^- and O^- were separately extracted; since no caesium has yet been introduced into the source, the expected ion currents are much lower than the target values, requiring a lower acceleration voltage (to keep the same perveance). Increasing the current in magnetic filter circuit, modifying its shape, and increasing the bias voltage were helpful to reduce the ratio of co-extracted electrons to negative ions (still very large: ~ 150 for oxygen, and ~ 40 for hydrogen), in qualitative agreement with theoretical and numerical models.

For the preliminary tests of the extraction system the source was operated in oxygen, whose high electronegativity allows to reach useful levels of extracted beam current. The efficiency of negative ions extraction is strongly influenced by the electron density and temperature close to the plasma grid, i.e. the grid of the acceleration system which faces the source. To support the tests, these parameters were measured by Optical Emission Spectroscopy, requiring the use of an oxygen-argon mixture⁹². The intensities of specific Ar I and Ar II lines were measured along lines-of-sight close to the plasma grid, and were interpreted with the ADAS package to get the desired information. This method was applied to the measured data so as to obtain electron density and temperature as functions of the main source parameters (RF power, pressure, bias voltage and magnetic filter field). It was found that not only the electron density but also the electron temperature increase with RF power; both decrease with increasing magnetic filter field. Variations of source pressure and plasma grid bias voltage appear to affect only electron temperature and electron density, respectively.

Both for the tests with oxygen and with hydrogen a 1D-CFC (carbon-fibre-carbon composite) tile was used as a calorimeter to determine the beam properties by observing the rear surface of the tile with an infrared camera⁹³; the same design was applied as for STRIKE, one of the diagnostics for SPIDER. A direct electrical measurement of the current impinging on the tile was also performed and was successfully cross-checked with the calorimetric estimate obtained by the infrared image. The large ratios (in the range 0.2-1.5) between the current impinging on the post-acceleration grid and that hitting the CFC tile suggest that beamlet divergence is

⁹² M. Barbisan et al., Electron Density and Temperature in NIO1 RF Source Operated in Oxygen and Argon, 5th International Symposium on Negative Ions, Beams and Sources 12-16 September 2016, Oxford, UK, poster MonP8; submitted to AIP Conf. Proc..

⁹³ A. Pimazzoni et al., A First Characterization of the NIO1 Particle Beam by Means of a Diagnostic Calorimeter, 5th International Symposium on Negative Ions, Beams and Sources 12-16 September 2016, Oxford, UK, poster MonP1; submitted to AIP Conf. Proc..

quite high, as expected for low current operation. Beamlets are in fact not yet distinguishable even if a global trapezoidal shape can be identified, due to the alternate deflection of the beamlet columns in the vertical direction caused by the permanent magnets in the extraction grid. The beam divergence is generally $>1^\circ$. Variations of the beam width can be seen on the calorimeter as voltages are changed. This behavior suggests that the beamlet deflection is large enough in this range of extraction voltages (U_{ex}) to overcome the effects of optics. As deflection is proportional to the inverse square root of the voltage ($U_{ex}^{-1/2}$), the effect of variation of the voltage ratio is expected to be seen clearly when the extraction voltage is increased. The best optics conditions with the present parameters were identified.

As already mentioned, at the end of 2016 an experimental campaign was devoted to the characterization of the plasma source by means of a Langmuir probe in different operating conditions; preliminary results show that the trends of electron temperature and density as functions of the source parameters have been obtained; detailed data analysis is in progress and will continue in 2017.

The experimental data, spectroscopic measurements, were interpreted also with the support of finite element simulations of the magnetic field and a dedicated particle in cell (PIC) numerical model for the electron transport across it, including Coulomb and gas collisions. The original filter field of NIO1, employing a current up to 400A flowing from the plasma grid into the bias plate electrodes was improved by realizing an alternative return circuit for the current using an external conductor. The integral of the magnetic field was enhanced by a factor of 2 in the extraction region of the experiment. The larger field, though penetrating the driver region, has no measurable effects on the RF coupling. The electron temperature, on the other hand, was effectively decreased, and the electron current recorded on the extraction grid power supply can be now decreased by 30% to 60% depending on feeding gas and operating pressure. These numerical results correspond to the measurements⁹⁴.

The numerical simulation activities in 2016 included the definition of an improved magnetic configuration, particularly concerning the co-extracted electron suppression magnets embedded in the present extraction grid and in the new extraction grid (with improved electrostatic optics) that will be installed in 2017. The finite element code OPERA 3D was used to investigate the effects of the three sets of magnets on

⁹⁴ P. Veltri et al., Study of electron transport across the magnetic filter of NIO1 Negative ion Source, 5th International Symposium on Negative Ions, Beams and Sources 12-16 September 2016, Oxford, UK, oral presentation FriO5; submitted to AIP Conf. Proc..

beamlet optics ⁹⁵. Comparisons of numerical results with measurements were performed when possible. Operations in oxygen and hydrogen gases were compared in the numerical investigations.

Beam energy recovery can be realized by decelerating the charged particle in collector electrodes. Recently an axi-symmetric collector was proposed for beam energy recovery of the non-neutralized fraction of the D beam. A specific axisymmetric collector was designed and simulated for the test of beam energy recovery in NIO1. The simulation, carried out with COMSOL and confirmed by OPERA, showed that the system could collect more than 98% of the ions with an average recovered energy of about 95% ⁹⁶.

During 2016 two molybdenum samples were exposed to the caesium vapour emitted by the caesium oven built for the NIO1 experiment; the deposition was performed in a dedicated vacuum vessel; the sample exposure time was different. Different positions over the sample surfaces were analysed by the XPS technique. The results show a larger presence of caesium on the sample exposed for the longer time; caesium is found to be oxidised probably due to exposure to some amount of air after the deposition. Fluorine and silicon are also detected, probably due to pollution by pump oil.

3.4.2 *Breakdown Modelling for HV Holding*

Breakdown events greatly limit the high-voltage insulating capability of a vacuum gap and thus a lot of studies have been dedicated to this subject from its very beginning. Nevertheless, a whole comprehensive and satisfactory picture is still missing.

In general, experiments show that the electric charge exchanges between electrodes reveal itself as very small current (nano-currents or dark currents); this current is often characterized by bursts (micro-currents), often coincident with pressure bursts; the breakdown is eventually characterized by high current, limited only by the external circuit impedance,

The proposed BIRD model is an attempt to put these experimental evidences inside a unique interpretative framework. It is based on the existence of a dielectric layer on the cathode surface which is subjected to charging process due to dark current.

⁹⁵ C. Baltador et al., Finite elements numerical codes as primary tool to improve beam optics and support measurements in NIO1, 5th International Symposium on Negative Ions, Beams and Sources 12-16 September 2016, Oxford, UK, poster MonP2; submitted to AIP Conf. Proc..

⁹⁶ V. Variale et al., Energy Recovery From Mixed H-/H⁰/H⁺ Beams and Collector Simulations, 5th International Symposium on Negative Ions, Beams and Sources 12-16 September 2016, Oxford, UK, poster MonP11; submitted to AIP Conf. Proc..

Above a certain electric field inside this layer, microbreakdown (“rupture”) occurs, generating current bursts that potentially develop into breakdown events.

Thus, in the BIRD model context, the breakdown is considered as a three-step process:

In each one of the three phases, there is

- A threshold value, necessary to switch-on the electric current
- A limiting process that counter-balances the current producing mechanisms and that could eventually damp down the current itself.

With regard to the current and pressure bursts, the model forecasts a threshold situation, when the internal electric field reaches the dielectric strength of the layer. If this threshold is reached a disruptive discharge through the material can be originated with the formation of a localized electrically conductive path, thus a burst of electrons is emitted from the cathode surface to the anode. The ionized desorbed gas could determine the capture of electrons, thus stopping the avalanche (exponential) process due to radiative emission of secondary electrons. This phenomenon, known as Photo-Electric Cascade Mechanism ⁹⁷, is compatible with the total voltage effect, as shown in ⁹⁸

Increasing voltage, the burst could evolve in the full breakdown. The possibility of a breakdown evolution is mainly determined by the rapidity of the current amplification mechanisms compared with the damping phenomena.

3.4.2.1 Results on model validation

In the year 2016 the activity was concentrated mainly on the investigation at a micro-current level.

It has been found a good correlation between the start-times of current, pressure bursts and X-rays radiation.

For a constant voltage difference, the rate of burst event is a decreasing function of



Fig. 3.4.1 Breakdown as a three step-process
time (see Fig. 3.4.2).

⁹⁷ R. Latham, High Voltage Vacuum Insulation New Perspective, 2006, AuthorHouse.

⁹⁸ A. De Lorenzi, N. Pilan, E. Spada, "Progress in the validation of the voltage holding prediction model at the high-voltage Padova test facility", IEEE Trans. Plasma Sci., vol. 41, no. 8, pp. 2128-2134, Aug. 2013

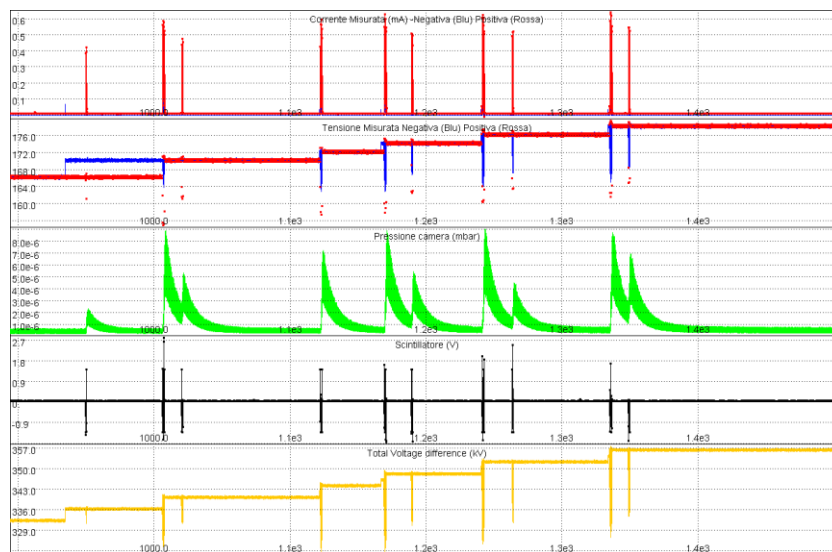


Fig. 3.4.2 #1602160931# signals

Further investigations have been carried out in an asymmetric setting of electrodes, like a sphere-plane configuration and the outcome should depend on the choice of the polarity. In fact if the starting process is essentially due to the cathodic electric field, it is known that it assumes different values on the two surfaces.

Let E_s and E_p be, respectively, the surface electric field on the spherical and plane electrode. It is that $E = f \beta \frac{V}{h}$ where $f_{s,p}$ is the shape factor due to geometry and β is the local amplification coefficient and v and h the voltage and distance.

Experiments with the negative polarized planes and spheres, at varying distances have been conducted and the first burst (breakdown) recorded. The valuable result is that the β values span in the range (1 ÷ 4.7) more credible than the much greater value ($\sim 10^2$) usually found analysing the dark-current behavior with the Fowler-Nordheim model.

3.4.3 Voltage Holding Prediction Model activities

In 2010 it has been proposed⁹⁹ the Voltage Holding Prediction Model VHPM, an innovative tool to face the problem of the voltage breakdown determination in an electrostatic system of any complexity, based on the following experimental evidences: i) the Total Voltage Effect; ii) the probabilistic nature of the breakdown voltage occurrence; iii) the electrodes area effect on the breakdown voltage (the

⁹⁹ N.Pilan, A. De Lorenzi and P. Veltri IEEE Trans. on Dielectr. and Elec. Insul. Vol. 18, No. 2; April 2011

larger the area, the lower the breakdown voltage; iv) the polarity effect (inverting the polarity for an electrostatic system with all the electrode in the same condition - material and treatment- the lowest breakdown voltage occurs when negative polarity is applied in the classical configuration of sphere/plane electrodes).

In 2016, the VHPM has been applied to the full scale prototype of the high voltage bushing SF6-Vacuum for the ITER NBI injector (1 MV max. voltage; multi electrode system, with the longest gap of 1300 mm to sustain 1 MV; a HV test campaign has been carried out at the QST laboratory in Naka. aimed to reach the full voltage holding capability. In this case, the model predictions based on eq. 1

$$P = 1 - \exp \left[- \int_{Ac} \left(\frac{E_A^\alpha \cdot E_C^\gamma \cdot U}{W_0} \right)^m \cdot dA \right] \quad 1)$$

have shown some inconsistencies with the measurements. A possible explanation has been envisaged in the inappropriate values of the exponents α, γ derived from Cranberg-Slivkov model ($\alpha=2/3, \gamma=1$).

During the year it has been proposed to keep the eq. 1 unvaried giving up the exponents α and γ so far adopted, the new values will be obtained fitting the experimental results of the HVPTF and QST laboratories.

The activity is ongoing, it foreseen a close collaboration with QST researchers to improve the VHPM model.

A new diagnostic system has been added in the HVPTF laboratory. A NaI probe has been implemented to obtain a better knowledge of the X ray emission which is typically observed during the high voltage conditioning phase.

The study of the X rays spectra, generated by the bremsstrahlung radiation of electrons at the anodic surface, could be the way to understand the energy of the impinging electrons at the anode side adding a further step in the explanation of the physical phenomena governing the voltage holding in vacuum.

A particular configuration, having a needle at the cathode side, has been implemented in order to calibrate the system through the enhance emission of electrons due to the electric field.

An interesting correlation between the energy of the X ray and the drained current has been observed during the tests.

3.4.4 *Modelling of beam acceleration*

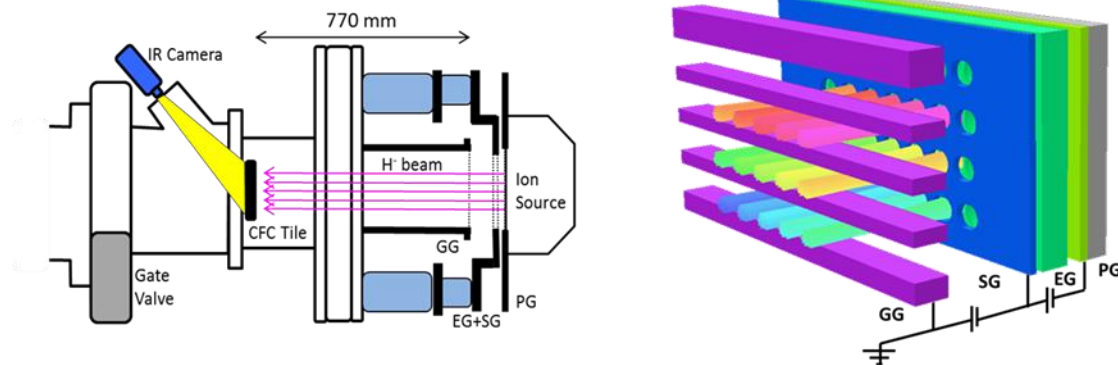


Fig. 3.4.3 Figure 1 a) Schematic of the RNIS beamline, with the CFC calorimetric target mini-STRIKE (MS) installed, top view. b) Sketch of the accelerator domain (3x5 beamlets corresponding to the PG mask) used in the numerical simulations. The beamlet trajectories calculated by the OPERA code are also shown.

The modeling activities on the beam acceleration during 2016 involved a thoroughly benchmark of the codes used for the design of the MITICA and SPIDER sources, against the results collected in existing experiment, mainly during the collaboration with the NIFS institute. In particular, the optics of the beam, simulated with the OPERA code, was compared against the infra-red images of 15 beamlet footprints collected on the beamlet monitor installed in the NIFS test stand. Fig. 3.4.3 reports the schematic of the diagnostic system installed on the NIFS test stand and the ray tracing model code OPERA used to model the beam acceleration.

The beam optics calculated with the ray tracing code OPERA shows a reasonable agreement with the experimental data both in terms of beam space charge (current

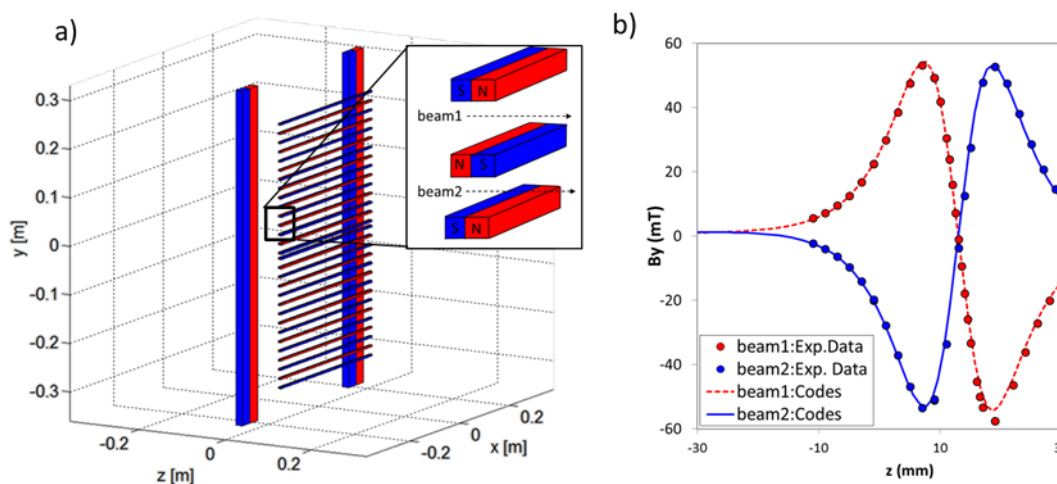


Fig. 3.4.4 Figure 3 a) layout of the permanent magnets in the NIFS test stand. In b) the magnetic field profile B_y calculated with the code NBIMAG (solid line) or measured with the Hall sensor are compared.

density) and focusing dependences. A careful estimation of the extracted beam current was fundamental to allow the comparison, and the availability of different diagnostics was important in this sense.

The codes for the pressure distribution (AVOCADO), secondary production (EAMCC) magnetic field profiles (NBI-MAG) were benchmarked as well (see Fig. 3.4.4). The models used for the simulation of the magnetic field distribution exhibit a high reliability, as resulting from the direct comparison of their results with measured values.

The application of the molecular flow code (AVOCADO) to a real vacuum system of nuclear fusion device was carried out: the measured gas pressures in the ion source

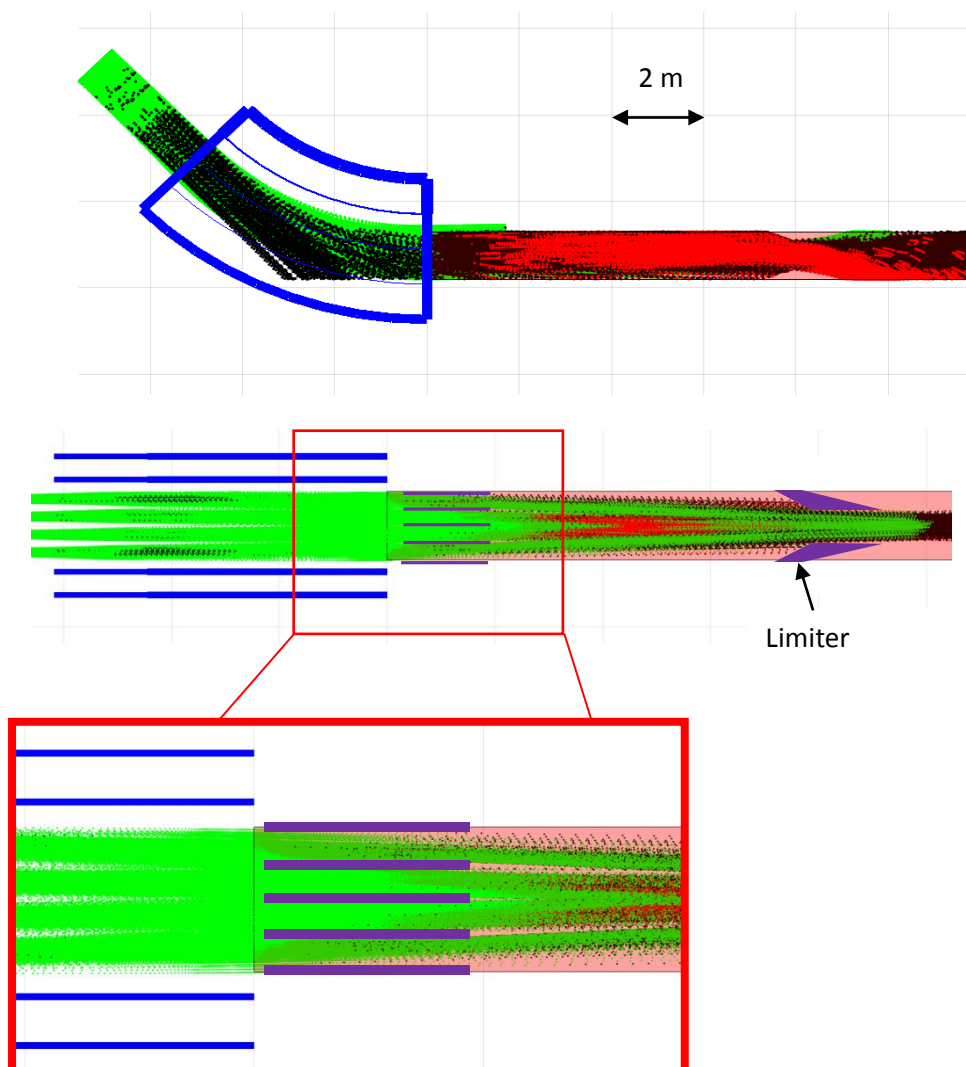


Fig. 3.4.5 Results of the ray tracing Monte Carlo code . Fast particles H-, H0 and H+ are represented respectively in green, black and red colors.

and in the vessel, and the metering valve settings controlling the injected throughput were used as benchmarks for the simulation showing a small discrepancy and highlighting uncertainties due to the operation in transient conditions of the ion source. The gas density profile along the accelerator was then included in the beamline models to calculate the H- beam losses.

The beam loss due to stripping caused by the gas density along the accelerator was included in the simulation to allow a more precise calculation of the beam space charge. A less satisfactory agreement was found concerning the simulation of beamlet deflection induced by magnetic and electrostatic effects, which appears to be underestimated by a factor of ~ 2 with respect to the experimental results. Since magnetic fields are measured exactly, the motivation of such discrepancy most likely resides in aspects not yet included in the OPERA code. A possible explanation, based on non-uniform H- extraction caused by the magnetic field, was proposed. This specific topic is of particular interest and surely deserves further investigations.

From the point of view of the beam transport through the accelerator and up to the calorimeter, simulated with the modified EAMCC code, a reasonable affinity with the IR data was found. Nonetheless some open points still needs further investigations, such as the alignment of the beamlet belonging to the same row, whose cause is not reproducible with the set of codes used so far. More in general, the use of the CFC calorimeter for the aim of the code benchmark was satisfactory, and the diagnostics showed a high reliability if a proper post processing of IR images is provided.

3.4.4.1 Modelling of secondary plasma formation by beam gas interaction and impact on alternative neutralization

The propagation of an ion beam is permitted by the production and confinement along the beam path of charged particles of opposed polarity. This process, called space charge compensation, for relatively high pressures such as the one of interest for neutral beam injectors, leads to the formation of a secondary plasma. An example of space charge compensation is shown in Fig. 3.4.6, which presents a transient simulation of space charge compensation and molecular ion plasma formation. The characteristics of the secondary plasma in negative-ion beam systems are of interest for their effect on beam optics and ion beam neutralization. All these aspects have direct implications in the ITER Heating Neutral Beam and the operation of the prototypes, SPIDER and MITICA, and also have important role in the conceptual studies for NBI systems of DEMO.

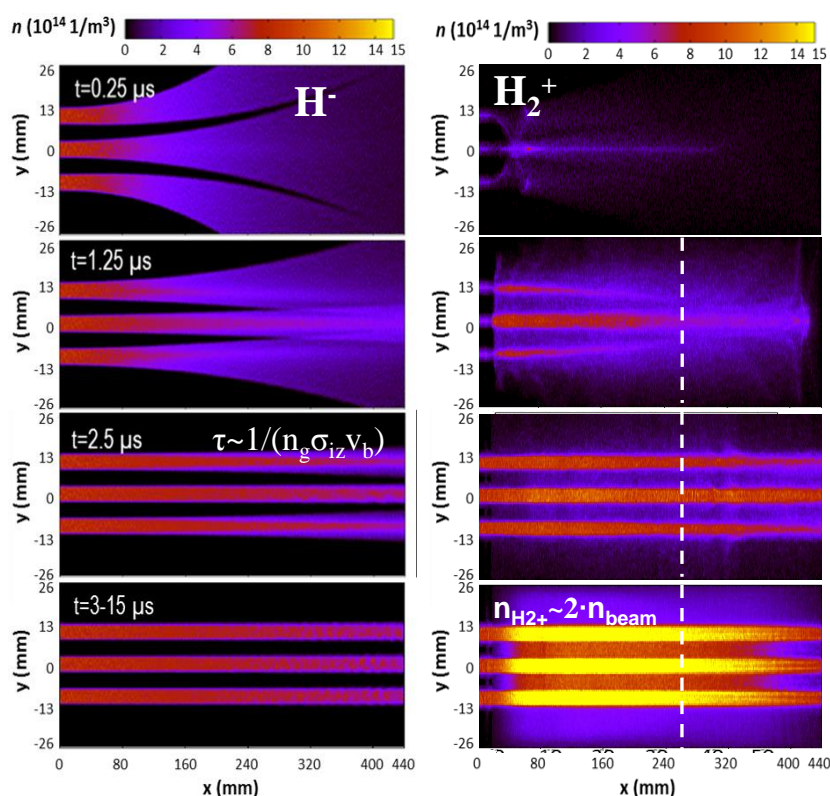


Fig. 3.4.6 Particle in cell transient simulation of a negative ion beam propagating through uniform background gas pressure of 50 mPa; on the left hand side, beam particle density; on the right hand side, density of the molecular ion secondary plasma

The measurement of the plasma density, plasma potential, and the energy spectrum of secondary particles in the drift region of a negative ion beam offers an insight into beam-induced plasma formation and beam transport in low pressure gasses. At present experimental data are lacking. Therefore during 2016, in collaboration with the National Institute for Fusion Science, the secondary plasma in the drift tube of a multibeamlet negative ion beam has been studied experimentally. Fig. 3.4.7 shows the experimental setup of the beam line diagnostics. The Retarding Field Energy Analyzer is highlighted on the side of the beam. An example of integral energy distribution function for ions and electrons is shown in Fig. 3.4.8, together with the dependency of plasma parameters on the background gas pressure.

The experimental results will be compared to the numerical simulations, in order to validate and possibly improve the models presently available.

It is well known that an ionized gas target offers higher cross sections for neutralizing a negative ion beam, with the main parameter being the ionization degree of the gas target. If the self-produced secondary plasma is very well confined, and its formation is enhanced, it is possible to improve the neutralization efficiency of neutral beam

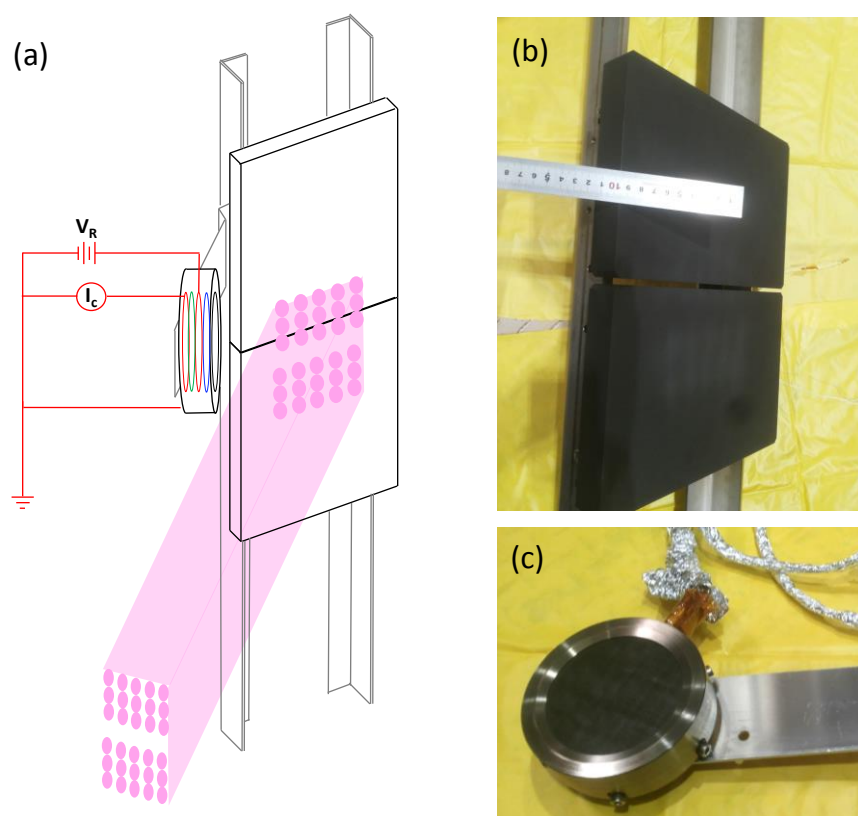


Fig. 3.4.7 (a) Sketch of carbon calorimeter and RFA installed in the NIRS (NIFS institute, japan); (b) picture of the carbon calorimeter after use and (c) picture of RFA after use

injectors. This improvement would not affect the system in terms of safety (passive system), with a minor cost in terms of complexity (magnetic field).

Anyway, since plasma formation is to be obtained by a special configuration of magnetic fields (preferably obtained by permanent magnet only) some trial experiments with reduced-size prototypes are necessary. The feasibility study of such a system for NIO1 has been carried out during 2016. The gas neutralizer has cylindrical symmetry and a simple magnetic configuration such as that produced by a coil.

A preliminary calculation of steady-state plasma density has been performed by a diffusive plasma model. The model takes into account the collisional frequency of charges against plasma particles and neutrals. It also assumes ambipolar diffusion along each direction parallel and perpendicular with respect to the magnetic field lines, and partially include the effect of “magnetic bottles” to confine the plasma at the open edges of the neutralizer.

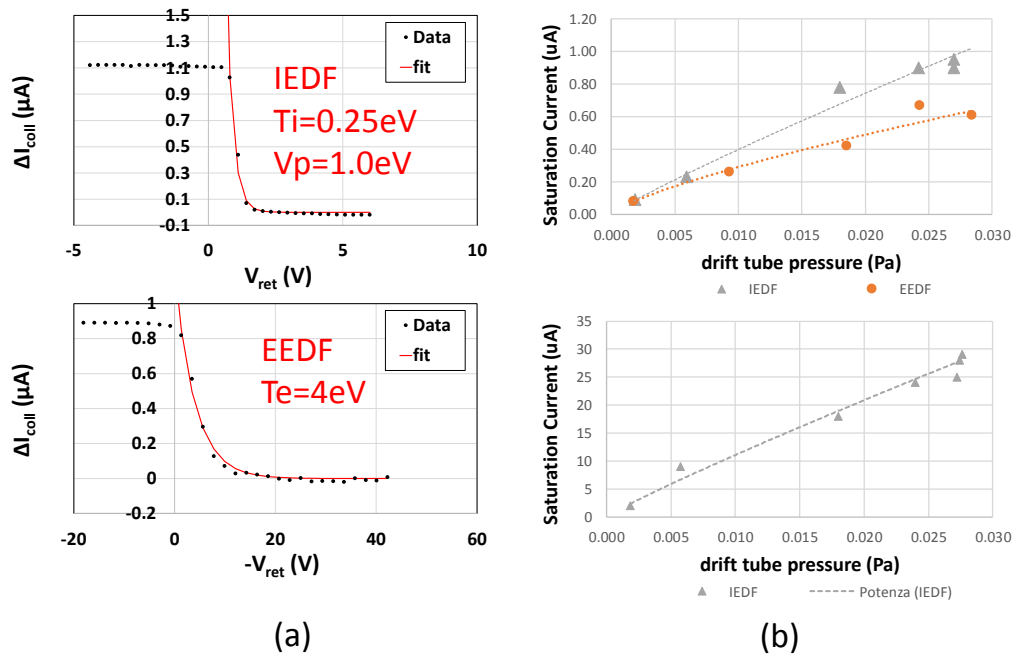


Fig. 3.4.8 (a) RFA characteristics and preliminary analysis to obtain the integral ion and electron energy distribution function; (b) dependence of the saturation current on the beamline pressure, obtain by the probe in RFA or Langmuir mode

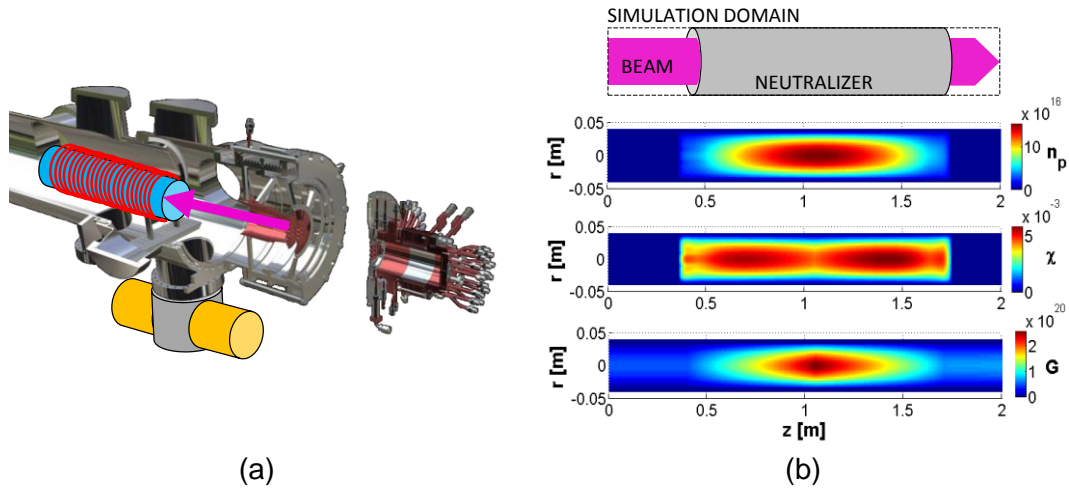


Fig. 3.4.9 (a) Scheme of installation in NIO1 with the neutralizer (blue) and the cryopumps (yellow) highlighted; (b) calculated plasma density, ionization degree, and source term for the ions

Preliminary calculations indicate that the secondary plasma could reach a density in the range of 10^{17} m^{-3} . Though the ionization degree (about 0.5%) is too low to produce a consistent effect on the neutralization yield, nevertheless, the proposed experiment could provide a proof of principle that high density plasmas can be generated by negative ion beams, and offers the possibility of testing advanced measurement to characterize such a plasma.

3.4.5 *Development of alternative concepts: the bent beam*

A further step in design the bent neural beam injector¹⁰⁰ has carried out in 2016. The Monte Carlo Code, utilized to simulate the injector performances, has been improved by adding a detailed geometry of the neutralizer. Five panels have been inserted in the neutralizer region in order to limit the flux of gas to the Beam Source. A limiter has been added to decrease the flux of molecules lost downward the neutralizer.

The distribution of the background gas along the injector has been verified by using lumped model and an equivalent scheme of conductances (see Fig. 3.4.10).

The same model has been adopted to verify the possibility to implement a set of vacuum pumps located at the plasma source potential, the pumps should be able to reduce the pressure downward the extraction grid decreasing the stripping losses inside the electrostatic accelerator.

3.4.6 *Collaboration with other Laboratories and Institutions*

3.4.6.1 IPP

During 2016 the collaboration with IPP involved the training in ELISE of 12 RFX personnel distributed over 4 weeks, regarding several aspects of the operation and of the plants. Specifically, concerning the latter, topics included electrical, mechanical, magnetic and radiofrequency aspects and also the description of the new features with respect to the past (like, among others, the new insulators of the RF coils as well as the addition of permanent magnets on the source walls, allowing to increase and to decrease the magnetic filter field).

The operation included experiments regarding the start-up phase of the machine and the characterization of the beam features (position, width) in correspondence to scans of the source and accelerator parameters; in particular the influence of the magnetic filter field on the broad component of the beam, in different conditions of beam optics, was investigated.

During 2016 a collaboration activity with IPP was dedicated to the characterization of the angular distribution of beam particles, as measured by the Beam Emission Spectroscopy (BES) diagnostic. The behavior of the beam was studied also by measuring the currents flowing through the Grounded Grid and the metal box surrounding its exit. The broader component of the beam was found to be reduced

100 N. Pisan, V. Antoni, A. De Lorenzi, G. Chitarin, P. Veltri, and E. Sartori, Rev. of Sci. Ins. 87, 02B325 (2016)

when the permanent magnets are weakening the magnetic field produced by the current through the plasma grid ¹⁰¹.

3.4.6.2 Collaboration with NIFS

The collaboration with the National Institute for Fusion Science during 2016 involved the study of negative ion beam optics and the influence of the space charge compensation in the drift region of the beam. The experimental campaign was carried out with a new version of the beamlet monitor used during 2014 and 2015 (MiniStrike) developed at NIFS. This new design includes a set of graphite tiles capable of accommodating more beamlet and is monitored with the infrared camera (FLIR) that looks at the thermal pattern from the front side (in former campaign the

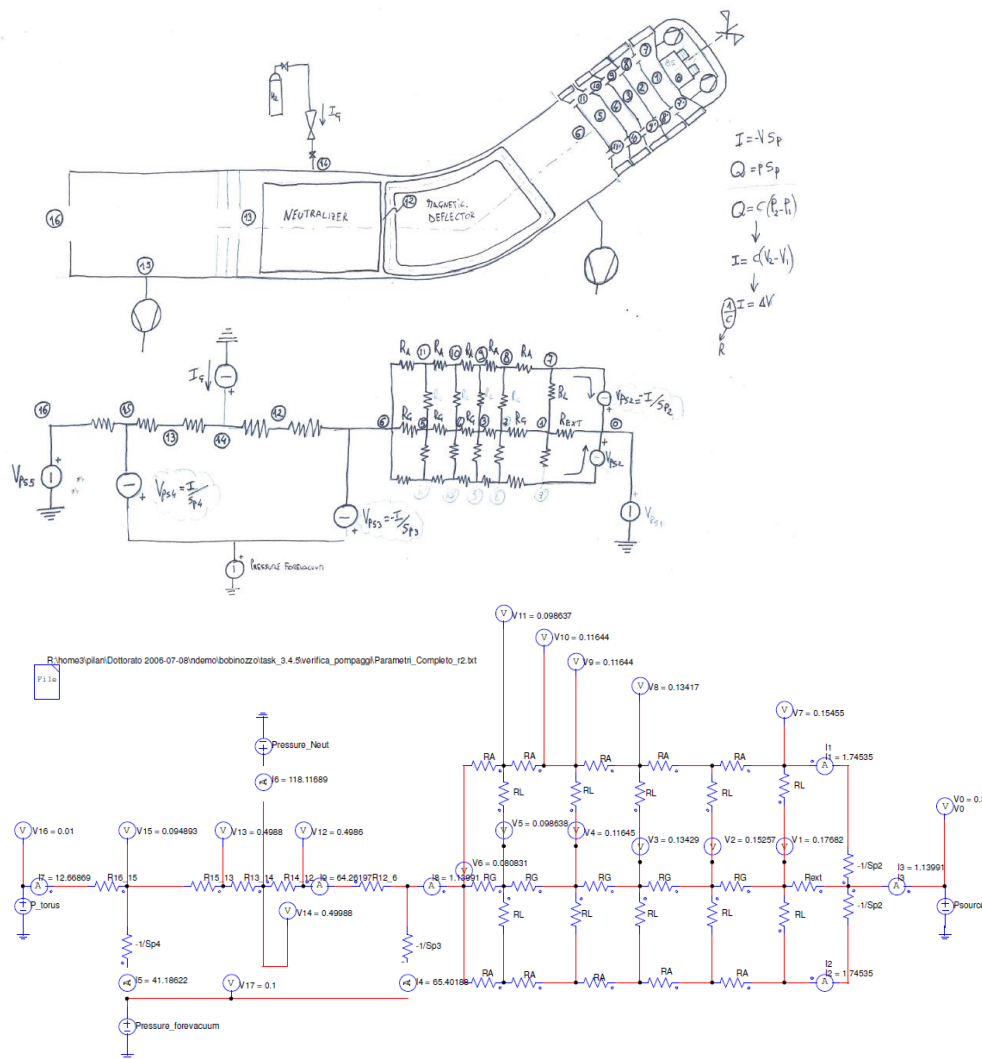


Fig. 3.4.10 Equivalent scheme of conductances adopted to calculate the pressure distribution in the bent beam line vessel.

camera was monitoring the rear tile. The graphite tiles were also insulated from the vessel, to carry out measurements of the beam current collected on them. Moreover, a novel diagnostic was installed in the beam line; it is a residual field energy analyzer (RFEA) developed at RFX and tested in the Magnetron sputtering device at RFX. This probe includes large collection area, to maximize the signal of the particle collected from the tenuous plasma formed by beam-gas interaction in the drift region. A 4 potential grid system discriminates the particles according to their energy (electron or molecular ions) so that the current collected on the last electrode can be used to infer the energy spectra of electrons and ions. During the campaign the probe was used during various scan of the source and beam parameters. A dedicated gas injection line was also installed, to increase the pressure of the residual gas in the beamline independently from the gas in the source.

3.4.6.3 Collaboration with QST

During 2016, the collaboration agreement established in 2015 between Consorzio RFX and QST (National Institutes for Quantum and Radiological Science and Technology, Neutral Beam Heating and Technology Group) Naka, Japan (formerly JAEA) has fostered several joint activities in support to the Neutral Beam Injector for ITER and JT60-SA:

- First experimental tests of the grid electrostatic configuration and magnetic configuration adopted for the MITICA and ITER HNB accelerator. The experiments have been jointly carried out on negative ion accelerator already available at QST, Naka.

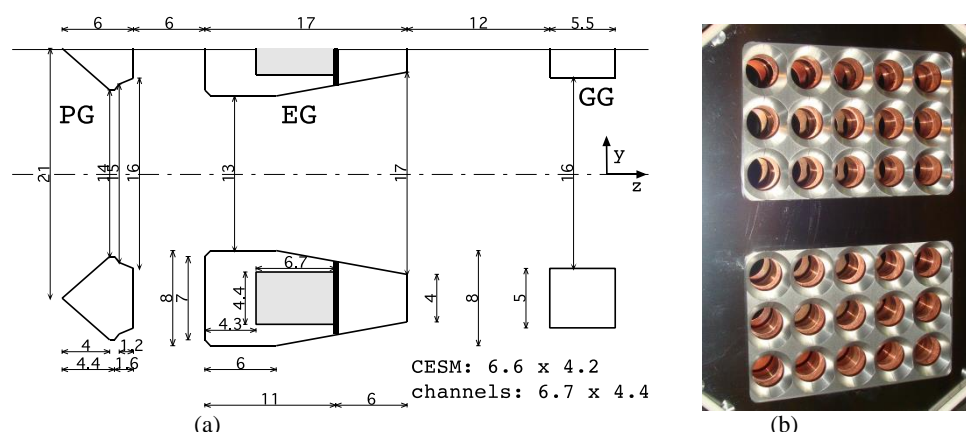


Fig. 3.4.11 (a) vertical cross section of the NITS accelerator with the EG (built by Consorzio RFX) and the PG (built by QST); the aperture profiles and gap lengths have been scaled so as to reproduce as close as possible the MITICA/HNB geometry. (b) photo showing the accelerator grids during assembly.

- Benchmark of the numerical simulation developed by QST and RFX teams, (using different codes SLACCAD, OPERA, BEAMORBT, COMSOL, EAMCC) against the experimental data obtained in the above mentioned campaign.

In agreement with QST Naka, the joint experiments have been designed mainly as relevant experimental benchmarks of the magnetic and electrostatic design of the MITICA and ITER/HNB accelerator. To this purpose, an accelerator grid system, based on the same design concepts and geometry and very similar to that of MITICA, was prepared and installed in the NITS (Negative Ion Test Stand) at the QST lab in Naka, Japan.

The Extraction Grid (EG), designed and built by Consorzio RFX, featured the same aperture profile as in MITICA and included both the standard Co-extracted Electron Suppression Magnets (CESM) and the Asymmetric Deflection Compensation Magnets (ADCM). The ADCM allow to counterbalance the undesired beam deflection caused by the electron-suppression magnetic field (also called criss-cross deflection), which is typical of negative ion accelerators. However, during the experiments, the ADCM were mounted only on half of the apertures, so as to provide direct comparison of the beamlet optics with and without ADCM.

The Plasma Grid (PG) was designed and built by QST, with a tapered aperture profile identical to that of MITICA. The grid profiles are shown in Fig. 3.4.12. The NITS device was also provided with an unidirectional CFC target and an IR camera with tele-lens, so as to directly measure the beam energy deposited and the negative ion beamlet deflection, divergence and power, see Fig. 3.4.12

The design of the EG is described in a paper presented at the SOFT 2016 conference [102]. The results of these experiments are reported a paper presented at

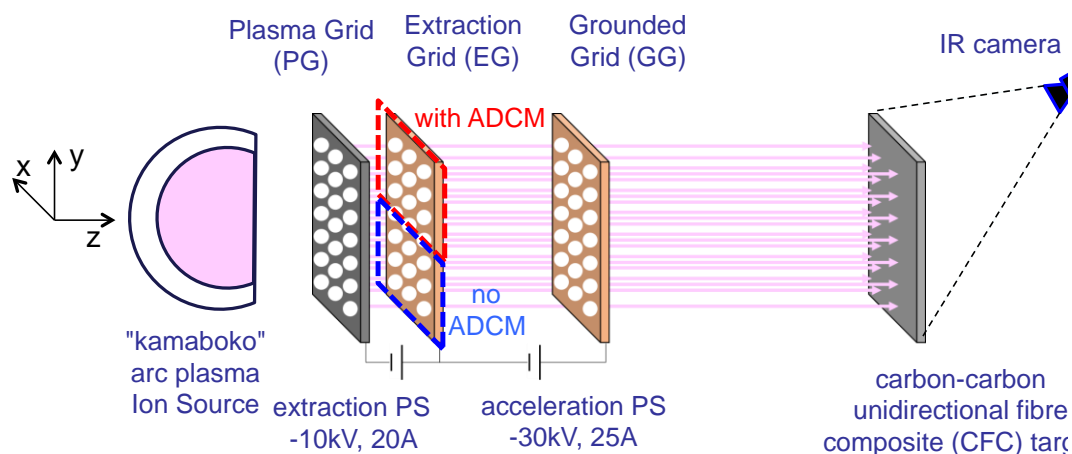


Fig. 3.4.12 conceptual scheme of NITS test facility at QST (Naka, Japan) and set-up for the joint experiments.

NIBS2016 [¹⁰³].

The joint experimental campaign was carried out on NITS first without Cs, reaching an acceleration voltage up to 30 kV and an extracted ion current density of $\sim 30 \text{ A/m}^2$. The joint experiments were then continued using Cs in the ion source, allowing to test for the first time the optics design of the MITICA/HNB accelerator. A beamlet divergence lower than 10 mrad was obtained, up to an extracted H⁻ ion current density of 170 A/m².

Divergence and deflection of the ion beamlets were measured under various conditions as shown in Fig. 3.4.13. The experiments showed that the ADCM can very well compensate the criss-cross deflection and guarantee good beamlet optics under a wide range of operating parameters. Both the simulations and the experiments showed linearity with magnet strength (additional simulations also show linearity with magnet size), even though the absolute deflection from the experimental results was slightly different from the one predicted using OPERA and COMSOL 3D codes.

Extensive code-to-code and code-to-experiment benchmarks have been developed in parallel with the experimental activities in order to better understand this mismatch. Additional optics numerical simulations showed that part of the "criss-cross" deflection of the ion beamlets could be related to a non-uniform H⁻ current distribution within each aperture, caused by the transverse "electron-suppression" magnetic field

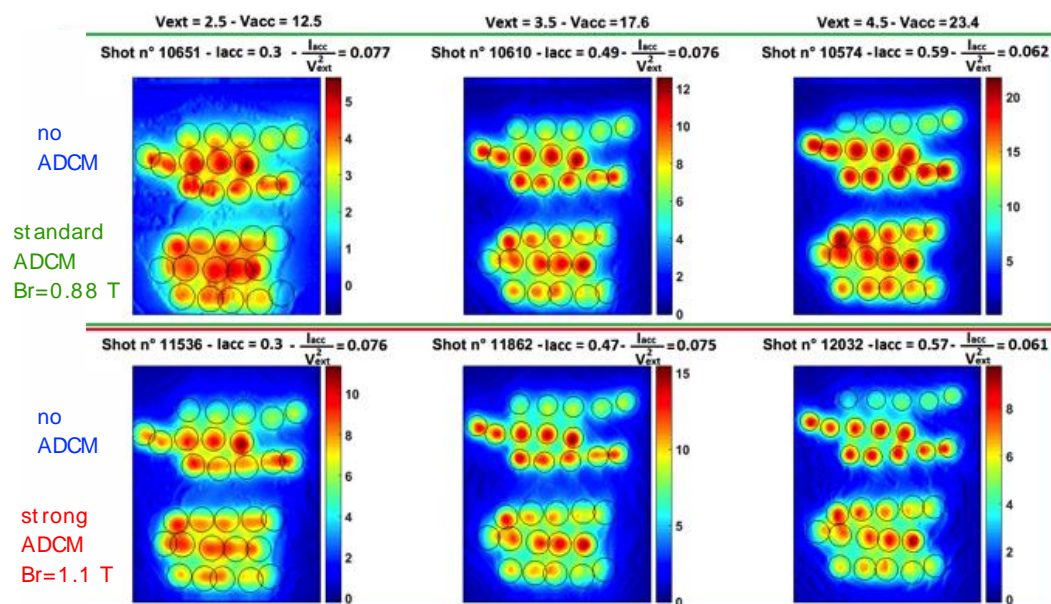


Fig. 3.4.13 Thermal images of beam pulses showing beamlet criss-cross deflection under various conditions, with the ADCM standard set ($Br=0.88 \text{ T}$) and with the augmented one ($Br= 1.1 \text{ T}$). The scale for the target temperature increase is shown on the right.

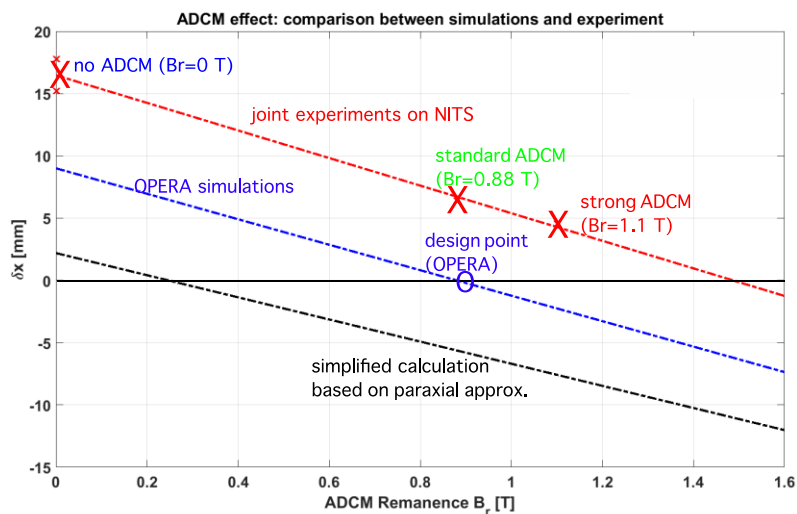


Fig. 3.5.1 beamlet criss-cross deflection on target (δx in mm) as a function of the ADCM strength (remanence B_r). In all cases ADCM size is assumed to be 16.4 x 6.6 x 1.0 mm. The trend obtained from the average experimental values (red) without ADCM, with standard ADCM ($B_r=0.88$ T) and with strong ADCM ($B_r=1.1$ T) is compared to the deflection calculated using simulations (blue and black).

produced by magnets in the Extraction Grid.

The effectiveness of ADCM is experimentally confirmed. Moreover, the scaling laws obtained from the experiments already guarantee an improvement of the final design of the MITICA and ITER/HNB accelerators.

The simulation and benchmarking activities are described in a paper by M. Ichikawa presented at NIBS2016 [104] and the main results are summarize in Fig. 3.5.1.

3.5 Power Plant Physics & Technology Projects

3.5.1 *Heating and Current Drive Systems for DEMO*

DEMO (DEMOⁿstration Fusion Power Plant) is a proposed nuclear fusion power plant that is intended to follow the ITER experimental reactor. While in ITER the goal is to demonstrate the possibility to obtain a plasma able to sustain the fusion nuclear reaction, in DEMO the main objective is to prove the industrial feasibility of fusion by showing the electricity production from the fusion reaction, the safety aspects and the Tritium self sufficiency.

¹⁰⁴ M. Ichikawa, A. Kojima, G. Chitarin, P. Agostinetti, D. Aprile, C. Baltador, M. Barbisan, R. Delogu, J. Hiratsuka, N. Marconato, R. Nishikiori, A. Pimazzoni, E. Sartori, G. Serrianni, H. Tobar, N. Umeda, P. Veltri, K. Watanabe, M. Yoshida, V. Antoni and M. Kashiwagi "Benchmark of single beamlet analysis to predict operational parameter for ITER in Japan - Italy joint experiments", presented at International Symposium on Negative Ions, Beams and Sources (NIBS2016), September 2016, St. Anne's College, Oxford, UK, to be published by AIP conference proceedings

The injection of high energy neutral beams is one of the main tools to heat the plasma up to fusion conditions. In the framework of the EUROfusion, a conceptual design of the Neutral Beam Injector (NBI) for the DEMO fusion reactor has been developed by Consorzio RFX in collaboration with other European research institutes and integrated into the DEMO1 reference design, as shown in Fig. 3.5.2. High efficiency and low recirculating power, which are fundamental requirements for the success of DEMO, have been taken into great consideration for the conceptual design of the DEMO NBI. Moreover, essential is the design of a system with the highest reasonably achievable Reliability, Availability, Maintainability and Inspectability (RAMI).

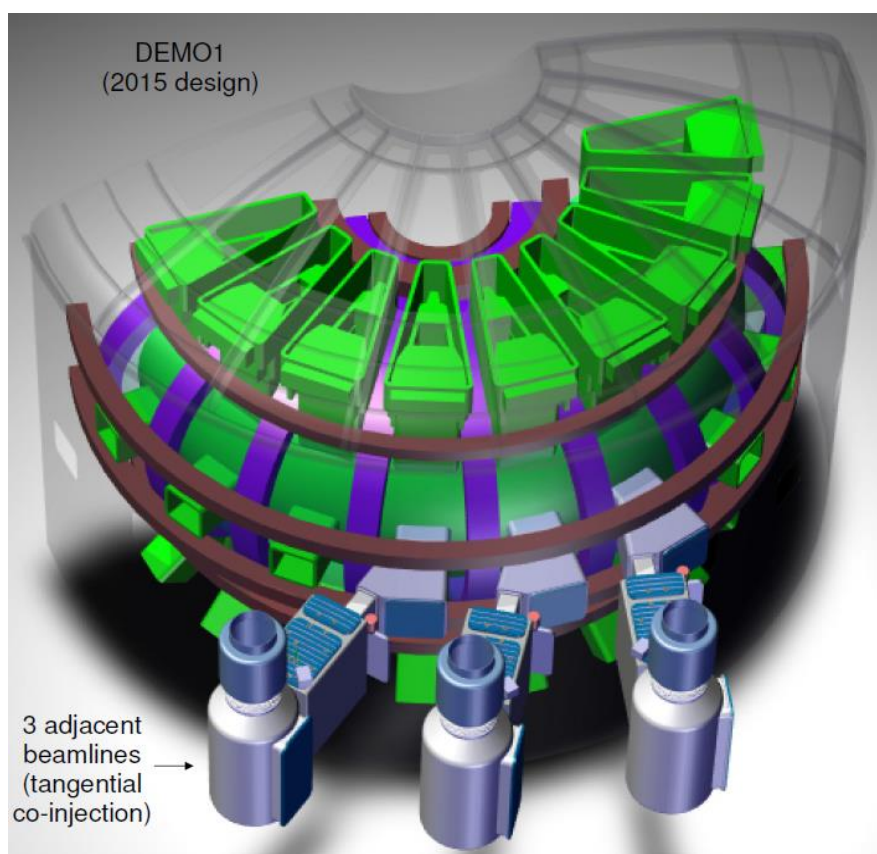


Fig. 3.5.2 Overall view of the DEMO NBIs after the conceptual design activities carried out during 2016.

An optimized design of the DEMO NBI based on the “closed recirculating cavity with nonlinear gating” (RING) concept was developed. The RING type of photoneutralizer uses two lasers with 35 kW power and 1.5 nm wavelength (infrared). By means of a second harmonic generator, only the second harmonic is circulated in the photoneutralizer, having a wavelength of 0.75 nm, half of the initial one injected by the laser. This harmonic remains trapped in the mirror system, given by 10 upper

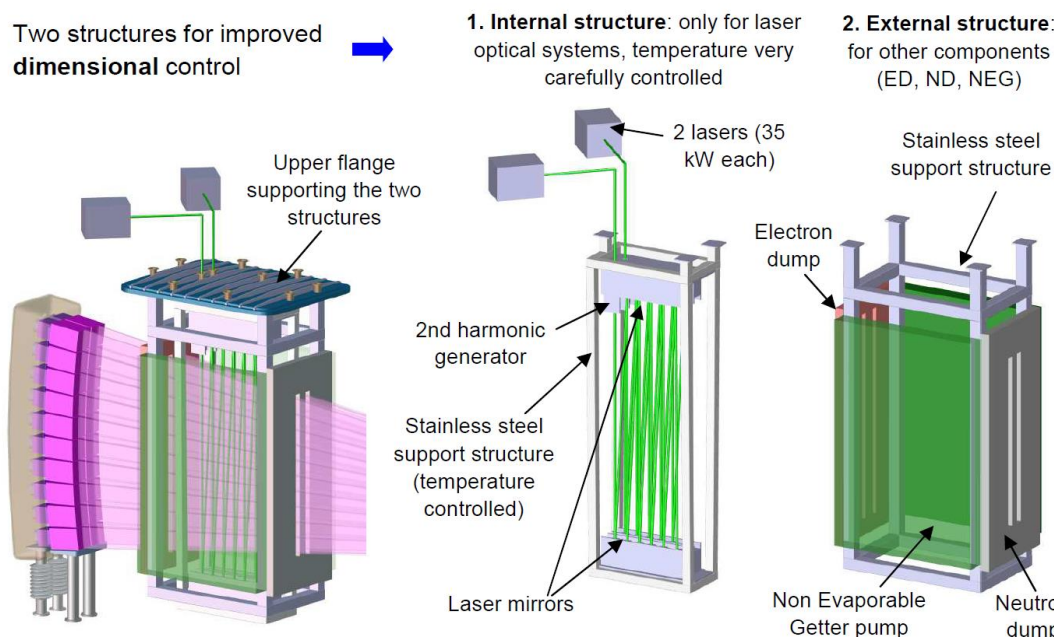


Fig. 3.5.3 Neutralizer conceptual design.

mirrors, 10 lower mirrors and 4 mirrors with a 45° angle. The beam must have the same width of the laser (limited to 70 mm for technological limitations) and intercept the laser many times.

The RF source is modular with 20 sub-sources, located with two vertical arrays of 10 sources each. The modular solution for the beam source is found to have the following main advantages:

- A better alignment between the corresponding apertures of the grids, also in presence of thermal expansion.
- A more uniform magnetic filter field inside each sub-source.
- A higher availability during the operations in DEMO.

On the other hand, there are also some drawbacks due to:

a more complex construction of the ion sources and a more complex construction of the extraction/acceleration system.

MITICA.

During 2016, the following activities for the design of the NBI system for DEMO have been carried out:

- General improvement of conceptual CAD of the NBI injector
- Development of the design of the accelerator
- Development of the design of the neutralizer
- Development of the design of the duct

- Modifications according to the indications from the studies of EUROfusion, CEA, CCFE and CIEMAT. In fact, working groups of these laboratories are collaborating with Consorzio RFX on the design of the DEMO NBI.
- Advancements on the R&D regarding the photo-neutralizer
- Advancements on the R&D regarding the energy recovery systems.

The impact of the advanced NBI concept on DEMO1 2015 plasma¹⁰⁵ has been studied with the Monte Carlo code BBNBI¹⁰⁶, which allows a detailed beamlet description of the injector. In particular the ionization of the neutral beam from a single injector in flat-top condition has been simulated. Fig. 3.5.4 shows a top view of the torus with the ionization traces for two NBI options (options 1 and 2 described in¹⁰⁷). The two different injection angles are clearly visible, with the beam aiming more on-axis for option 1. From these simulations it results that all the test particles are ionized inside the plasma, i.e. there is no shine-through neither on internal nor on external wall for both options. This work is being published and further studies including the investigation of NB fast ion slowing down are ongoing.

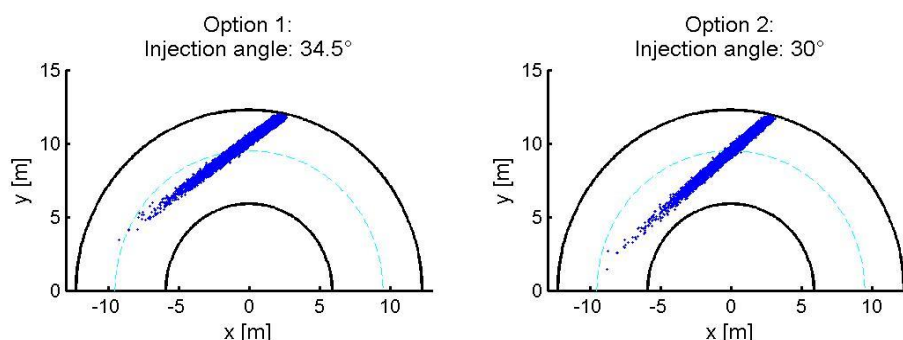


Fig. 3.5.4 Ionization pattern of NB particles, top view. Black line is the wall, dotted cyan line is the plasma magnetic axis.

The impact of NB design choices on DEMO1 plasma has been also investigated with a parametric scan by means of the fast tokamak simulator METIS¹⁰⁸. It is shown that the overall effect on DEMO1 plasma of using the advanced NBI concept instead of an ITER-like NBI is negligible, mainly because the NBI is not the main scenario actuator for DEMO1, which is dominated by alpha power and inductive currents.

¹⁰⁵ R. Wenninger, Nucl. Fusion 57 (2017) 016011 (11pp)

¹⁰⁶ Asunta O. et al 2015 Computer Physics Communications 188 33–46

¹⁰⁷ P. Sonato, 2016, “Conceptual Design of the DEMO Neutral Beam Injectors: Main Developments and R&D Achievements”, submitted to NF

¹⁰⁸ Artaud J. F. et al., Nucl. Fusion 50, 043001 (2010)

3.5.2 Plant Level System Engineering, Design Integration and Physics Integration

In 2016 the reference design data remained based on PROCESS run April 2015, even if for some engineering quantities more realistic values have been discussed in several meetings during the year. The task work of 2015 prosecuted in 2016 with the aim of updating and completing the electrical load list, contributing to the definition of realistic operative scenarios and starting the analysis of the electrical system configuration and circuits of the pulsed power supply system. The available operative scenarios have been discussed with PMI Physics in some meetings, identifying the criticality for the power supplies and allowing to define a set of more realistic input data for the design of the plant electrical system. On this basis, the ratings of the power supplies have been updated and the circuits of the pulsed power supply system have been outlined. Some considerations on the design of the main ac/dc converters have been performed. The steady state electrical load list has been completed also on the basis of the latest available information available from ITER design.

Consorzio RFX contribution on DEMO scenario modeling focused in 2016 on the optimization of Ramp-Up (RU) and Ramp-Down phases (RD) by numerical transport studies for DEMO1 (pulsed reactor) EUROfusion design. The optimization was driven by the improvement of the scenario robustness and the definition of Heating and Current Drive requirements.

In the RU case, the simplified 0.5D METIS (Fig. 3.5.5) code was used to simulate several trajectories for different current ramp rates and

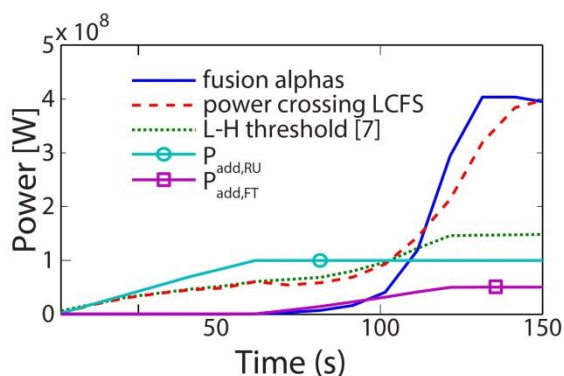


Fig. 3.5.5 Power balance for L-H transition during DEMO1 RU

several plasma density waveforms. The latter parameter was investigated in particular to lower the additional power requests for the L-H transition. Depending on the L-H threshold scaling adopted, a minimum of 70-100 MW was found to be required, at least when accepting a transition to H-mode at full plasma current, but at low plasma densities, of the order of 0.3-0.4 n/n_G (1.2 n/n_G being the target normalized density for the DEMO1 working point). A typical case for DEMO1 ramp-up is shown (Fig. 3.5.5) optimization strategies are aimed to reduce the required additional power.

The transport study of the ramp-down phase focused on the study of impurity transport and radiation, which are critical during DEMO ramp-down. DEMO1 2015 reference scenario¹⁰⁹ presents a high content of impurities ($Z_{\text{eff}}=2.6$ in flat-top phase) which may pose serious issues to plasma survival during ramp-down. JINTRAC transport suite of codes¹¹⁰ has been employed, coupling the 1.5D transport model with SANCO¹¹¹ for impurity transport and radiation. The power balance is indeed delicate due to the high power losses from radiation and the decreasing alpha power during ramp-down. These studies are necessary to estimate the amount of the necessary heating power and to validate the reference DEMO1 scenario.

Results of ramp-up and ramp-down studies have been presented in SOFT conference¹¹².

3.5.3 Magnet System Protection

The studies on the Quench Protection System of the DEMO superconducting coils have continued in 2016, in the frame of the working group WPMAG^{113, 114}.

Since the design of the winding pack of the Toroidal Field Coils (TFC) is more advanced with respect to the one of the Central Solenoid (CS) and of the Equilibrium Field Coils (EFC), Consorzio RFX work was mainly concentrated on the TFC circuit definition. It was studied the possibility to group TFCs in sectors, in order to minimize the number of Quench Protection Circuits (QPC), Current Leads (CL) and busbars which can result both in investment reduction and in efficiency increase due to the limitation of the recirculating power. Furthermore, the crowded area of the cryostat would see the presence of only half of the connections to the coils. The price to pay is a higher voltage to ground of the coil terminals, that could be afforded by a suitable design of the insulation of the coils.

Four different topologies have been studied for the TF circuits, in normal operation of QPS and in fault conditions, with different earthing circuit for the ground reference and with a different connection of the Dump Resistor (DR) in the circuit. The aim of

¹⁰⁹ R. Wenninger, Nucl. Fusion 57 (2017) 016011 (11pp)

¹¹⁰ M. Romanelli et al., Plasma and Fusion Research 9, 3403023 (2014)

¹¹¹ Lauro-Taroni L. et al 1994 Proc. 21st EPS Conf. on Controlled Fusion and Plasma Physics (Montpellier, France) vol 1, p 102

¹¹² P. Vincenzi et al., SOFT 2016, submitted to Fus. Eng. Design

¹¹³ L. Zani, et al., "Overview of Progress on the EU DEMO Reactor Magnet System Design", IEEE T Appl Supercon **26**, No. 4, (2016) 4204505

¹¹⁴ L. Zani, et al., "Evolutions of EU DEMO Reactor Magnet System Design Along the Recent Years and Lessons Learned for the Future", presented at IAEA-FEC 2016, FIP/P7-10

the analyses was to estimate the maximum voltage applied at the coils terminals with respect to ground, the voltage across each coil and the equivalent time constant for the discharge. The quantification of the peak voltage reached is important to verify the margins of the coil insulation, while the time constant of the discharge is important for the winding pack designers to verify if the coil can survive the quench.

The analyzed earthing circuit topologies derive from those adopted in ITER and JT-60SA; the first consisting in a couple of terminal resistors connected one side to the coil terminals and the other side to a common earthing resistor grounded.

The earthing system topology ITER-like seems to lead to lower peak voltages in most of the case analysed with numerical simulations.

As far as the connection of the DR is concerned, in both ITER and JT-60SA the DR are connected in parallel the circuit breaker of the QPC; other possibilities are the connection of the DR to the coil terminals (Fig. 3.5.6) or a mix of the two approaches; these case have been analyzed to identify the most suitable solution for DEMO.

The conceptual design of TF QPC has been started making reference to the design of ITER Fast Discharge Units, which make use of a mechanical ByPass Switch to

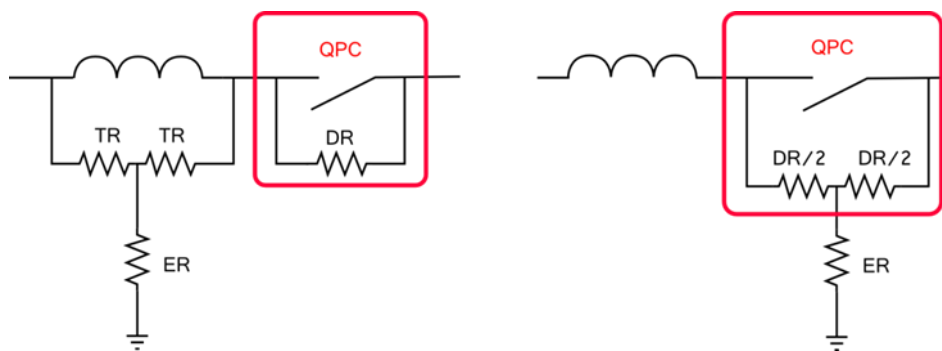


Fig. 3.5.6 One sector of ITER TF Circuit (left), One sector of JT-60SA TF Circuit (right)

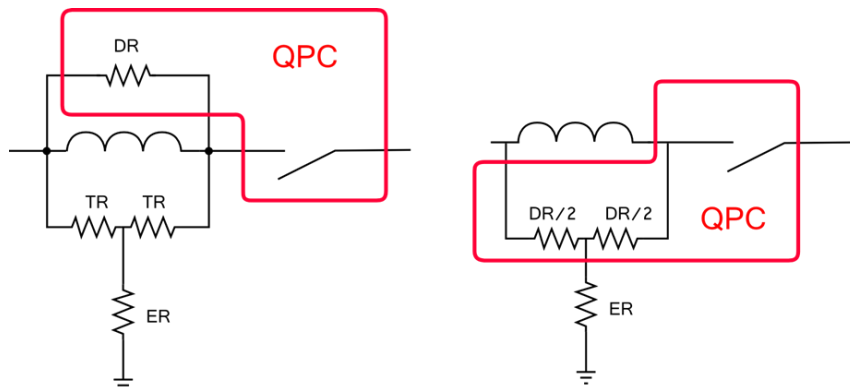


Fig. 3.5.7 Dump resistor in series to the main circuit breaker, earthing circuits used in ITER and JT-60SA

sustain the TFC current, a Vacuum Circuit Breaker and a CounterPulse Network to interrupt the dc current, a Dump Resistor to discharge the coil energy and a PyroBreaker as backup protection.

3.5.4 *Diagnostic and Control*

The aim of the Work Package Diagnostics and Control for DEMO (2015-2020) is to develop an integrated concept design of the DEMO diagnostic and control systems, taking into account the pulse duration and the harsh environmental conditions, mainly due to the neutron flux, which limit the possibility of relying on the magnetic measurement systems of present Tokamak experiments. In fact, their availability, reliability and lifetime in DEMO conditions is now under investigation and the study of an alternative strategy to provide basic information for plasma position and shape control by reflectometric measurements is in progress, taking advantage of the dedicated experiments carried out on ASDEX-Upgrade.

In this framework the RFX contribution focused on the preliminary assessment of the minimum number of channels needed to achieve a sufficiently accurate and reliable reconstruction of the plasma boundary along with their location and line of sight directions.

A purely geometric approach has been investigated to reconstruct the DEMO plasma boundary by means of active contour methods, widely used in computer vision application (image recognition) and already proposed in fusion devices, even if assuming the availability of a flux map provided by magnetic measurements. The basic underlying assumption is the possibility to represent the plasma boundary as a “regular” continuous curve instead of a set of discrete quantities such as gaps or flux control points.

The B-spline is a particularly convenient piecewise polynomial curve since the resulting contour shape can be modified by acting on a finite number of Control Points (CP) related to the curve points through a time invariant matrix. Following previous application of the method, the number of CP was chosen close to the number of active poloidal field coils. Thus a deformable template based on B-splines was implemented and the full plasma boundary reconstructed with fairly good accuracy by an iterative procedure. A cost function is defined by evaluating the distances between a limited number of estimated and “measured” plasma boundary points along the designed lines of sight of the reflectometric diagnostic. The minimization of the corresponding cost function is then formulated as an optimization

problem and solved by a simulated annealing technique. The number of degrees of freedom is given by the allowed position variation of the control points. In our application the limited number required in these examples favours the possibility of a prospective real time implementation of the method.

The present design number of 15 reflectometric measurements seems to be adequate for a reliable reconstruction except for the X-point region. The method proved to be more robust with respect to a random 10 cm error than to a reduction in the number of measurements. In fact, a sensitivity to the direction of the line of sights and to the selected set of measurements was observed in tests with a reduced number of measurements (10).

The main equilibrium parameters (elongation, triangularity, plasma centre position, plasma cross section area,...) were computed and compared to the corresponding quantities of a DEMO reference equilibrium and a satisfactory agreement was observed with the full set of 15 measurements. In Fig. 3.5.8 the initial estimate and the final reconstruction of the plasma boundary are shown against the reference boundary corresponding to a standard DEMO SOF (Start of Flat-top) equilibrium configuration.

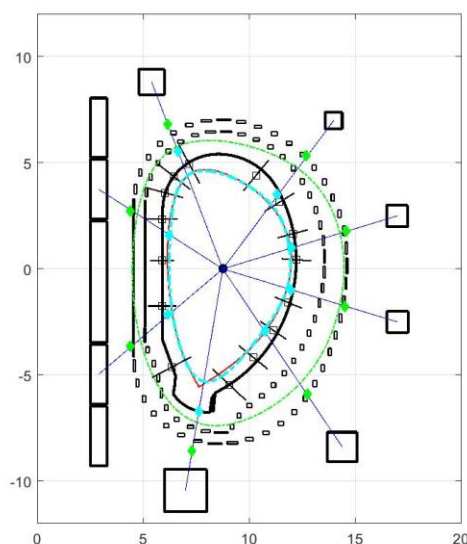


Fig. 3.5.8 Reference plasma boundary (red), initial estimate (green) and final reconstruction (cyan)

4 Broader Approach

4.1 Contribution to the JT-60SA project

After the completion in 2015 of the procurement of the JT-60SA “Quench Protection Circuits” (QPC), Consorzio RFX team continued participating in JT-60SA International Project Team activities¹¹⁵.and working on the second system to be procured for JT-60SA: the “Power Supplies for the in-vessel sector coils for RWM control”.

This Power Supply (PS) system will feed the 18 in-vessel coils of JT-60SA devoted to control a set of plasma instabilities called Resistive Wall Modes (RWM). Each coil will be fed by a dedicated inverter (300 A, 240 V), which has to guarantee very high dynamic performance, beyond the standard industrial practice¹¹⁶. In particular, a current bandwidth of 3 kHz and latency between output voltage and reference lower than 50 μ s are required. After the development of a prototype of the key part of the system, to prove the feasibility at

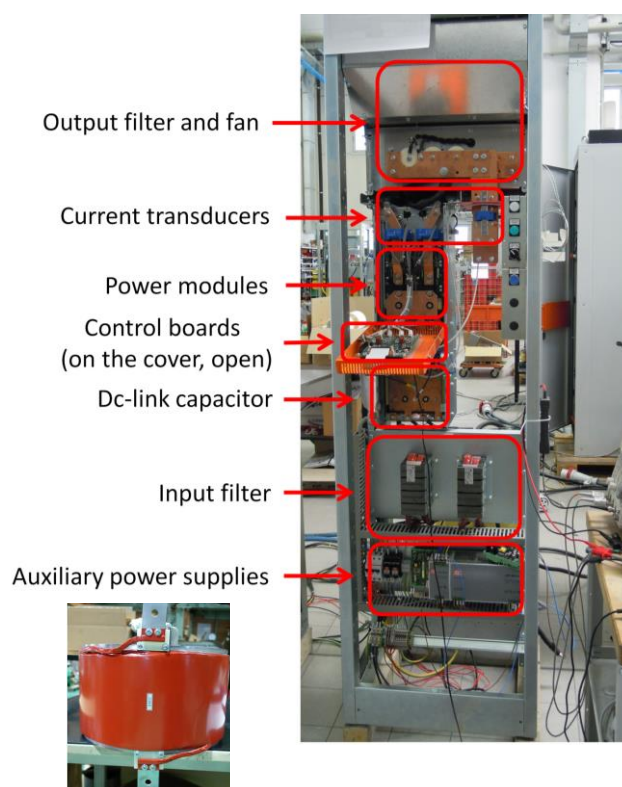


Fig. 4.1.1 RWM-PS inverter prototype (right), Dummy load provided by QST (left)

reasonable cost, and the positive results of the relevant tests, the reference design of the system was fixed in 2015 and the Procurement Arrangement for the full system and relevant accompanying documentation were prepared and signed. The call for tender was launched at the beginning of 2016 and the contract has been awarded in March to the same company who developed the prototype. The Supplier started the detailed design of the system in April; in parallel, further tests on the

¹¹⁵ L. Novello, et al., “Analysis of Maximum Voltage Transient of JT-60SA Toroidal Field Coils in Case of Fast Discharge”, IEEE T Appl Supercon **26**, NO. 2, (2016) 4700507

¹¹⁶ E. Gaio, et al., “Power Amplifiers Based on SiC Technology for MHD Mode Control in Fusion Experiments”, IEEE T Plasma Sci **44**, 9 (2016) 1654 - 1661

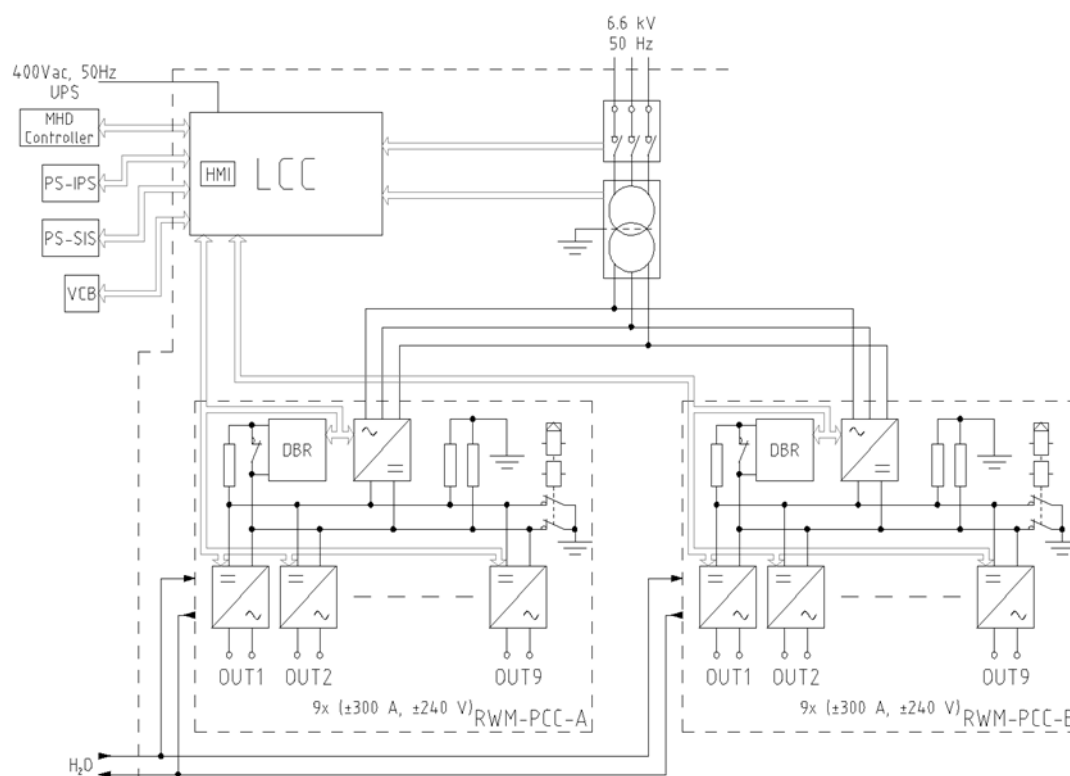


Fig. 4.1.2 Scheme of the full RWM-PS from the final design report (courtesy of E.E.I.)

inverter prototype were carried out, first at Consorzio RFX and then at Compagny. premises, to study some still open issues and to verify the feasibility of some improvements¹¹⁷.

The full system will be composed of an air-insulated ac disconnecter, a dry step-down transformer, two ac/dc converters and 18 inverters (divided in two groups). The final scheme is shown in Fig. 4.1.2. A new inverter control board is being specifically developed for this application, based on the experience gained with the prototype, and integrating both microcontroller and FPGA. The final design of the RWM-PS has been presented at the 29th SOFT conference¹¹⁸.

The first version of the Design Report has been delivered by the Supplier in November 2016 and deeply reviewed by Consorzio RFX. A Design Review Meeting with all the stakeholders has been held in December and concluded with the approval of the design and release of the next manufacturing phase.

¹¹⁷ F. Gasparini, "Characterization and optimization of a fast converter to control plasma instabilities in JT-60SA", Master Degree Thesis in Electrical Engineering, University of Padova, 2016.

¹¹⁸ E. Gaio, et al., "Final Design of SiC-based Power Supply system for Resistive-Wall-Mode control in JT-60SA", 29th Symposium on Fusion Technology, Prague, 5-9 September 2016

4.2 Remote Participation

In 2016 several activities related to remote data access have been carried out in the context of the OFC-OPE 566 F4E contract. In particular, the performance in remote data access of the MDSplus data system, jointly developed by MIT and Consorzio RFX, has been assessed in remote communication between Europe and Japan. A generic Data Model view has been developed in order to present different remote experiments using a common data ontology. The remaining activity foreseen in 2017 is the integration of secure communication in remote data access.

5 **Socio economic studies**

5.1 Fusion Energy as base-load electricity source

The FRESCO code developed by Consorzio RFX for technical and economic evaluations of fusion power plants has been further enhanced with an optimization tool based on a genetic algorithm. The 2016 research activities focused on pulsed fusion power plants, specifically on the duty cycle which largely affects the cost of electricity. Specifically, a pulsed DEMO-like power plant was modeled with the FRESCO code and the optimization of the operative cycle was carried out with the genetic algorithm in order to find the economic optimal solution. The duration of each cycle phase (current ramp up and ramp down, plasma heating, burn, central solenoid recharge) was changed randomly in order to identify the set of phase durations that minimizes the cost of electricity. The results were presented at SOFT16 [Bustreo, 2016]. The study demonstrates that the solution region is populated by local minima and the absolute minimum is achieved when the dwell time is minimized. Moreover the power plant under study generates cheaper electricity when operating in hybrid mode and the optimum flat top duration is a function of the heating and current drive costs.

5.2 Long term scenarios for power generation and the role of Fusion

Work is ongoing for the enhancement of the COMESE code developed by Consorzio RFX for the economic assessment of different future electricity generation mix. COMESE is being structured in a modular manner in order to increase flexibility in managing the input/output data. The code is equipped with a Monte Carlo routine for stochastic analysis and is ready to be coupled to an optimization algorithm also. Researches have been carried out to model the electricity generation from renewable

energy sources in Europe and estimate the storage capacity required to balance the intermittent generation. Work is underway for the implementation in COMESE.

The results of the scenarios analyses (Fig. 5.2.1) were presented at the IAEA conference [Cabal,2016]. The outcomes also demonstrate the great sensitivity of fusion technology penetration to investment cost variations going from 13% to 42% when investment costs are 30% lower than in the Reference case and from 13% to 1% when those costs are 30% higher.

Besides the scenario analysis, assessments on the relation between technical safety-related aspects to internal and external costs have been carried out.

6 Industrial Collaborations

6.1 Model for the electrostatic design a new VCB prototype

The “Agreement on a Development Order”, between the Centro Ricerche Fusione (the University Padova Representative Entity of the Consorzio RFX) and Siemens Aktengesellschaft, Berlin, aimed to apply the Voltage Holding Predictive Model – VHPM developed at RFX- to the design of the Vacuum Interrupter (VCBs) produced by Siemens, has been continued along the 2016 because of some delay in the completion of experimental campaign performed at the VCB Siemens factory in Berlin.

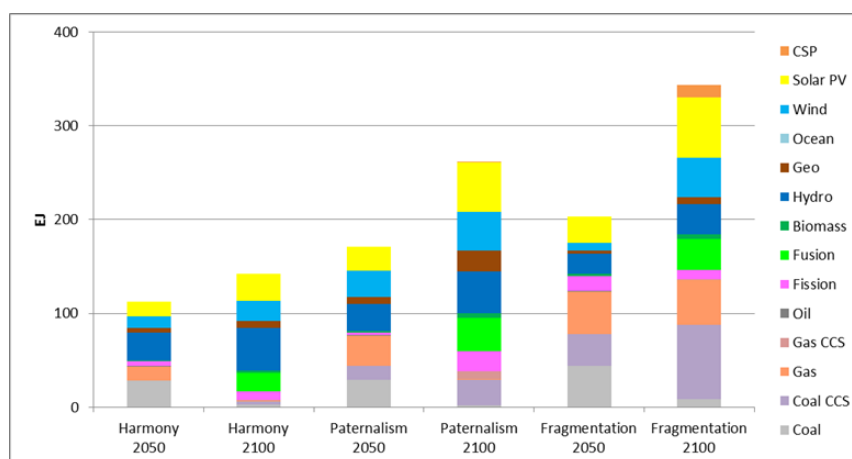


Fig. 5.2.1 Fusion penetration in the global electricity system

Basically, experimental campaigns have been carried out to collect data for the determination of the Lightning Impulse Voltage (LIV) breakdown probability of different medium-voltage Vacuum Interrupter (VI) tubes manufactured by Siemens.

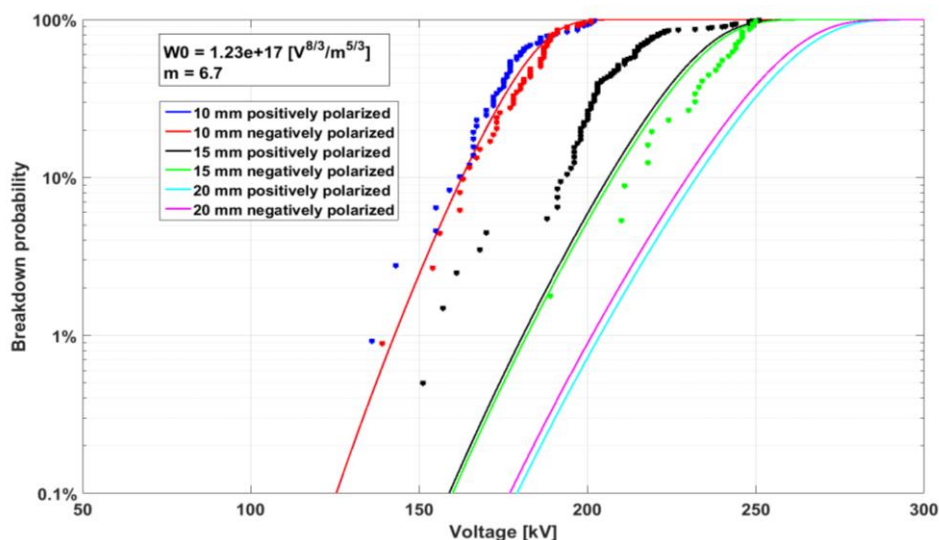


Fig. 6.1.1: Plots of calculated Weibull distributions (continuous lines) and experimental data (points) for all analyzed cases with positive and negative polarity. Gap 10 mm: blue (pos.) and red (neg.), gap 15 mm: black (pos.) and green (neg.), gap 20 mm: light blue (pos.) and magenta (neg.).

The Voltage Holding Prediction Model (VHPM) developed at Consorzio RFX to calculate the overall Weibull breakdown probability curve of multi-electrode systems insulated in vacuum under dc voltage has been tested to verify its prediction capability even for this different kind of voltage application. LIV experiments have been done with pulsed voltage up to 250 kV, at the Siemens VI factory in Berlin on different VI configurations. The VHPM model predictive capability has been evaluated applying to a tube configuration with unknown voltage breakdown characteristics the Weibull parameters obtained from the analysis of tube configurations with known LIV features.

Fig. 6.1.1 shows how the model is able to predict the voltage holding increase consequent to the contact gap increase from 10 to 15 mm. The quality of the agreement is quoted acceptable; the discrepancy with the prediction of the 15 mm case are mainly due to the fact the voltage breakdown distribution does not represent the voltage breakdown sequence typical of the fully conditioned VI, so that the breakdown voltage breakdown distribution deviates from the Weibull distribution.

In 2016 the program plan asked also for the extension of the VHPM to fully 3D formulation. Only partial experimental campaign has been carried out to compare the effectiveness of the model, so at the present stage it is not possible to derive conclusions concerning the 3D-VHPM prediction capability.

From the computational point of view, the upgrade was a success. In fact, with an innovative approach based on the complementary application of standard FEM

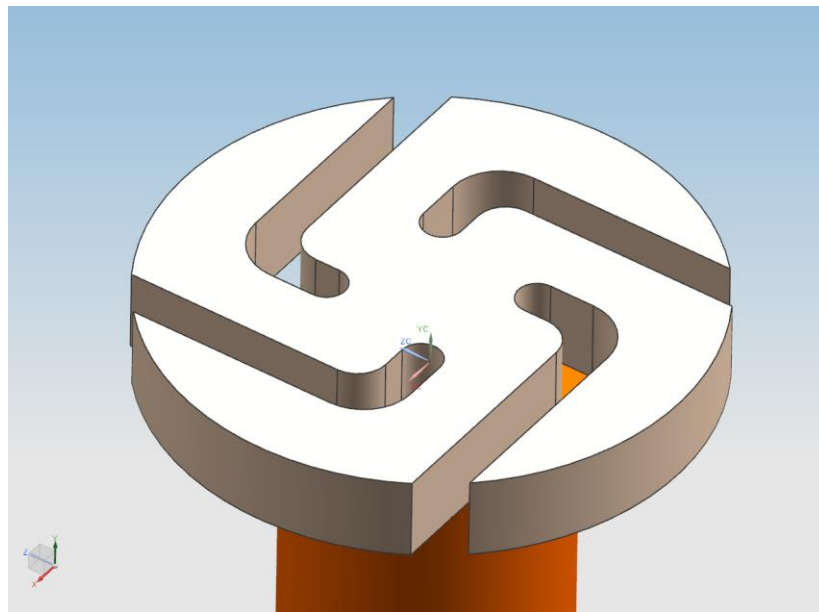


Fig. 6.1.2: Detail of the RMF tube showing the moving electrode.

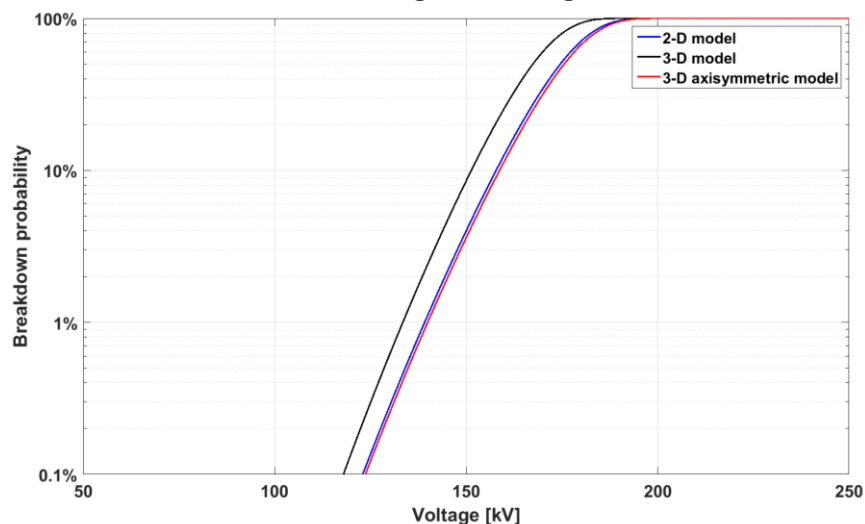


Fig. 6.1.3: Plot of the Weibull distribution calculated for the RMF tube positively polarized with the parameters obtained from the other tube type data. Results from 2-D (blue), 3-D (black) and 3-D axisymmetric (red) models.

electric scalar potential formulation combined with an original formulation that employs the electric vector potential, it was possible to obtain very accurate results optimizing the number of elements, rapidly converging towards the “true” solution.

The model was applied to a fully 3D Vacuum Interrupter, with the contact shaped as shown in Fig. 6.1.2.

This contact (used for Rotating Magnetic Field Interrupters) is only representative of the reality, which cannot be shown for IPR restriction from Siemens.

Fig. 6.1.3 shows the results in terms of comparison with breakdown probability curve for a 2D configuration calculated by 3D VHPM and 2D VHPM. The two curves

overlap. Applying the 3D VHPM to the real geometry, it is clearly visible the reduction of the breakdown voltage (left shift of the curve), which the expected result from the experiment (not yet available) should confirm.

6.2 Biomedical plasma applications

In the course of 2016 the development of the industrial-grade prototype of the plasma source for biomedical applications jointly patented by Consorzio RFX and University of Padova has been advanced by the company which holds the patent license. Some problems have been evidenced, mainly the heating of some circuit elements in the power supply circuit and some arcing occurring inside the source. These problems have been diagnosed with the active contribution of scientists at Consorzio RFX, and will be solved in the course of 2017.

Meanwhile, further studies have been carried, in collaboration with the Department of Molecular Medicine and other departments of the University of Padova, concerning possible therapeutic applications of the plasma source. In particular, an in-vitro study on cancer treatment has been carried out¹¹⁹. In this study, primary cells extracted from samples of laryngeal cancer and healthy tissue coming from the same patients were treated with the plasma. The effect was an increase in intracellular Reactive Oxygen Species, more pronounced in the case of cancer cells, which led to apoptosis (programmed cell death) in a higher proportion of cancer cells than in the healthy counterparts. This differential effect was emphasized by the addition of antimycin-A, a molecule promoting ROS production, suggesting a possible synergy between plasma and chemotherapy.

Another study was carried out on the topic of wound healing¹²⁰. This was an in-vivo study, where wounds were produced on the skin of sheep, and then treated with plasma and other treatments. The plasma was shown to bring an acceleration of the wound healing, both with respect to the control case and to the other treatments. Furthermore, known effects such as disinfection and intracellular ROS production could be confirmed in vivo.

¹¹⁹ E. Martines, et al., *Effect of indirect plasma treatment on laryngeal cancer cells*, 6th International Conference on Plasma Medicine, Bratislava, 4-9 September 2016.

¹²⁰ E. Martines, et al., *Plasma treatment of sheep skin wounds in veterinary medicine*, 6th International Conference on Plasma Medicine, Bratislava, 4-9 September 2016.

7 Education, Training and Information to the public

7.1 Education and Training

7.1.1 International Doctorate in Fusion Science and Engineering

In 2016 the Joint Research Doctorate in Fusion Science and Engineering (by Padua University, Lisbon Instituto Superior Tecnico and Naples Federico II University) and the European Interuniversity Doctoral Network in Fusion Science and Engineering (same Universities, plus the Munich Ludwig Maximilians University and the Tampere University of Technology) continued under the responsibility of the University of Padua and of the Consorzio RFX. Also the correlated participation to the Erasmus Mundus International Doctoral College in Fusion Science and Engineering (Fusion DC), Coordinated by the Ghent University, continued very fruitfully. In particular, 2 new PhD students started their research activity at RFX, at the beginning of 2016 (XXXI cycle, starting November 2015), and further 8 students (one by Fusion DC) are now beginning their research activity (XXXII cycle, starting October 2016).

At the same time in April 2016, 7 PhD students passed the Final Doctoral Examination and obtained the Joint International Doctoral Diploma. Three of them 7 continue working at the Consorzio, one with an EuroFusion Engineering Grant and two with an RFX grant, whilst other 3 went to different Fusion Laboratories.

Three Advanced Courses of 6 ECTS each were taught to the students of the Doctorate: one at IPP (Garching) on *Physics of Controlled Thermonuclear Fusion*, one at IST (Lisbon) on *Diagnostics and experimental tools for real-time control of fusion relevant plasmas* and one at RFX (Padua) on *Engineering of a Magnetically Confined Fusion Reactor*.

7.1.2 Other education and training activities

The other educational and training actions carried out at Consorzio RFX continued with the tutorial activity for the thesis of master and bachelor students and the organization of summer stages for high school students.

Also the educational activity for the RFX staff continued with the following courses:

- Transmission lines for EM signals,
- MDS-Plus,
- Introduction to Linux and Raspberry Pi.

Moreover the following 7 regular courses on Plasma Physics and Fusion were held by teachers from Consorzio RFX at Padua University:

- Basic principles of Plasma Physics (6 ECTS, 1st Level Degree, Physics)
- Physics of Nuclear Fusion and Applications of Plasmas (6 ECTS, 2nd Level Degree, Physics)
- Fluid and Plasmas Physics (6 ECTS, 2nd Level Degree, Physics)
- Fission and Fusion Nuclear Plants (9 ECTS, 2nd Level Degree, Engineering)
- Energy Technology and Economics (9 ECTS, 2nd Level Degree, Engineering)
- Thermonuclear Fusion (6 ECTS, 2nd Level Degree, Engineering)
- Industrial Applications of Plasmas (6 ECTS, 2nd Level Degree, Engineering).

7.2 Information to the public

The decision to include the NBTF project among the high-priority actions of the ITER project entailed the need of giving a larger visibility to the achievements of its milestones, within a collaboration activity among ITER, F4E and RFX. In this framework a first joint meeting among responsables and communicators from F4E, ITER and RFX was held in June in Padova, to agree the communication plan.

On this basis, in 2016 Consorzio RFX produced a large quantity of photographic and information material and 2 professional videos on the progress of on-site activities. Two articles were published on ITER Newline and a communication campaign started to diffuse information on the project: contacts were taken with the main local newspapers to present RFX-mod and the NBTF. Participations to programs and round tables at local TV stations were undertaken. Press notes were elaborated and released for the best thesis in Fusion Science and Engineering Award 2016, the main NBTF milestone achievements and the events organized at Consorzio RFX.

Talks and lectures were given by scientists from Consorzio RFX for several external initiatives and workshops. Moreover 2 main events were organized to present both the NBTF and the RFX-mod projects:

- The European Night of Research in Padova on 30 September 2016 that had a good resonance on the press, also at a national level.
- TEDxCNR in Rome on 8 October 2016 - Consorzio RFX participated with a booth presenting fusion research in Padova and in particular the NBTF project. The resonance on the media was high and benefited from the TEDxCNR event press campaign. Two interviews were broadcasted on RAI and CNR website.

Some new initiatives were undertaken in the field of arts, in particular comics, with the Walt Disney Topolino Italia, and music, with the pop-rap group "Supplenti italiani".

Information material on RFX-mod and NBTF was made available on the web: along the RFX website, also social media such as the facebook page of the Consorzio RFX were regularly updated and a twitter account @ConsorzioRFX was opened.

As for the information to schools, besides continuing the program of visits to the Consorzio, the new project of a thesis on fusion was launched. It consists of an educational kit in Power Point, with content on fusion, proposed to high school students for their final degree thesis, with the support of scientist from the Consorzio RFX. A first test was successfully performed in November with a group of 4 classes and, on the basis of the positive result, the Regional School Office in Padova decided to distribute it to all schools in the district. The thesis on fusion is available on Consorzio RFX and Padova CNR Research Area websites.

Finally Consorzio RFX contributes to the Social Economic Studies in the frame of the EURO fusion work packages.

8 PUBLICATIONS 2016

NATIONAL AND INTERNATIONAL JOURNALS

1. **Evaluation of reconstruction errors and identification of artefacts for JET gamma and neutron tomography** T. Craciunescu, A. Murari, V. Kiptily, I. Lupelli, A. Fernandes, S. Sharapov, I. Tiseanu, V. Zoita and JET Contributors *Rev. Sci. Instrum.* **87**, 013502 (2016)
2. **Performance of the full size nGEM detector for the SPIDER experiment** Muraro, G. Croci, G. Albani, G. Claps, M. Cavenago, C. Cazzaniga, M. Dalla Palma, G. Grosso, F. Murtas, R. Pasqualotto, E. Perelli Cippo, M. Rebai, M. Tardocchi, M. Tollin, G. Gorini *Nucl Instrum Meth A* **813** (Jan 2016) 147–152
3. **Detailed design optimization of the MITICA negative ion accelerator in view of the ITER NBI** P. Agostinetti, D. Aprile, V. Antoni, M. Cavenago, G. Chitarin, H.P.L. de Esch, A. De Lorenzi, N. Fonnesu, G. Gambetta, R.S. Hemsworth, M. Kashiwagi, N. Marconato, D. Marcuzzi, N. Pilan, E. Sartori, G. Serianni, M. Singh, P. Sonato, E. Spada, V. Toigo, P. Veltri and P. Zaccaria *Nucl. Fusion* **56** (2016) 016015
4. **Conceptual design of a polarimetric Thomson scattering diagnostic in ITER** L. Giudicotti, M. Bassan, F.P. Orsitto, R. Pasqualotto, M. Kempenaars and J. Flanagan *Journal of Instrumentation* **11** (2016)
5. **Application of symbolic regression to the derivation of scaling laws for tokamak energy confinement time in terms of dimensionless quantities** A. Murari, E. Peluso, M. Lungaroni, M. Gelfusa and P. Gaudio *Nucl. Fusion* **56** 026005 (2016)
6. **Application of transfer entropy to causality detection and synchronization experiments in tokamaks** A. Murari, E. Peluso, M. Gelfusa, L. Garzotti, D. Frigione, M. Lungaroni, F. Pisano, P. Gaudio and JET Contributors *Nucl. Fusion* **56** (2016) 026006
7. **First hydrogen operation of NIO1: Characterization of the source plasma by means of an optical emission spectroscopy diagnostic** M. Barbisan, C.

-
- Baltador, B. Zaniol, M. Cavenago, U. Fantz, R. Pasqualotto, G. Serianni, L. Vialetto and D. Wunderlich *Rev. Sci. Instrum.* **87**, 02B319 (2016)
8. **Particle transport and heat loads in NIO1** N. Fonnesu, M. Cavenago, G. Serianni and P. Veltri *Rev. Sci. Instrum.* **87**, 02B905 (2016)
 9. **Ion collector design for an energy recovery test proposal with the negative ion source NIO1** V. Variale, M. Cavenago, P. Agostinetti, P. Sonato and L. Zanotto *Rev. Sci. Instrum.* **87**, 02B305 (2016)
 10. **Simulation of diatomic gas-wall interaction and accommodation coefficients for negative ion sources and accelerators** E. Sartori, L. Brescaccin, G. Serianni *Rev. Sci. Instrum.* **87**, 02A502 (2016)
 11. **Simulation of space charge compensation in a multibeamlet negative ion beam** Sartori E., Maceina T.J., Veltri P., Cavenago M., Serianni G. *Rev. Sci. Instrum.* **87** 02B917 (2016)
 12. **Multi-beamlet investigation of the deflection compensation methods of SPIDER beamlets** C. Baltador, P. Veltri, P. Agostinetti, G. Chitarin and G. Serianni *Rev. Sci. Instrum.* **87** 02B141 (2016)
 13. **Development and tests of molybdenum armored copper components for MITICA ion source** Mauro Pavei, Bernd Böswirth, H. Greuner, D. Marcuzzi, A. Rizzolo and M. Valente *Rev. Sci. Instrum.* **87**, 02B126 (2016)
 14. **The characterization and optimization of NIO1 ion source extraction aperture using a 3D particle-in-cell code** F. Taccogna, P. Minelli, M. Cavenago, P. Veltri and N. Ippolito *Rev. Sci. Instrum.* **87**, 02B145 (2016)
 15. **Design optimization of RF lines in vacuum environment for the MITICA experiment** Michela De Muri, Mauro Pavei, Federico Rossetto, Diego Marcuzzi, Enrico Miorin and Silvia M. Deambrosis *Rev. Sci. Instrum.* **87**, 02B314 (2016)
 16. **Steady state thermal-hydraulic analyses of the MITICA cooling circuits** M. Zaupa, E. Sartori, M. Dalla Palma, F. Fellin, D. Marcuzzi, M. Pavei and A. Rizzolo *Rev. Sci. Instrum.* **87**, 02B323 (2016)
 17. **Final design of the beam source for the MITICA injector** D. Marcuzzi, P. Agostinetti, M. Dalla Palma, M. De Muri, G. Chitarin, G. Gambetta, N. Marconato, R. Pasqualotto, M. Pavei, N. Pilan, A. Rizzolo, G. Serianni, V. Toigo, L. Trevisan, M. Visentin, P. Zaccaria, M. Zaupa, D. Boilson, J. Graceffa, R. S. Hemsworth, C. H. Choi, M. Marti, K. Roux, M. J. Singh, A. Masiello, M. Froeschle, B. Heinemann, R. Nocentini, R. Riedl, H. Tobar, H. P. L. de Esch and V. N. Muvvala *Rev. Sci. Instrum.* **87**, 02B309 (2016)
 18. **Preliminary results concerning the simulation of beam profiles from extracted ion current distributions for mini-STRIKE** P. Agostinetti, M. Giacomini, G. Serianni, P. Veltri, F. Bonomo and L. Schiesko *Rev. Sci. Instrum.* **87**, 02B913 (2016)
 19. **Preliminary design of electrostatic sensors for MITICA beam line components** S. Spagnolo, M. Spolaore, M. Dalla Palma, R. Pasqualotto, E. Sartori, G. Serianni and P. Veltri *Rev. Sci. Instrum.* **87**, 02B931 (2016)
 20. **Transmission of electrons inside the cryogenic pumps of ITER injector** P. Veltri and E. Sartori *Rev. Sci. Instrum.* **87**, 02B313 (2016)
 21. **First experiments with the negative ion source NIO1** M. Cavenago, G. Serianni, M. De Muri, P. Agostinetti, V. Antoni, C. Baltador, M. Barbisan, L. Baseggio, M. Bigi, V. Cervaro, F. Degli Agostini, E. Fagotti, T. Kulevoy, N. Ippolito, B. Laterza, A. Minarello, M. Maniero, R. Pasqualotto, S. Petrenko, M. Poggi, D. Ravarotto, M. Recchia, E. Sartori, M. Sattin, P. Sonato, F. Taccogna, V. Variale, P. Veltri, B. Zaniol, L. Zanotto and S. Zucchetti *Rev. Sci. Instrum.* **87**, 02B320 (2016)

-
22. **Negative ion production and beam extraction processes in a large ion source** K. Tsumori, K. Ikeda, H. Nakan, M. Kasaki, S. Geng, M. Wada, K. Sasaki, S. Nishiyama, M. Goto, G. Serianni, P. Agostinetti, E. Sartori, M. Brombin, P. Veltri, C. Wimmer, K. Nagaoka, M. Osakabe, Y. Takeiri and O. Kaneko *Rev. Sci. Instrum.* **87**, 02B936 (2016)
 23. **A feasibility study of a NBI photoneutralizer based on nonlinear gating laser recirculation** Fassina, F. Pretato, M. Barbisan, L. Giudicotti and R. Pasqualotto *Rev. Sci. Instrum.* **87**, 02B318 (2016)
 24. **A new deflection technique applied to an existing scheme of electrostatic accelerator for high energy neutral beam injection in fusion reactor devices** N. Pilan, V. Antoni, A. De Lorenzi, G. Chitarin, P. Veltri and E. Sartori *Rev. Sci. Instrum.* **87**, 02B325 (2016)
 25. **Background gas density and beam losses in NIO1 beam source** E. Sartori, P. Veltri, M. Cavenago and G. Serianni *Rev. Sci. Instrum.* **87**, 02B118 (2016)
 26. **Castellated tiles as the beam-facing components for the diagnostic calorimeter of the negative ion source SPIDER** S. Peruzzo, V. Cervaro, M. Dalla Palma, R. Delogu, M. De Muri, D. Fasolo, L. Franchin, R. Pasqualotto, A. Pimazzoni, A. Rizzolo, M. Tollin, L. Zampieri and G. Serianni *Rev. Sci. Instrum.* **87**, 02B925 (2016)
 27. **Analysis of diagnostic calorimeter data by the transfer function technique** R. S. Delogu, C. Poggi, A. Pimazzoni, G. Rossi and G. Serianni *Rev. Sci. Instrum.* **87**, 02B932 (2016)
 28. **Numerical simulations of the first operational conditions of the negative ion test facility SPIDER** G. Serianni, P. Agostinetti, V. Antoni, C. Baltador, M. Cavenago, G. Chitarin, N. Marconato, R. Pasqualotto, E. Sartori, V. Toigo and P. Veltri *Rev. Sci. Instrum.* **87**, 02B927 (2016)
 29. **Off-normal and failure condition analysis of the MITICA negative-ion accelerator** Giuseppe Chitarin, Piero Agostinetti, Daniele Aprile, Nicolò Marconato, Diego Marcuzzi, Gianluigi Serianni, Pierluigi Veltri and Pierluigi Zaccaria *Rev. Sci. Instrum.* **87**, 02B311 (2016)
 30. **Optics of the NIFS negative ion source test stand by infrared calorimetry and numerical modelling** P. Veltri, V. Antoni, P. Agostinetti, M. Brombin, K. Ikeda, M. Kasaki, H. Nakano, E. Sartori, G. Serianni, Y. Takeiri and K. Tsumori *Rev. Sci. Instrum.* **87**, 02B908 (2016)
 31. **Optimization of ICRH for core impurity control in JET-ILW** E. Lerche, M. Goniche, P. Jacquet, D. Van Eester, V. Bobkov, L. Colas, C. Giroud, I. Monakhov, F.J. Casson, F. Rimini, C. Angioni, M. Baruzzo, T. Blackman, S. Brezinsek, M. Brix, A. Czarnecka, K. Crombé, C. Challis, R. Dumont, J. Eriksson, N. Fedorczak, M. Graham, J.P. Graves, G. Gorini, J. Hobirk, E. Joffrin, T. Johnson, Y. Kazakov, V. Kiptily, A. Krivska, M. Lennholm, P. Lomas, C. Maggi, P. Mantica, G. Mathews, M.-L. Mayoral, L. Meneses, J. Mlynar, P. Monier-Garbet, M.F. Nave, C. Noble, M. Nocente, I. Nunes, J. Ongena, G. Petravich, V. Petrzilka, T. Pütterich, M. Reich, M. Santala, E.R. Solano, A. Shaw, G. Sips, M. Stamp, M. Tardocchi, M. Tsalas, M. Valisa and JET Contributors *Nucl. Fusion* **56** (2016) 036022 (19pp)
 32. **Aspect ratio scaling of the single helical states in the reversed field pinch plasmas** R. Paccagnella *Nucl. Fusion* **56** 046010 (2016)
 33. **A Metric to Improve the Robustness of Conformal Predictors in the Presence of Error Bars** Andrea Murari, Saeed Talebzadeh, Jesús Vega, Emmanuele Peluso, Michela Gelfusa, Michele Lungaroni, Pasqualino Gaudio *Conformal and Probabilistic Prediction with Applications*, Vol. 9653 of the series *Lecture Notes in Computer Science* (Apr 2016) 105-115

-
34. **On the statistics and features of turbulent structures in RFX-mod** N Vianello, M Spolaore, M Agostini, R Cavazzana, G De Masi, E Martines, B Momo, P Scarin, S Spagnolo and M Zuin *Plasma Phys. Control. Fusion* 58 (2016) 044009 (10pp)
 35. **Analysis of Maximum Voltage Transient of JT-60SA Toroidal Field Coils in Case of Fast Discharge** L. Novello, P. Cara, A. Coletti, E. Gaio, A. Maistrello, M. Matsukawa, G. Phillips, V. Tomarchio, and K. Yamauchi *IEEE T Appl Supercon* 26, NO. 2, (2016) 4700507
 36. **Characterization of small thermal structures in RFX-mod electron temperature profiles** A Fassina, M Gobbin, S Spagnolo, P Franz and D Terranova *Plasma Phys. Control. Fusion* 58 (2016) 055017
 37. **Excitation of external kink mode by trapped energetic particles** S.C. Guo, X.Y. Xu, Y.Q. Liu and Z.R. Wang *Nucl. Fusion* 56 (2016) 056006
 38. **Toroidal modelling of RMP response in ASDEX Upgrade: coil phase scan, q_{95} dependence, and toroidal torques** Yueqiang Liu, D. Ryan, A. Kirk, Li Li, W. Suttrop, M. Dunne, R. Fischer, J.C. Fuchs, B. Kurzan, P. Piovesan, M. Willensdorfer, the ASDEX Upgrade Team and the EUROfusion MST1 Team *Nucl. Fusion* 56 (2016) 056015
 39. **Evaluation of thermal helium beam and line-ratio fast diagnostic on the National Spherical Torus Experiment-Upgrade** J. M. Muñoz Burgos, M. Agostini, P. Scarin, D. P. Stotler, E. A. Unterberg, S. D. Loch, O. Schmitz, K. Tritz, and Stutman *Phys. Plasmas* 23, 053302 (2016)
 40. **The radiofrequency magnetic dipole discharge** Martines, M. Zuin, M. Marcante, R. Cavazzana, A. Fassina and M. Spolaore *Phys. Plasmas* 23, 053511 (2016)
 41. **Internal Transport Barrier Broadening through Subdominant Mode Stabilization in Reversed Field Pinch Plasmas** R. Lorenzini, F. Auremma, A. Fassina, E. Martines, D. Terranova, and F. Sattin *Phys. Rev. Lett.* 116, 185002 (May 2016)
 42. **Classification of JET Neutron and Gamma Emissivity Profiles** T. Craciunescu, A. Murari, V. Kiptily, J. Vega and JET Contributors *Journal of Instrumentation*, *JINST* 11 C05021 (May 2016)
 43. **New analysis methods to push the boundaries of diagnostic techniques in the environmental sciences** M. Lungaroni, A. Murari, E. Peluso, M. Gelfusa, A. Malizia, J. Vega, S. Talebzadeh and P. Gaudio *Journal of Instrumentation*, Apr 2016 *JINST* 11 (May 2016)
 44. **Characterisation of the properties of a negative hydrogen ion beam by several beam diagnostic techniques** R. Maurizio, U. Fantz, F. Bonomo and G. Serianni *Nucl. Fusion* 56 (2016) 066012 (11pp)
 45. **The influence of grid positioning on the beam optics in the neutral beam injectors for ITER** Veltri P., Agostinetti P., Marcuzzi D., Sartori E., Serianni G. *Fusion Eng. and Design* 107, (June 2016) 64–69
 46. **The external kink mode in diverted tokamaks** Turnbull A.D., Hanson J.M., Turco F., Ferraro N.M., Lanctot M.J., Lao L.L., Strait E.J., Piovesan P., Martin P. *Journal of Plasma Physics* 82, Issue 3 (Jun 2016) 515820301
 47. **Overview of Progress on the EU DEMO Reactor Magnet System Design** L. Zani, C. M. Bayer, M. E. Biancolini, R. Bonifetto, P. Bruzzone, C. Brutti, D. Ciazynski, M. Coleman, I. Duran, M. Eisterer, W. H. Fietz, P. V. Gade, E. Gaio, F. Giorgetti, W. Goldacker, F. Gömöry, X. Granados, R. Heller, P. Hertout, C. Hoa, A. Kario, B. Lacroix, M. Lewandowska, A. Maistrello, L. Muzzi, A. Nijhuis, F. Nunio, Panin, T. Petrisor, J.-M. Poncet, R. Prokopec, M. Sanmarti Cardona, L.

-
- Savoldi, S. I. Schlachter, K. Sedlak, B. Stepanov, I. Tiseanu, A. Torre, S. Turtù, R. Vallcorba, M. Vojenciak, K.-P. Weiss, R. Wesche, K. Yagotintsev, and R. Zanino *IEEE T Appl Supercon* **26**, No. 4, (2016) 4204505
- 48. Upgrades of Diagnostic Techniques and Technologies for JET Next D-T Campaigns** Murari, J. Figueiredo, N. Bekris, C. Perez von Thun, P. Batistoni, D. Marocco, F. Belli, M. Tardocchi *IEEE T. Nucl Sci* **63**, No. 3, 7497673, (June 2016), 1674-168
- 49. How to assess the efficiency of synchronization experiments in tokamaks** A. Murari, T. Craciunescu, E. Peluso, M. Gelfusa, M. Lungaroni, L. Garzotti, D. Frigione, P. Gaudio and JET Contributors *Nucl. Fusion* **56** (2016) 076008
- 50. Heating Neutral Beams for ITER: Present Status** Singh M.J., Boilson D., Hemsworth R.S., Chareyre J., Decamps H., Geli F., Graceffa J., Schunke B., Svensson L., Shah D., El Ouazzani A., Urbani M., De Esch H.P.L., Delmas E., Antoni V., Chitarin G., Serianni G., Marcuzzi D., Toigo V., Zaccaria P., Fantz U., Franzen P., Heinemann B., Kraus W., Kashiwagi M., Hanada M., Tobar H., Kuriyama M., Masiello A., Bonicelli T. *IEEE T. Plasma Sci* **44**, 9 (2016) 1496 - 1505
- 51. Design and Test of Readout Electronics for Thermocouples on Ion Beam Sources** Brombin, Ghirardelli, Molon Pasqualotto, Serianni *IEEE T. Plasma Sci* **44**, 9 (2016) 1619 - 1624
- 52. Power Amplifiers Based on SiC Technology for MHD Mode Control in Fusion Experiments** Elena Gaio, Alberto Ferro, Luca Novello, and Makoto Matsukawa *IEEE T. Plasma Sci* **44**, 9 (2016) 1654 - 1661
- 53. Progress in the Design and Testing of In-Vessel Magnetic Pickup Coils for ITER** S. Peruzzo, M. Brombin, M. Furno Palumbo, W. Gonzalez, N. Marconato, A. Rizzolo, S. Arshad, Y. Ma, G. Vayakis, A. Suarez, I. D'uran, L. Viererbl, and Z. Lahodová *IEEE T. Plasma Sci* **44**, 9 (2016) 1704 – 1710
- 54. MHD spectra and coordinate transformations in toroidal systems I.** Predebon, B. Momo, D. Terranova and P. Innocente *Phys. Plasmas* **23**, 092508 (2016)
- 55. Relaxation models for single helical reversed field pinch plasmas** R. Paccagnella *Phys. Plasmas* **23**, 092512 (2016)
- 56. Heating Neutral Beams for ITER : Present Status** Singh, M.J., Boilson, D., Hemsworth, R., Chareyre, J., Decamps, H., Delmas, E., Geli, F., Graceffa, J., Schunke, B., Svensson, L., Shah, D., El Ouazzani, A., Urbani, M., De Esch, H.P.L., Antoni, V., Chitarin, G., Serianni, G., Marcuzzi, D., Toigo, V., Zaccaria, P., Fantz, U., Franzen, P., Heinemann, B., Kraus, W., Kashiwagi, M., Hanada, M., Tobar, H., Kuriyama, M., Masiello, A., Bonicelli, T. *IEEE T. Plasma Sci*, **44**, 9, (Sept 2016)
- 57. Interaction of external $n = 1$ magnetic fields with the sawtooth instability in low- q RFX-mod and DIII-D tokamaks** C. Piron, P. Martin, D. Bonfiglio, J. Hanson, N.C. Logan, C. Paz-Soldan, P. Piovesan, F. Turco, J. Bialek, P. Franz *Nucl. Fusion* **56** (2016) 106012
- 58. Optimization of ICRH for core impurity control in JET-ILW Geodesic distance on Gaussian manifolds for the robust identification of chaotic systems** T. Craciunescu, A. Murari *Nonlinear Dynamics* **86** Issue 1, (Oct 2016) 677–693
- 59. Characterization of electromagnetic fluctuations in a HiPIMS plasma** S Spagnolo, M Zuin, R Cavazzana, E Martines, A Patelli, M Spolaore and M Colasuonno *Plasma Sources Sci Technol.* **25** 065016 (Oct 2016)

-
60. **Upgrades and application of FIT3D NBI-plasma interaction code in view of LHD deuterium campaigns** P. Vincenzi, T. Bolzonella, S. Murakami, M. Osakabe, R. Seki, M. Yokoyama *Plasma Phys. Control. Fusion* **58** 125008 (Oct 2016)
 61. **Design and operation of the RFX-mod plasma shape control system** G. Marchiori, C. Finotti, O. Kudlacek, F. Villone, P. Zanca, D. Abate, R. Cavazzana, G.L. Jackson, T.C. Luce, L. Marrelli *Fusion Eng. and Design* **108** (Oct 2016) 81–91
 62. **Plasma-resistivity-induced strong destabilization of the kinetic resistive wall mode** V. V. Yanovskiy *Phys. Plasmas* **23**, 102510 (2016)
 63. **The Full-Size Source and Injector Prototypes for ITER Neutral Beams** G. Serianni, P. Agostinetti, V. Antoni, D. Aprile, C. Baltador, M. Cavenago, G. Chitarin, N. Marconato, D. Marcuzzi, E. Sartori, P. Sonato, V. Toigo, P. Veltri And P. Zaccaria *Plasma and Fusion Research*, 11, 2402119 (2016)
 64. **Study of a high power hydrogen beam diagnostic based on secondary electron emission** Sartori E., Panasenkov A., Veltri P., Serianni G., Pasqualotto R. *Rev. Sci. Instrum.* **87**, 11D438 (2016)
 65. **Performance of the prototype LaBr3 spectrometer developed for the JET gamma-ray camera upgrade** Rigamonti D., Muraro A., Nocente M., Perseo V., Boltruczyk G., Fernandes A., Figueiredo J., Giacomelli L., Gorini G., Gosk M., Kiptily V., Korolczuk S., Mianowski S., Murari A., Pereira R.C., Cippo E.P., Zychor I., Tardocchi M. *Rev. Sci. Instrum.* **87**, 11E717 (2016)
 66. **Final design of thermal diagnostic system in SPIDER ion source** M. Brombin, M. Dalla Palma, R. Pasqualotto and N. Pomaro *Rev. Sci. Instrum.* **87**, 11D433 (2016)
 67. **SPIDER beam dump as diagnostic of the particle beam** M. Zaupa, M. Dalla Palma, E. Sartori, M. Brombin and R. Pasqualotto *Rev. Sci. Instrum.* **87**, 11D415 (2016)
 68. **Implementation of the new multichannel X-mode edge density profile reflectometer for the ICRF antenna on ASDEX Upgrade** D. E. Aguiam, A. Silva, V. Bobkov, P. J. Carvalho, P. F. Carvalho, R. Cavazzana, G. D. Conway, O. D’Arcangelo, L. Fattorini, H. Faugel, A. Fernandes, H. Fünfgelder, B. Gonçalves, L. Guimaraes, G. De Masi, L. Meneses, J. M. Noterdaeme, R. C. Pereira, G. Rocchi, J. M. Santos, A. A. Tuccillo, O. Tudisco and ASDEX Upgrade Team *Rev. Sci. Instrum.* **87**, 11E722 (2016)
 69. **JET diagnostic enhancements in preparation for DT operations** J. Figueiredo, A. Murari, C. Perez Von Thun, D. Marocco, M. Tardocchi, F. Belli, M. García Muñoz, A. Silva, S. Soare, T. Craciunescu, M. Santala, P. Blanchard, I. Balboa, N. Hawkes and JET Contributors *Rev. Sci. Instrum.* **87**, 11D443 (2016)
 70. **First neutron spectroscopy measurements with a pixelated diamond detector at JET** Muraro A., Giacomelli L., Nocente M., Rebai M., Rigamonti D., Belli F., Calvani P., Figueiredo J., Girolami M., Gorini G., Grosso G., Murari A., Popovichev S., Trucchi D.M., Tardocchi M., Contributors J. *Rev. Sci. Instrum.* **87**, 11D833 (2016)
 71. **Two key improvements to enhance the thermo-mechanic performances of accelerator grids for neutral beam injectors** P. Agostinetti, G. Chitarin, G. Gambetta, D. Marcuzzi *Fus. Eng. and Design*, **109–111, Part A**, (Nov 2016) 890–894
 72. **Vacuum boundary modifications of the RFX-mod machine** N. Patel, M. Dalla Palma, S. Dal Bello, L. Grando, S. Peruzzo, P. Sonato *Fus. Eng. and Design*, **109–111, Part A**, (Nov 2016) 777–783

-
- 73. Electro-mechanical connection system for ITER in-vessel magnetic sensors** A. Rizzolo, M. Brombin, W. Gonzalez, N. Marconato, S. Peruzzo, S. Arshad, Y. Ma, G. Vayakis, A. Williams *Fus. Eng. and Design*, **109–111, Part A**, (Nov 2016) 201–206
- 74. JET experiments with tritium and deuterium–tritium mixtures** Lorne Horton, P. Batistonic, H. Boyerd, C. Challisd, D. ‘Ciri’, A.J.H. Donnée, L.G. Erikssonb, Garciag, L. Garzotti, S. Geed, J. Hobirrh, E. Joffring, T. Jones, D.B. Kingd, S. Kniped, X. Litaudone, G.F. Matthews, I. Monakhovd, A. Murari, Nunesj, V. Riccardo, A.C.C. Sips, R. Warren, H. Weisen.-D. Zastrow, JET Contributors *Fus. Eng. and Design*, **109–111, Part A**, (Nov 2016) 925–936
- 75. Modelling of cyclic plasticity for austenitic stainless steels 304L, 316L, 316L(N)-IG** Mauro Dalla Palma *Fus. Eng. and Design*, **109–111, Part A**, (Nov 2016) 20–25
- 76. Solutions to mitigate heat loads due to electrons on sensitive components of ITER HNB beamlines** E. Sartori, P. Veltri, M. Dalla Palma, P. Agostinetti, R. Hemsworth, M. Singh, G. Serianni *Fus. Eng. and Design*, **109–111, Part A**, (Nov 2016) 377–382
- 77. Analysis of twisted tape solutions for cooling of the residual ion dump of the ITER HNB** S. O. Guamána, S. Hanke, E. Sartori, M. Dalla Palma *Fus. Eng. and Design*, **109–111, Part A**, (Nov 2016) 437–442
- 78. Beam calorimetry at the large negative ion source test facility ELISE: Experimental setup and latest results** R. Nocentini, F. Bonomo, M. Ricci, A. Pimazzoni, U. Fantza, B. Heinemann, R. Riedl, D. Wunderlich *Fus. Eng. and Design*, **109–111, Part A**, (Nov 2016) 673–677
- 79. MDSplus quality improvement project** Thomas W. Fredian, Joshua Stillerman, G. Manduchi, Andrea Rigoni, Keith Erickson *Fus. Eng. and Design*, **112**, (Nov 2016) 906–909
- 80. Integrating supervision, control and data acquisition-The ITER Neutral Beam Test Facility experience** A. Luchetta, G. Manduchi, C. Taliercio, M. Breda, R. Capobianco, F. Molon, M. Moressa, P. Simionato, E. Zampiva *Fus. Eng. and Design*, **112**, (Nov 2016) 928–931
- 81. Continuous State-Space Model in dq Frame of the Thyristor AC/DC Converters for Stability Analysis of ITER Pulsed Power Electrical System** C. Finotti, E. Gaio, I. Benfatto, I. Song, J. Tao *IEEE T. Plasma Sci* **44**, 11 (2016)
- 82. The Full-Size Source and Injector Prototypes for ITER Neutral Beams** G. Serianni, P. Agostinetti, V. Antoni, D. Aprile, C. Baltador, M. Cavenago, G. Chitarin, N. Marconato, D. Marcuzzi, E. Sartori, P. Sonato, V. Toigo, P. Veltri And P. Zaccaria *Plasma and Fusion Research* **11**, 2402119 (2016)
- 83. Tomographic reconstruction of the beam emissivity profile in the negative ion source NIO1** N. Fonnesu, M. Agostini, R. Pasqualotto, G. Serianni and P. Veltri *Nucl. Fusion* **56** (2016) 126018
- 84. Modelling plasma response to RMP fields in ASDEX Upgrade with varying edge safety factor and triangularity** L. Li, Y.Q. Liu, A. Kirk, N. Wang, Y. Liang, D. Ryan, W. Suttrop, M. Dunne, R. Fischer, J.C. Fuchs, B. Kurzan, P. Piovesan, M. Willensdorfer, F.C. Zhong, the ASDEX Upgrade Team⁹ and the EUROfusion MST1 Team *Nucl. Fusion* **56** (2016) 126007
- 85. The physics and technology basis entering European system code studies for DEMO** R. Wenninger, R. Kembleton, C. Bachmann, W. Biel, T. Bolzonella, S. Ciattaglia, F. Cismonti, M. Coleman, A.J.H. Donnè, T. Eich, E. Fable, G. Federici, T. Franke, H. Lux, F. Maviglia, B. Meszaros, T. Putterich, A. Snickers,

- F. Villone, P. Vincenzi, D. Wol and H. Zohm *Nucl. Fusion* 57 (2017) 016011 (11pp)
- 86. Runaway electron mitigation by applied magnetic perturbations in RFX-mod tokamak plasmas** M. Gobbin, M. Valisa, R.B. White, D. Cester, L. Marrelli, M. Nocente, P. Piovesan, L. Stevanato, M.E. Puiatti and M. Zuin *Nucl. Fusion* 57 (2017) 016014 (16pp)
- 87. Gyrokinetic study of turbulent convection of heavy impurities in tokamak plasmas at comparable ion and electron heat fluxes** Angioni, R. Bilato, F.J. Casson, E. Fable, P. Mantica, T. Odstrcil, M. Valisa, ASDEX Upgrade Team and JET Contributors *Nucl. Fusion* 57 (2017) 022009 (11pp)
- 88. Axisymmetric oscillations at L–H transitions in JET: M-mode** Emilia R. Solano, N. Vianello, E. Delabie, J.C. Hillesheim, P. Buratti, D. Réfy, I. Balboa, A. Boboc, R. Coelho, B. Sieglin, S. Silburn, P. Drewelow, S. Devaux, D. Dodt, A. Figueiredo, L. Frassinetti, S. Marsen, L. Meneses, C.F. Maggi, J. Morris, S. Gerasimov, M. Baruzzo, M. Stamp, D. Grist, I. Nunes, F. Rimini, S. Schmuck, I. Lupelli, C. Silva and JET contributors *Nucl. Fusion* 57 (2017) 022021 (12pp)
- 89. Ion beam transport: modelling and experimental measurements on a large negative ion source in view of the ITER heating neutral beam** P. Veltri, E. Sartori, P. Agostinetti, D. Aprile, M. Brombin, G. Chitarin, N. Fonnesu, K. Ikeda, M. Kisaki, H. Nakano A. Pimazzoni, K. Tsumori and G. Serianni *Nucl. Fusion* 57 (2017) 016025 (14pp)
- 90. Avoidance of tearing mode locking with electro-magnetic torque introduced by feedback-based mode rotation control in DIII-D and RFX-mod** M. Okabayashi, P. Zanca, E.J. Strait, A.M. Garofalo, J.M. Hanson, Y. In, R.J. La Haye, L. Marrelli, P. Martin, R. Paccagnella, C. Paz-Soldan, P. Piovesan, C. Piron, L. Piron, D. Shiraki, F.A. Volpe and The DIII-D and RFX-mod Teams *Nucl. Fusion* 57 (2017) 016035 (13pp)
- 91. Sawtooth mitigation in 3D MHD tokamak modelling with applied magnetic perturbations** D Bonfiglio, M Veranda, S Cappello, L Chacón and D F Escande *Plasma Phys. Control. Fusion* 59 (2017) 014032 (10pp)
- 92. Impact of ideal MHD stability limits on high-beta hybrid operation** P. Piovesan, V Igochine, F Turco, D A Ryan, M R Cianciosa, Y Q Liu, L Marrelli, D Terranova, R S Wilcox, A Wingen *Plasma Phys. Control. Fusion* 59 (2017) 014027 (13pp)

Communications to Workshops and Conferences

IPAB 2016

Status of NBI for ITER and the related test facility G. Serianni, and NBI team
IPAB 2016, INFN Legnaro, Italy May 5 – June 3 2016

PSI2016, Roma May 30 – June 2 to be published in Nuclear Materials and Energy

Electromagnetic ELM and inter-ELM filaments detected in the COMPASS Scrape Off Layer M. Spolaore, K. Kovařík, J. Stöckel, J. Adamek, R. Dejarnac, I. Đuran, M. Komm, T. Markovic, E. Martines, J. Seidl, N. Vianello and the COMPASS team

Heat flux measurements and modeling in the RFX-mod experiment P. Innocente, H. Bufferand, A. Canton, G. Ciraolo, N. Visonà

Boundary plasma response in RFX-mod to 3D magnetic field perturbations P. Scarin, M. Agostini, L. Carraro, G. Spizzo, M. Spolaore, N. Vianello

The electrostatic response to edge islands: a comparison between the RFP and the tokamak G. Spizzo, O.Schmitz, R.B.White, S.S.Abdullaev, M.Agostini, R.Cavazzana, G. DeMasi, T.E. Evans, H. Frerichs, G. Granucci, G. Pucella, P. Scarin, M. Spolaore, O. Tudisco, N. Vianello, M. Zuin

Dynamics and frequency behaviour of the MARFE instability on FTU C.Mazzotta, E.Giovanozzi, G.Pucella, G.Spizzo, O.Tudisco, W.Bin, B.Esposito and the FTU team

Changeover from Deuterium to Helium with Ion Cyclotron Wall Conditioning and diverted plasmas in ASDEX Upgrade D. Douai, T. Wauters, V. Rohde, A. Garcia-Carrasco, V. Bobkov, S. Brezinsek, D. Carralero, R. Cavazzana, A. Hakola, A. Lyssoivan, S. Möller, R. Ochoukov, P. Peterson, P. Schneider, M. Spolaore, the EUROfusion MST1 Team and ASDEX Upgrade Team

The 6th Asian-Pacific Transport Working Group (APTWG) Meeting, June 21 – 25 2016, Korea

Physics of Reversed Field Pinch Relaxation S. Cappello- Invited talk

18th International Congress on Plasma Physics (ICPP 2016), 2016/6/27 ~ 2016/7/1, Taiwan

Magnetic chaos healing and transport barriers in new stimulated helical regimes of the Reversed Field S. Cappello, D. Bonfiglio¹, D. F. Escande², M. Veranda¹, A. Fassina¹, P. Franz¹, M. Gobbin¹, M. E. Puiatti

2016 IEEE Power Modulator and High Voltage Conference, S. Francisco CA, July 5-9 2016

High Voltage Radio Frequency Test Facility for the characterization of the dielectric strength in vacuum of RF drivers for Neutral Beam Injectors Ion Sources A. Maistrello, J. Palak, M. Recchia, M. Bigi, E. Gaio and V. Toigo

21st Joint EU-US Transport Task Force Meeting - Leysin (Switzerland), 5-8 September 2016

The electrostatic response to edge islands: a comparison between the RFP and the tokamak G. Spizzo, O. Schmitz, R.B. White, S. S. Abdullaev, M. Agostini, R. Cavazzana, G. De Masi, T.E. Evans, H. Frerichs, G. Granucci, C. Mazzotta, G. Pucella, P. Scarin, M. Spolaore, O. Tudisco, N. Vianello, M. Zuin Invited

Thermal gradients of QSH states in RFX-mod Y. Zhang, F. Auriemma, B. Momo, F. Sattin, R. Lorenzini, E. Martines, A. Fassina, D. Lopez-Bruna and D. Terranova

Impurity injection in RFX-mod Reversed Field Pinch for impurity transport studies L. Carraro, F. Auriemma, A. Fassina, P. Franz, I. Predebon, P. Scarin, D.Terranova

102° Congresso Nazionale Società di Fisica, Padova 26-30 settembre 2016

A polarimetric Thomson scattering diagnostic in ITER L. Giudicotti and R. Pasqualotto

High power Negative ion beams: main physics issues M. Cavenago, V. Antoni, P. Agostinetti, D. Aprile, G. Chitarin, N. Marconato, R. Pasqualotto, N. Pilan, E. Sartori, P. Veltri

Beam and ion source diagnostics for the ITER NBI system R. Pasqualotto, M. Brombin, G. Serianni, B. Zaniol, M. Spolaore, M. Dalla Palma, M. Barbisan, S. Gorini

Experimental analysis of MHD instability in a wide range of plasma equilibria for magnetic fusion confinement in RFX-mod M. Zuin and the RFX-mod Team and Collaborators

Interaction of a low-temperature plasma with pathogens and eukaryotic cells E. Martines, M. Zuin, P. Brun, R. Cavazzana, L. Cordaro, G. De Masi, A. Fassina

Plasma sustainment by Neutral Beam Injection (NBI): from current leading experiments to future nuclear fusion reactors P. Vincenzi, T. Bolzonella, M. Vallar

58th Annual Meeting of the APS Division of Plasma Physics, October 31 - November 4, 2016, San Jose, California

Electrical modeling of the Reversed Field Pinch configuration R. Cavazzana

Spectral properties of VMEC equilibria Predebon, B Momo, D Terranova, P Innocente

A polarimeter for JT-60SA: chords layout study with V3FIT for q profile reconstruction D. Terranova, A. Boboc, C. Gil, S. Soare, F.P. Orsitto

Helical self-organization in the reversed-field pinch: detection of barriers to transport M. Veranda, D. Bonfiglio, S. Cappello, D. F. Escande, F. Auriemma, D. Borgogno, L. Chacòn, D. Grasso, G. Rubino, A. Fassina, P. Franz, M. Gobbin, M.E. Puiatti

Density and magnetic fluctuations at JET: experimental observation and numerical characterization G. De Masi, I. Predebon, I. Lupelli, S. Spagnolo, J. C. Hillesheim, L. Menezes, E. Delabie, C. Maggi

APPC 2016 (joint 13th Asia Pacific Physics Conference and 22nd Australian Institute of Physics Congress), Brisbane, Australia, 4-8 Dec. 2016

Further progress on integrated transport analysis suite, TASK3D-a, and its contributions for promoting scientific understandings of LHD plasmas M. Yokoyama, R. Seki, C. Suzuki, M. Sato, M. Emoto, S. Murakami, M. Osakabe, T. Ii, Tsujimura, Y. Yoshimura, K. Ogawa, S. Satake, Y. Suzuki, T. Goto, K. Ida, N. Pablant, F. Warmer, P. Vincenzi

Conference participations

RT2016 - 20th Real Time Conference, Padova, Italy, June 05-10 2016 to be published in IEEE Transactions on Nuclear Science

Current status of SPIDER CODAS and its evolution towards the ITER compliant NBI CODAS MANDUCHI G., Adriano Luchetta, C. Taliercio, Andrea Rigoni

Distributed continuous event – based data acquisition using FlexRIO FPGA C. Taliercio, A. Luchetta, G. Manduchi and A. Rigoni

Assessment of General Purpose GPU systems in real-time control Tj. Maceina, G. Manduchi

Real Time Control of Electron Density on RFX-mod Tokamak Discharges R. Cavazzana, C. Taliercio, G. Manduchi, L. Marrelli, P. Franz, P. Piovesan and C. Piron

Control system optimization techniques for real-time applications in fusion plasmas: the RFX-mod experience L. Pigatto, M. Baruzzo, P. Bettini, T. Bolzonella, G. Manduchi, G. Marchiori

29th SOFT 2016, Sept 5-9 2016, Prague, Czech Republic (to be published in *Fus. Eng. and Design* special Issue, except for *)

A substantial step forward in the realization of the iter HNB system: the iter NBI test facility V. Toigo, D. Boilson, T. Bonicelli, R. Piovan, M. Hanada, A. Chakraborty and NBTF Team and the contributing Staff of IO, F4E, JADA and INDA – **Invited** - In press *Fusion Eng. Des.* (2016), <http://dx.doi.org/10.1016/j.fusengdes.2016.11.007>

Design of machine upgrades for the RFX-mod experiment S. Peruzzo, P. Bettini, A. Canton, R. Cavazzana, S. Dal Bello, M. Dalla Palma, L. Grando, P. Innocente, G. Marchiori, L. Marrelli, N. Patel, M. Siragusa, A. Zamengo, P. Zanca, L. Zanotto, P. Sonato **Oral talk**

Economic assessment of different operational reactor cycle structures in a pulsed DEMO-like power plant C. Bustreo, G. Zollino, D. Maggio

Final Design of SiC-based Power Supply system for Resistive- Wall-Mode control in JT-60SA E. Gaio, A. Ferro, L. Novello, M. Matsukawa, M. Shimada

Requirements and modelling of fast particle injection in RFX-mod tokamak plasmas M. Vallar, JF. Artaud, T. Bolzonella, M. Valisa, P. Vincenzi,

Implementation of the SPIDER Central Interlock N. Pomaro, A. Luchetta, C. Taliercio, M. Moressa, L. Svensson, F. Paolucci, F. Sartori, C. Labate

3D electromagnetic analysis of the MHD control system in RFX-mod Upgrade P. Bettini, P. Alotto, T. Bolzonella, R. Cavazzana, L. Grando, G. Marchiori, L. Marrelli, L. Pigatto, R. Specogna, P. Zanca

Comparison of three methods for the solution of eddy current problems in fusion devices R. Specogna, P. Bettini

Final design of the diagnostic calorimeter for the negative ion source SPIDER A. Rizzolo, M. Tollin, M. Brombin, V. Cervaro, M. Dalla Palma, M. De Muri, D. Fasolo, L. Franchin, S. Peruzzo, A. Pimazzoni, R. Pasqualotto, G. Serianni (* **not submitted Fus. Eng. and Design**)

Final design and prototyping of the SPIDER caesium ovens A. Rizzolo, M. Froschle, B. Laterza, M. De Muri, F. Rossetto

Modeling and mitigation of the magnetic field errors in RFX-mod Upgrade L. Grando, P. Bettini, C. Finotti, G. Marchiori, R. Specogna,

Installation and site testing of the SPIDER Ion Source and Extraction Power Supplies M. Bigi, S. Carrozza, G. Corbucci, A. Luchetta, M. Moressa, L. Rinaldi, M. Simon, L. Sita, G. Taddia, A. Zamengo, H. Decamps, P. Simionato, C. Taliercio, D. Zella, V. Toigo (* **not submitted Fus. Eng. and Design**)

SPIDER Gas injection and Vacuum System: from design to site acceptance test S. Dal Bello, M. Fincato, E. Bragulat, M. Breda, F. Buffa, L. Grando, A. Luchetta, F. Paolucci, A. Principe, P. Simionato, F. Siroti, L. Svensson, P. Zaccaria

Commissioning and First Operation of the SPIDER Control and Data Acquisition System A. Luchetta, G. Manduchi, C. Taliercio, P. Barbato, R. Capobianco, S. Polato, P. Simionato, E. Zampiva, L. Svensson, F. Paolucci, F. Sartori, C. Labate

Manufacturing and assembly of the cooling plant for SPIDER experiment F. Fellin, M. Bigi, M. Breda, G. Lazzaro, A. Luchetta, M. Maniero, N. Pilan, P. Zaccaria, M. Zaupa, G. Agarici, V. Pilard, G. Cenedella, M. Tamagnone, N. Granzotto, A. Turetta

3D magnetic surfaces reconstruction in RFX-mod F. Ledda, P. Bettini, A. Chiariello, Gaetano, A. Formisano, G. Marchiori,; R. Martone, F. Pizzo, D. Terranova

Upgraded electromagnetic measure system for RFX-mod G. Marchiori, R. Cavazzana, P. Bettini, L. Grando, S. Peruzzo,

Integration of the state observer RAPTOR in the real-time MARTe framework at RFX-mod C. Piron, G. Manduchi, P. Bettini, F. Felici, G. Finotti, P. Franz, O. Kudlacek, G. Marchiori, L. Marrelli, O. Sauter, P. Piovesan, C. Taliercio

Final design of the HV deck1 and bushing for the ITER Neutral Beam Injector M. Boldrin, T. Bonicelli, H. Decamps, C. Finotti, G.E. Gomez, M. Krohn, E. Sachs, M. Simon, V. Toigo

Final design of acceleration grid power supply conversion system of MITICA neutral beam injector L. Zanotto, E. Gaio, D. Gutierrez, M. Simon, H. Decamps, M. Perna, F. Guarda, C. Panizza, C. Brocca

The design of the Residual Ion Dump Power Supply for ITER Neutral Beam Injector A. Ferro, E. Gaio, L. Sita, L. Rinaldi, G. Taddia, D. Gutierrez, M. Simon, H. Decamps

The transmission line for the SPIDER experiment: from design to installation M. Boldrin, V. Toigo, D. Gutierrez, M. Simon, G. Faoro, E. Maggiora, D. Pedron, A. Guion, H. Decamps

SPIDER High Voltage Bushings: design, development and first experimental tests N. Pilan, L. Grando, A. De Lorenzi, A. Masiello, L. Christophe

Realization of a magnetically compensated extraction grid for performance improvement of next generation NBI D. Aprile, P. Agostinetti, C. Baltador, G. Chitarin, N. Marconato, E. Sartori, G. Serianni, P. Veltri

Application of the VTTJ cold junction technique to fusion reactor relevant geometry and materials P. Agostinetti, F. Degli Agostini, P. Sonato

Multi-design innovative cooling research & optimization (MICRO): novel proposals for high performance cooling in DEMO novel proposals for high performance cooling in DEMO G. Gambetta, P. Agostinetti, P. Sonato

Inverse heat flux evaluation from thermographic measurements in SPIDER R.S. Delogu, A. Pimazzoni, G. Serianni,

EU DEMO transient phases: main constraints and heating mix studies for ramp-up and ramp-down P. Vincenzi, R. Ambrosino, J.F. Artaud, T. Bolzonella, L. Garzotti, G. Giruzzi, G. Granucci, F. Kochl, M. Mattei, M.Q. Tran, R. Wenninger

Feasibility study of a flux-gate magnetic field sensor suitable for ITER Neutral Beam Injectors G. Chitarin, D. Aprile, M. Brombin, N. Marconato, L. Svensson,

Current status of the EU DEMO Project on the inner fuel cycle systems Day, C., Butler, B., Giegerich T., B. Ploekl, F. Cismondi, A. Frattolillo, M. Gethins, S. Hanke, A. Hollingsworth, Horstensmeyer, Y.1; Igitkhanov, P. T. Lang, R. Lawless, X. Luo, S. A. Medley, C. Moreno, S. S. Naris, Y. Ochoa, B. Pegourie, B. Peters, M. Rollig, A. Santucci, E. Sartori, M. Scannapiego, R. Shaw, P. Sonato, H. Strobel, S. Tosti, S. Varoutis, R. J. Walker, D. Whittaker, Oral -

The DTT device: systems for heating G. Granucci, P. Agostinetti, T. Bolzonella, A. Bruschi, A. Cardinali, S. Ceccuzzi, L. Figini, S. Garavaglia, G. Giruzzi, R. Maggiora, D. Milanese, F. Mirizzi, S. Nowak, G.L. Ravera, P. Sonato, C. Sozzi, A.A. Tuccillo, P. Vincenzi,

The DTT device: power supply and electrical distribution system A. Lampasi, P. Zito, F. Starace, P. Costa, G. Maffia, E. Gaio, V. Toigo, L. Zanotto, S. Minucci, S. Ciattaglia, M.C. Falvo

Experimental characterization of the MITICA neutralizer gas injection nozzles S. Hanke, V. Hauer, C. Day, E. Sartori, S. Dal Bello, P. Zaccaria, M. Zhang, M. Dalla Palma

Implementation of the soft X-ray multi-camera tomography diagnostic in the Wendelstein 7-X stellarator C. Brandt, T. Broszat, P. Franz, M. Schulke, M. Sieber, H. Thomsen, S. Weißflog, M. Marquardt,

Experimental investigation of beam-target neutron emission at the ELISE neutral beam test facility G. Croci, M. Nocente, D. Wunderlich, F. Bonomo, U. Fantz, B. Heinemann, W. Kraus, R. Pasqualotto, M. Tardocchi, G. Gorini

Heating & Current Drive Efficiencies, TBR and RAMI considerations for DEMO Franke, P. Agostinetti, K. Avramidis, A. Bader, C. Bachmann, W. BieT. I, T. Bolzonella, S. Ciattaglia, M. Coleman, F. Cismondi, G. Granucci, G. Grossetti, J. Jelonnek, I. Jenkins, M. Kalsey, R. Kempleton, N. Mantel, J.M. Noterdaeme, N. Rispoli, A. Simonin, P. Sonato, M.Q. Tran, P. Vincenzi, R. Wenninger

Advanced probe for transport measurements in mediumsize tokamaks B.S. Schneider, S. Costea, C. Ionita, R. Schrittwieser, V. Naulin, J.J. Rasmussen, N. Vianello, M. Spolaore, J. Kovacic, T. Gyergyek, R. Starz

X-mode raw data analysis of the new AUG ICRF antenna edge density profile reflectometer Aguiam, E. Diogo, A. Silva, P.J. Carvalho, P. Carvalho, R. Cavazzana, G.D. Conway, O. D'arcangelo, L. Fattorini, H. Faugel, A. Fernandes, H. Funfgelder, B. Goncalves, L. Guimaraes, G. De Masi, L. Meneses, J.M. Noterdaeme, R. Pereira, G. Rocchi, J. Santos, A. Tuccillo, O. Tudisco, Team, Asdex Upgrade

The influence of dust characteristics on re-suspension: test with tungsten and data discussion A. Malizia, I. Cacciotti, M. Gelfusa, A. Murari, L. Poggi, Antonio, Ciparisse, P. Gaudio

5th International Symposium on Negative Ions, Beams and Sources (NIBS`16), 12th - 16th September 2016, St. Anne's College, Oxford, UK to be published by AIP conference proceedings series

Test of 1D carbon-carbon composite prototype tiles for the SPIDER diagnostic calorimeter G. Serianni, A. Pimazzoni, A. Canton, M. Dalla Palma, R. Delogu, D. Fasolo, L. Franchin, R. Pasqualotto, M. Tollin

Finite elements numerical codes as primary tool to improve beam optics and support measurements in NIO1 C. Baltador, P. Veltri, M. Cavenago, G. Serianni

Control, Interlock, Acquisition and Data Retrieval Systems for the Negative Ion Source NIO1 P. Serianni, P. Barbato, L. Baseggio, M. Cavenago, M. De Muri, B. Laterza, L. Migliorato, F. Molon, G. Moro, D. Ravarotto, R. Pasqualotto, M. Recchia, C. Taliercio, P. Veltri

Does viscous and transient effects, dissociation, heating and surface scattering play a role in the gas density distribution along SPIDER E. Sartori, G. Serianni

Preliminary studies for a beam-generated plasma neutralizer test in NIO1 E. Sartori, P. Veltri, L. Balbinot, M. Cavenago, V. Antoni, G. Serianni

Development of an energy analyzer as diagnostic of beam-generated plasma in negative ion beam system E. Sartori, G. Carozzi, P. Veltri, M. Spolaore, V. Antoni, G. Serianni

Progress on development of SPIDER diagnostics R. Pasqualotto, M. Agostini, M. Barbisan, M. Brombin, R. Cavazzana, G. Croci, M. Dalla Palma, R. S. Delogu, G. Gorini, A. Muraro, N. Pomaro, G. Serianni, S. Spagnolo, M. Spolaore, M. Zaupa, B. Zaniol

Experimental validation of an innovative deflection compensation method in a multi-beamlet negative-ion accelerator G. Chitarin, A. Kojima, P. Agostinetti, D. Aprile, C. Baltador, J. Hiratsuka, M. Ichikawa, N. Marconato, E. Sartori, G. Serianni, P. Veltri, M. Yoshida, M. Kashiwagi, M. Hanada, V. Antoni

A first characterization of NIO1 particle beam by means of a diagnostic calorimeter A. Pimazzoni, M. Cavenago, V. Cervaro, D. Fasolo, G. Serianni, M. Tollin, P. Veltri

Study of electron transport across the magnetic filter of NIO Negative ion P. Veltri, M. Cavenago, E. Sartori and G. Serianni

Electron density and temperature in NIO1 RF source, operated in oxygen and argon M. Barbisan, M. Cavenago, R. Pasqualotto, G. Serianni and B. Zaniol

Influence of the magnetic filter field topology on the beam divergence at the ELISE test facility M. Barbisan, U. Fantz and D. Wunderlich

Improvements of the Versatile Multiaperture Negative Ion Source NIO1 M. Cavenago, G. Serianni, M. De Muri, P. Veltri, V. Antoni, C. Baltador, M. Barbisan, M. Brombin, A. Galatà, N. Ippolito, T. Kulevoy, R. Pasqualotto, S. Petrenko, A. Pimazzoni, M. Recchia, E. Sartori, F. Taccogna, V. Variale, B. Zaniol, P. Barbato, L. Baseggio, V. Cervaro, D. Fasolo, L. Franchin, R. Ghirdelli, B. Laterza, M. Maniero, D. Martini, L. Migliorato, A. Minarello, F. Molon, G. Moro, T. Patton, D. Ravarotto, R. Rizzieri, A. Rizzolo, M. Sattin, F. Stivanello and S. Zucchetti

Benchmark of single beamlet analysis to predict operational parameter for ITER in Japan - Italy joint experiments M. Ichikawa, A. Kojima, G. Chitarin, P. Agostinetti, D. Aprile, C. Baltador, M. Barbisan, R. Delogu, J. Hiratsuka, N. Marconato, R. Nishikiori, A. Pimazzoni, E. Sartori, G. Serianni, H. Tobar, N. Umeda, P. Veltri, K. Watanabe, M. Yoshida, V. Antoni and M. Kashiwagi

Energy recovery from mixed H⁻/H⁰/H⁺ beams and collector simulations V. Variale, M. Cavenago, C. Baltador, G. Serianni, P. Veltri, E. Sartori, P. Agostinetti

Particle model of a cylindrical inductively coupled ion source N. D. Ippolito, F. Taccogna, P. Minelli, M. Cavenago, P. Veltri

27th International Symposium on Discharges and Electrical Insulation in Vacuum (27th ISDEIV), Suzhou, China, Sept 18-23, 2016 To be published in IEEE Transactions on Plasma Science Special Issue

Prediction of Lightning Impulse Voltage Induced Breakdown in Vacuum Interrupters N. Marconato, A. De Lorenzi, N. Pilan, P. Bettini, A. Lawall, N. Wenzel

XXI Convegno AIPT, Reggio Emilia, 30-09-2016, Proc. to be published

Thermo-hydraulic design and monitoring of high heat flux components for the ITER NBTF Dalla Palma M., R. Pasqualotto, P. Zaccaria

FUNFI2, Enea, Frascati, 26-28 Ottobre 2016 Proc. to be published

The reversed field pinch as neutron source for fusion-fission hybrid systems: strengths and issues R. Piovan, M.E. Puiatti, M. Valisa, G. Zollino, C. Bustreo, S. Martini, D. Escande

Characterization of Neutron Production and Fast Particle Dynamics in Reversed-Field Pinch Plasmas M. Zuin, L. Stevanato, E. Martines, F. Auriemma, M. Gobbin, B. Momo, R. Cavazzana, G. De Masi, W. Gonzalez, R. Lorenzini, M.E. Puiatti, P. Scarin, S. Spagnolo, M. Spolaore, M. Valisa, N. Vianello, W. Schneider, D. Cester, G. Nebbia, L. Sajo-B

21st Workshop on MHD Stability Control – A US-Japan Workshop San Diego, CA on November 7-9, 2016 To be published in Special Issue PPCF

Model-based real-time scenario monitoring for transient event prediction with RAPTOR C. Piron, invited talk,

Effects of 3D fields on disruption generated runaway electrons in AUG, TCV and RFX-mod Marco Gobbin, invited talk

Conference proceedings

High Temperature Plasma Diagnostics HTPD 2016, June 5-9 2016, Madison – Wisconsin USA

Study of a high power hydrogen beam diagnostic based on secondary electron emission Sartori E., Panasenkov A., Veltri P., Serianni G., Pasqualotto R

Design of in-vacuum sensors for the beamline components of the ITER neutral beam test facility M. Dalla Palma, R. Pasqualotto, E. Sartori, S. Spagnolo, M. Spolaore, and P. Veltri

Design and status of the electrostatic probe system for the SPIDER experiment M. Spolaore, M. Brombin, R. Cavazzana, G. Serianni, R. Pasqualotto, N. Pomaro, G. Taliercio

Extending the T_e range of the ITER core Thomson scattering system by detection of the unpolarized scattering radiation L. Giudicotti^{1,2}, R. Pasqualotto² and O. McCormack

Final design of SPIDER thermal diagnostic system M. Brombin, M. Dalla Palma, R. Pasqualotto, and N. Pomaro

SPIDER beam dump as diagnostic of the particle beam M. Zaupa, M. Dalla Palma, R. Pasqualotto, E. Sartori

Dual-laser, self-calibrating Thomson scattering measurements in RFX-MOD O. McCormack,^{a,1} L. Giudicotti,^{a,b} A. Fassina,^a and R. Pasqualotto

43rd European Physical Society Conference on Plasma Physics, Leuven, Belgium, 4 - 8 July 2016 Published in European Physical Society Conference on Plasma Physics – ECA Vol. 40A

Impact of ideal MHD stability limits on high-beta hybrid operation P. Piovesan, V Igochine, F Turco, D A Ryan, M R Cianciosa, Y Q Liu, L Marrelli, D Terranova, R S Wilcox, A Wingen **Invited talk published in PPCF 2017**

Connections between RFP, Tokamak and Stellarator physics as highlighted in 3D nonlinear MHD modeling D. Bonfiglio, S. Cappello, D.F. Escande, M. Veranda, D. Borgogno, L. Chacón, D. Grasso, G. Rubino **Invited talk published in PPCF 2017**

Characterising W radiation in JET-ILW plasmas Emilia R. Solano, I. Coffey, A. Huber, S. S. Henderson, M. O'Mullane, F. Casson, H. Summers, T. Pütterich, M.E. Puiatti, L. Carraro, M. Valisa, S. Menmuir, K. Lawson, M. Sertoli, B. Lomanowski, M. Reinke, M. Bernert, P. Drewelow, M. Maslov, J. Flanagan, G. Sergienko, M. Stamp, S. Brezinsek, L. Meneses, S. Schmuck, J. Boom, C. Giroud, C. Guillemaut, E. de la Luna, A. Baciero and JET Contributors – P2.005

Characterization of first wall materials in RFX-mod A. Canton, P. Innocente, S. Deambrosis, L. Grando, E. Miorin, M. Siragusa, N. Visonà – P5.012

Entrainment of MHD modes in ASDEX Upgrade using non-axisymmetric coils R.Paccagnella, M.Maraschek, P.Zanca, S.Fietz, L.Giannone, A.Gude, V.Igocine, A. Lazaros, L.Marrelli, P.Piovesan, M.Reich, W.Suttrop, and the ASDEX Upgrade and EUROfusion MST1 teams – P1.027

Non-linear evolution of RFX-mod tokamak equilibria during L-H transition including 3D wall effects D. Abate, G. Marchiori, F. Villone – P5.013

Tokamak experiments in RFX-mod with polarized insertable electrode L. Carraro, R. Cavazzana, S. Dal Bello, G. De Masi, A. Ferro, C. Finotti, P. Franz, L. Grando, P. Innocente, O. Kudlacek, G. Marchiori, L. Marrelli, E. Martines, R. Paccagnella, P. Piovesan, C. Piron, M.E. Puiatti, M. Recchia, P. Scarin, S. Spagnolo, M. Spolaore, C.Taliercio, B. Zaniol, L. Zanutto, M. Zuin – P5.014

Resistive Wall Mode Stability in JT-60SA High β_N Scenarios L. Pigatto, T. Bolzonella, J. Garcia, S. C. Guo, Y.Q. Liu, X. Xu – P4.078

Sensitivity of Thomson Scattering measurements on electron distribution modelling in low density RFP Plasmas A. Fassina, P. Franz – P5.016

Current sheet fragmentation following magnetic reconnection in RFP plasmas L. Cordaro, M. Zuin, B. Momo, E. Martines, M. Spolaore, F. Auriemma, R. Cavazzana, G. De Masi, P. Scarin, S. Spagnolo, N. Vianello, D. Cester, L. Stevanato, H. Isliker, L. Vlahos, W. Schneider – P5.015

Parametrisation of optimal RMP coil phase on ASDEX Upgrade D. A. Ryan, Y. Liu, A. Kirk, M. Dunne, L. Li, B. Dudson, P. Piovesan, W. Suttrop, M. Willensdorfer, the ASDEX-Upgrade team and the EUROfusion MST1 team – P1.057

JET disruption simulations H. Strauss, R. Paccagnella, J. Breslau, E. Joffrin, V. Riccardo, I. Lupelli, M. Baruzzo and JET Contributors – P2.012

Reconstruction of 3-D VMEC equilibria with helical cores in DIII-D A. Wingen, R.S. Wilcox, M.R. Cianciosa, S.K. Seal, E.A. Unterberg, S.P. Hirshman, P. Piovesan and F. Turco – P5.025

The External Kink Mode and the Role of q_{95} in Diverted Tokamaks A.D. Turnbull, J.M. Hanson, F.Turco, N.M. Ferraro, M.J. Lanctot, L.L. Lao, E.J. Strait, P. Piovesan and P. Martin – O3.109

International Symposium on Electromagnetic Theory (EMTS 2016), 14–18 August 2016, Espoo, Finland

Fast computational techniques for modeling RFX-mod fusion devices on hybrid CPU-GPU architectures D. Abate, B. Carpentieri, A. G. Chiariello, G. Marchiori, N. Marconato, S. Mastrostefano, G. Rubinacci, S. Ventre, F. Villone – **Invited** - Special Issue of the 2016 URSI Commission B International Symposium on Electromagnetic Theory

26th IAEA Fusion Energy Conference, Kyoto, Japan, 17–22 October 2016

Overview of the RFX-Mod Fusion Science Activity M. Zuin, M. E. Puiatti, L. Marrelli, and S. Dal Bello , OV/P-2

Extended Scenarios Opened by the Upgrades of the RFX-Mod Experiment M. E. Puiatti, M. Agostini, P. Bettini, A. Canton, R. Cavazzana, S. Dal Bello, M. Dalla Palma, R. S. Delogu, G. De Masi, A. Fassina, P. Innocente, L. Grando, O. Kudlacek, G. Marchiori, L. Marrelli, N. Patel, S. Peruzzo, M. Siragusa, P. Sonato, M. Spolaore, M. Valisa, P. Zanca, and L. Zanotto, 26th, EX/P5-23

The ITER Neutral Beam Test Facility toward SPIDER Operation V. Toigo, D. Boilson, T. Bonicelli, A. K. Chakraborty, U. Fantz and the contributing Staff of IO2, F4E3, IPR4 and IPP , FIP/P4-28

H-Mode Achievement and Edge Features in RFX-Mod Tokamak Operation M. Spolaore, R. Cavazzana, L. Marrelli, L. Carraro, P. Franz, S. Spagnolo, B. Zaniol, M. Zuin, L. Cordaro, S. Dal Bello, G. De Masi, A. Ferro, C. Finotti, L. Grando, P. Innocente, O. Kudlacek, G. Marchiori, E. Martines, B. Momo, R. Paccagnella, P. Piovesan, C. Piron, M. E. Puiatti, M. Recchia, P. Scarin, C. Taliercio, N. Vianello, L. Zanotto , EX/P5-24

Synergy of Numerical Simulations and Experimental Measurements to Improve the Interpretation of Negative Ion Beam Properties G. Serianni, P. Agostinetti, V. Antoni, D. Aprile, M. Brombin, M. Cavenago, G. Chitarin, R. S. Delogu, N. Marconato, R. Pasqualotto, A. Pimazzoni, E. Sartori, P. Veltri, O. Kaneko, Y. Takeiri, M. Osakabe, K. Nagaoka, K. Ikeda, H. Nakano, M. Kisaki, and K. Tsumori , FIP/P4-31

Conceptual Design of the DEMO NBIs: Main Developments and R&D Achievements P. Sonato, M. Q. Tran, U. Fantz, I. Furno, P. Agostinetti, T. Franke, A. Fassina, L. Zanotto, E. Sartori, A. Simonin, and C. Hopf , FIP/P7-5

Kinetic Properties of Edge Plasma with 3D Magnetic Perturbations in RFX-Mod M. Agostini, P. Scarin, G. Spizzo, F. Auriemma, D. Bonfiglio, S. Cappello, L. Carraro, M. Spolaore, M. Veranda, N. Vianello, M. Zuin and RFX-mod Team , EX/P5-25

Transport Studies with Magnetic Islands in Fusion Plasmas R. Lorenzini, F. Auriemma, A. Fassina, B. Momo, I. Predebon, F. Sattin, D. Terranova, D. López-Bruna, Y. Narushima, Y. Suzuki and the LHD experiment group, EX/P5-26

The Role of ELMs and Inter-ELM Phases in the Transport of Heavy Impurities in JET M. Valisa, L. Amicucci, C. Angioni, R. Cesario, L. Carraro, D. Coster, F. J. Casson, E. de la Luna, I. Coffey, P. Devynck, P. Drewelow, L. Frassinetti, C. Giroud, F. Koechl, M. Leyland, A. Loarte, M. Marinucci, M. O'Mullane, V. Parail, M. E. Puiatti, M. Romanelli, and E. Stefanikova , EX/P6-17

Physics, Control and Mitigation of Disruptions and Runaway Electrons in the EUROfusion Medium Size Tokamaks Science Programme P. Martin, T. Blanken, D. Carnevale, J. Decker, B. Duval, B. Esposito, E. Fable, F. Felici, A. Fil, M. Gobbin, G. Granucci, M. Hoelzl, O. Kudlacek, M. Maraschek, L. Marrelli, J. Mlynář, E. Nardon, M. Nocente, R. Paccagnella, G. Papp, G. Pautasso, P. Piovesan, C. Piron, V. V. Plyusnin, C. Sommariva, C. Sozzi, M. Valisa, and P. Zanca , EX/P6-23

Role of MHD Dynamo in the Formation of 3D Equilibria in Fusion Plasmas P. Piovesan, D. Bonfiglio, S. Cappello, L. Chacón, C. Chrystal, D. Escande, P. Franz, C. T. Holcomb, V. Igoshine, T. C. Luce, L. Marrelli, M. Nornberg, C. Paz-Soldan, L. Piron, J. S. Sarff, N. Taylor, D. Terranova, F. Turco, P. Zanca, and B. Zaniol , EX/1-1

Securing High-N JT-60SA Operational Space by MHD Stability and Active Control Modelling T. Bolzonella, P. Bettini, S. C. Guo, Y. Liu, G. Marchiori, G. Matsunaga, S. Mastrostefano, S. Nowak, L. Pigatto, O. Sauter, M. Takechi, F. Villone, X. Xu, N. Aiba, J. Garcia, L. Garzotti, N. Hayashi, P. Lauber, M. Romanelli, J. Shiraishi, and C. Sozzi , TH/P1-18

Progress in Theoretical RFP Studies: New Stimulated Helical Regimes and Similarities with Tokamak and Stellarator D. Bonfiglio, M. Veranda, M. Agostini, S. Cappello, D. Borgogno, L. Chacón, D. Escande, A. Fassina, P. Franz, M. Gobbin, D. Grasso, P. Piovesan, I. Predebon, G. Rubino, F. Sattin, and M. Zuin , TH/P3-35

Enhancement of Helium Exhaust by Resonant Magnetic Perturbation Fields O. Schmitz, K. Ida, M. Kobayashi, A. Bader, S. Brezinsek, T. E. Evans, Y. Feng, H. Funaba, M. Goto, C. C. Hegna, O. Mitarai, T. Morisaki, G. Motojima, Y. Narushima, D. Nicolai, U. Samm, G. Spizzo, H. Tanaka, M. Yoshinuma, and Y. Xu , EX/1-4

Overview of MST Reversed Field Pinch Research in Advancing Fusion Science J. S. Sarff, J. K. Anderson, P. Brunzell, D. L. Brower, B. E. Chapman, D. Den Hartog, W. X. Ding, L. Frassinetti, R.W. Harvey, V. Mirnov, M. Nornberg, S. Polosatkin, C. Sovinec, D. Spong, P.W. Terry, A. F. Almagri, J. Boguski, P. Bonofiglio, M. Borchardt, W. Capecchi, C. Cook, D. Craig, J. Egedal, A. DuBois, J. Duff, X. Feng, D. Demers, P. Fimognari, C. Forest, M. Galante, J. Goetz, C. C. Hegna, D. Holly, C. Jacobson, J. Johnson, J. Kim, S. Kubala, L. Lin, K. McCollam, M. McGarry¹, L. Morton, S. Munaretto, T. Nishizawa, R. Norval, P. Nonn, S. Oliva, M. J. Pueschel, J. Reusch, L. Reusch, J. Sauppe, S. Sears, A. Seltzman, J. Triana, D. Thuecks, G. Whelan, Z. Williams, A. Xing, O. Schmitz, T. Crowley, V. Belykh, V. Davydenko, A. A. Ivanov, R. Fridström, P. Franz, S. Hirshman, E. Parke, H. Stephens, M. Tan, and J. Titus , OV/P-5

Overview of Progress in European Medium Sized Tokamaks towards an Integrated Plasma-Edge/Wall Solution H. Meyer, T. Eich, M. Beurskens, S. Coda, A. Hakola, and P. Martin , OV/P-12

On Filamentary Transport in the TCV Tokamak: Addressing the Role of the Parallel Connection Length N. Vianello, C. Tsui², C. Theiler, S. Allan, J. A. Boedo, B. Labit, H. Reimerdes, K. Verhaegh, W. Vijvers, N. Walkden, S. Costea, J. Kovacic, C. Ionita, V. Naulin, A. H. Nielsen, J. J. Rasmussen, B. Schneider, R. Schrittwieser, M. Spolaore, D. Carralero, and J. Madsen , EX/P8-26

Recent Progress towards a Quantitative Description of Filamentary SOL Transport D. Carralero, H.W. Müller, M. Groth, J. Adamek, L. Aho-Mantila, S. Artene, G. Birkenmeier, M. Brix, G. Fuchert, P. Manz, J. Madsen, S. Marsen, U. Stroth, H. J. Sun, N. Vianello, M. Wischmeier, and E. Wolfrum , EX/2-2

TCV Experiments towards the Development of a Plasma Exhaust Solution H. Reimerdes, J. Harrison, P. Innocente, B. Lipschultz, M. Spolaore, C. Theiler, C. Tsui, W. Vijvers, J. A. Boedo, G. Calabrò, F. Crisanti, B. Duval, B. Labit, T. Lunt, R. Maurizio, V. Pericoli, U. Sheikh, K. Verhaegh, and N. Vianello , EX/2-3

Joint Experiments Tailoring the Plasma Evolution to Maximize Pedestal Performance I. Chapman, S. Saarelma, R. Cesario, S. Coda, E. de la Luna, A. Kirk, C. Maggi, A. Merle, R. Scannell, H. Urano, J. Connor, M. Dunne, R. Fisher, C. Ham, J. Hastie, J. Hobirk, O. McCormack, M. Peterka, O. Sauter, J. Simpson, E. R. Solano, and W. Wright , EX/3-6

Disruption Study Advances in the JET Metallic Wall E. Joffrin, P. Drewelow, P. de Vries, S. Gerasimov, M. Lehnen, P. Martin, G. Matthews, A. Murari, E. Nardon, D.

Paccagnella, C. Reux, G. Pautasso, R. Roccella, C. Sozzi, H. Strauss, M. Barruzo, A. Fil, T. Hender, S. Jachmich, U. Kruezi, B. N'Konga, R. Moreno, A. Pau, V. Riccardo, F. Rimini, J. Vega, and F. Villone , EX/9-1

Runaway Electron Generation and Mitigation on the European Medium Sized Tokamaks ASDEX-Upgrade and TCV G. Papp, G. Pautasso, J. Decker, M. Gobbin, P. J. McCarthy, D. Choi, S. Coda, B. Duval, R. Dux, B. Erdos, O. Ficker, C. Fuchs, L. Giannone, G. Anja, K. Lackner, L. Marelli, A. Mlynek, M. Maraschek, M. Nocente, P. Piovesan, V. V. Plyusnin, I. P. Gergo, P. Z. Poloskei, S. Potzel, C. Reux, B. Sieglin, C. Sommariva, W. Suttrop, G. Tardini, W. Treutterer, and M. Valisa , EX/9-4

Enhanced Measurements for MHD Validation Using Integrated Data Analysis on the MST Fusion Research Experiment D. Den Hartog, A. F. Almagri, D. Craig, P. Franz, M. Galante, C. Jacobson, J. Johnson, K. McCollam, M. Meghan, L. Morton, M. Nornberg, E. Parke, J. Reusch, L. Reusch, J. S. Sarff, J. Sauppe, C. Sovinec, H. Stephens, and J. Triana , EX/P5-15

Improved Low-Aspect-Ratio RFP Performance with Active MHD Control and Associated Change in Magnetic Topology in RELAX S. Masamune, A. Sanpei, Y. Aoki, T. Nagano, M. Higuchi, S. Nakanobo, R. Tsuboi, H. Himura, N. Mizuguchi, T. Akiyama, T. Mizuuchi, K. McCollam, D. Den Hartog, and R. Paccagnella , EX/P5-22

Ion Cyclotron Resonance Heating for Tungsten Control in JET H-Mode Scenarios M. Goniche, R. Dumont, V. Bobkov, P. Buratti, S. Brezinsek, C. Challis, F. J. Casson, L. Colas, A. Czarnecka, N. Fedorczak, J. Garcia, C. Giroud, M. Graham, J. Graves, P. Jacquet, E. A. Lerche, P. Mantica, I. Monakhov', P. Monier-Garbet, M. F. Nave, I. M. Ferreira Nunes, T. Pütterich, F. Rimini, M. Valisa, and D. Van Eester , EX/P6-16

MHD Limits and Plasma Response in High- Hybrid Operations in ASDEX-Upgrade V. Igochine, P. Piovesan, P. Bettini, T. Bolzonella, I. Classen, M. Dunne, A. Gude, P. Lauber, Y. Liu, M. Maraschek, N. Marconato, L. Marelli, S. Mastrostefano, P. J. McCarthy, R. McDermott, M. Reich, D. Ryan, M. Schneller, E. Strumberger, W. Suttrop, G. Tardini, F. Villone, and D. Yadikin , EX/P6-24

Comparison of Runaway Electron Generation Parameters in Small, Medium-sized and Large Tokamaks: A Survey of Experiments in COMPASS, TCV, ASDEX-Upgrade and JET V. V. Plyusnin, C. Reux, V. Kiptily, P. Lomas, V. Riccardo, G. Pautasso, J. Decker, G. Papp, J. Mlynář, S. Jachmich, A. Shevelev, E. Khilkevitch, S. Coda, B. Alper, Y. M. Martin, V. Weinzettl, R. Dux, B. Duval, S. Gerasimov, P. Martin, M. Nocente, and M. Vlainic , EX/P6-33

Losses of Runaway Electrons in MHD-Active Plasmas of the COMPASS Tokamak J. Mlynář, O. Ficker, M. Vlainic, V. Weinzettl, S. Coda, J. Decker, P. Martin, E. Nardon, G. Papp, V. V. Plyusnin, C. Reux, F. Saint-Laurent, C. Sommariva, J. Havlicek, O. Hronova, T. Markovic, R. Paprok, R. Panek, and J. Urban , EX/P6-34

First Experimental Results of Runaway Beam Control in TCV B. Esposito, D. Carnevale, M. Gospodarczyk, M. Gobbin, S. Galeani, C. Galperti, J. Decker, B. Duval, H. Anand, P. Buratti, F. Causa, G. Papp, S. Coda, and P. Martin, EX/P8-27

Real-Time Model-Based Plasma State Estimation, Monitoring and Integrated Control in TCV, ASDEX-Upgrade and ITER F. Felici, T. Blanken, B. Maljaars, H. Van den Brand, J. Citrin, D. Hogeweij, M. Scheffer, M. De Baar, M. Steinbuch, S. Coda, C. Galperti, J.-M. Moret, O. Sauter, A. Teplukhina, T. Vu, R. Nouailletas, O.

Kudlacek, C. Piron, P. Piovesan, W. Treutterer, C. Rapson, L. Giannone, and M. Willensdorfer , EX/P8-33

Physics and Operation Oriented Activities in Preparation of the JT-SA Tokamak Exploitation G. Giruzzi, E. Joffrin, J. Garcia, D. Douai, J.-F. Artaud, B. Pégourié, P. Maget, Y. Kamada, M. Yoshida, S. Ide, N. Hayashi, G. Matsunaga, T. Nakano, K. Shinohara, S. Sakurai, T. Suzuki, H. Urano, M. Enoda, H. Kubo, K. Kamiya, M. Takechi, Y. Miyata, A. Isayama, T. Kobayashi, S. Moriyama, K. Shimizu, K. Hoshino, H. Kawashima, A. Bierwage, D. C. McDonald, C. Sozzi, L. Figini, S. Nowak, A. Moro, P. Platania, D. Ricci, G. Granucci, T. Bolzonella, P. Bettini, P. Innocente, D. Terranova, L. Pigatto, F. Villone, A. Pironti, S. Mastrostefano, G. De Tommasi, M. Mattei, A. Mele, F. P. Orsitto, D. Dunai, T. Szepesi, E. Barbato, V. Vitale, M. Romanelli, L. Garzotti, A. Boboc, S. Saarelma, M. Wischmeier, P. Lauber, P. Lang, R. Neu, C. Day, C. Gleason-Gonzalez, M. Scannapiego, R. Zagorski, K. Galazka, W. Stepniewski, N. Cruz, E. de la Luna, M. Garcia-Munoz, J. Vega, S. Clement-Lorenzo, F. Sartori, S. Coda, T. P. Goodman, and S. Soare , EX/P8-40

Progress in the Theoretical Description and the Experimental Characterization of Tungsten Transport in Tokamaks C. Angioni, E. A. Belli, R. Bilato, V. Bobkov, F. J. Casson, E. Fable, A. Loarte, P. Mantica, R. Ochoukov, T. Odstrcil, T. Pütterich, M. Sertoli, J. Stober, and M. Valisa , TH/P2-6

Recent EUROfusion Achievements in Support to Computationally Demanding Multiscale Fusion Physics Simulations and Integrated Modelling I. Voitsekhovitch, R. Hatzky, D. Coster, F. Imbeaux, D. C. McDonald, T. B. Fehér, K. S. Kang, H. Leggate, M. Martone, S. Mochalsky, X. Sáez, T. Ribeiro, T.-M. Tran, A. Gutierrez-Milla, S. Heurax, S. D. Pinches, F. da Silva, D. Tskhakaya, T. Aniel, D. Figat, L. Fleury, O. Hoenen, J. Hollocombe, D. Kaljun, G. Manduchi, M. Owsiak, V. Pais, B. Palak, M. Plociennik, J. Signoret, C. Voulard, and D. Yadikin , TH/P2-12

Investigation of Sustainable Reduced-Power Noninductive Scenarios on JT-60SA M. Romanelli, L. Garzotti, S. Wiesen, M. Wischmeier, R. Zagorski, J. Garcia, P. Maget, E. de la Luna, M. Yoshida, H. Urano, P. da Silva Arresta Belo, G. Corrigan, S. Saarelma, T. Bolzonella, and H. Derek , TH/P2-20

EUROfusion Integrated Modelling (EU-IM) Capabilities and Selected Physics Applications G. Falchetto, M. I. Airila, A. Alberto Morillas, C. Boulbe, R. Coelho, D. Coster, T. Johnson, D. Kalupin, A. H. Nielsen, G. Vlad, E. Andersson Sundén, T. Aniel, J.-F. Artaud, O. Asunta, C. V. Atanasiu, M. Baelmans, V. Basiuk, R. Bilato, M. Blommaert, X. Bonnin, D. Borodin, S. Briguglio, J. Buchanan, F. J. Casson, G. Ciralo, J. Citrin, S. Conroy, V. Doriæ, R. Dumont, E. Fable, B. Faugeras, J. Ferreira, L. Figini, A. Figueiredo, G. Fogaccia, C. Fuchs, K. Ghos, E. Giovannozzi, C. Gleason-Gonzalez, V. Goloborod'ko, O. Hoenen, N. Horsten, P. Huynh, F. Imbeaux, I. Ivanova-Stanik, L. Kos, V. Kotov, J. Krek, C. Lechte, E. A. Lerche, R. Lohner, J. Madsen, O. Maj, G. Manduchi, M. Mantsinen,, Y. Marandet, N. Marushchenko, S. Mastrostefano, R. Mayo-Garcia, P. J. McCarthy, A. Merle, S. Moradi, E. Nardon, W. Natorf, S. Nowak, M. O'Mullane, M. Owsiak, V. Pais, B. Palak, G. Pelka, V. Pericoli-Ridolfini, M. Plociennik, G. I. Pokol, E. Poli, D. Poljak, H. Radhakrishnan, H. Reimerdes, D. Reiser, P. Rodrigues, X. Sáez, D. Samaddar, O. Sauter, K. Schmid, M. B. Schneider, B. D. Scott, S. Šesni'c, J. Signoret, S. K. Sipilä, R. Stankiewicz, E. Suchkov, A. Šušnjara, G. Szepesi, D. Tegnered, L. Tophøj, K. T'okési, D. Tskhakaya, J. Urban, P. Vallejos, D. Van Eester, S. Varoutis, L. Villard, F. Villone, B. Viola, E. Westerhof, D. Yadikin, R. Zagorski, F. Zaitsev, T. Zok, W. Zwingmann, and S. Äkäsloppolo , TH/P2-13

Progress of Experimental Study on Negative Hydrogen Ion Production and Extraction M. Kasaki, K. Tsumori, K. Ikeda, H. Nakano, S. Geng, T. Tokuzawa, M. Osakabe, K. Nagaoka, P. Agostinetti, M. Brombin, A. Hatayama, S. Nishioka, E. Sartori, G. Serianni, P. Veltri, O. Kaneko, and Y. Takeiri, FIP/1-4

EU DEMO Heating and Current Drive: Physics and Technology M. Q. Tran, T. Franke, G. Granucci, G. Grossetti, J. Jelonnek, I. Jenkins, J.-M. Noterdaeme, A. Simonin, P. Sonato, R. Wenninger, and H. Zohm , FIP/7-7

Evolutions of EU DEMO Reactor Magnet System Design Along the Recent Years and Lessons Learned for the Future L. Zani, M. Biancolini, R. Bonifetto, P. Bruzzone, C. Brutti, D. Ciazynski, M. Coleman, G. Federici, E. Gaiò, F. Giorgetti, P. Hertout, C. Hoa, B. Lacroix, M. Lewandowska⁷, A. Maistrello, L. Muzzi, A. Nijhuis, F. Nunio, A. Panin, J.-M. Poncet, L. Savoldi, K. Sedlak, B. Stepanov, I. Tiseanu, A. Torre, S. Turtu, R. Vallcorba, R. Wesche, K. Yagotintsev, and R. Zanino , FIP/P7-10

Extended Capability of the Integrated Transport Analysis Suite, TASK3D-a, for LHD Experiment, and its Impacts on Facilitating Stellarator-Heliotron Research M. Yokoyama, R. Seki, C. Suzuki, M. Sato, A. Shimizu, M. Emoto, S. Murakami, M. Osakabe, T. I. Tsujimura, Y. Yoshimura, K. Ogawa, S. Satake, Y. Suzuki, T. Goto, K. Ida, N. Pablant, D. Gates, A. Y. Pankin, F. Warmer, and P. Vincenzi , FIP/P7-35

Exploration of Fusion Power Penetration under Different Global Energy Scenarios Using the EFDA Times Energy Optimization Model H. Cabal, Y. Lechón, F. Gracceva, D. Ward, M. Biberacher, C. Bustreo, D. N. Dongiovanni, and P. E. Grohnheit , SEE/P7-4